

# Antidepressant effects of valproic acid in an animal model of depression

Original paper

Buzgoova K.<sup>1,2✉</sup>, Balagova L.<sup>1</sup>, Hlavacova N.<sup>1</sup>, Jezova, D.<sup>1</sup>

<sup>1</sup>Slovak Academy of Sciences, Biomedical Research Center,  
Institute of Experimental Endocrinology;

<sup>2</sup>Comenius University in Bratislava, Faculty of Pharmacy,  
Department of Pharmacology and Toxicology,  
Bratislava, Slovakia

Received 18 May, 2019, accepted 22 May, 2019

**Abstract** Valproic acid, beside its anticonvulsant action, is widely used as a mood stabilizer in the therapy of bipolar disorder. The potential antidepressant action of valproic acid has not been sufficiently characterized so far. The aim of the present study was to evaluate the antidepressant effect of valproic acid in an aldosterone model of depression. Subchronic treatment with valproic acid resulted in a reduction of the time spent in immobility in the forced swim test. In conclusion, the present study provides evidence on antidepressant effects of valproic acid using a classical behavioral approach for testing the efficacy of antidepressant drug in animal models.

**Keywords** sodium valproate – forced swimming test – antidepressant effect

## INTRODUCTION

Valproic acid is an antiepileptic drug used in the clinical practice for a long time. Beside its anticonvulsant action, it is widely used as a mood stabilizer in the therapy of bipolar disorder. Together with other thymoprophylactics and anticonvulsants, such as tiagabine, it also exhibits antidepressant effect (Pistovcakova et. al 2008). The exact mechanism of antidepressant action is still unknown, and therefore, it is tested in various animal models of depression (Lima et al. 2017, Qiu et. al 2015). However, the data from the literature are still insufficient to fully elucidate the potential antidepressant action of valproic acid.

The aim of the present study was to evaluate the antidepressant effect of valproic acid in an animal model of depression based on elevated circulating concentrations of aldosterone, which was shown to induce increased anxiety and depression-like behaviors (Hlavacova & Jezova, 2008; Hlavacova et al. 2012).

## MATERIAL AND METHODS

Forty male adult Sprague-Dawley rats were used. Animals were housed individually in standard cages with free access to rat chow and water. All experimental procedures were approved by the Animal Health and Animal Welfare

Division of the State Veterinary and Food Administration of the Slovak Republic. Animals were divided into four groups (n = 9–10 per group) based on the treatment administered. Aldosterone (d-aldosterone, Sigma, USA) or vehicle was continuously administered via subcutaneous osmotic minipumps for 14 days (Model 2002, Alzet, Alza Corp., USA). The dose of aldosterone was chosen based on our previous studies (Hlavacova & Jezova, 2008; Hlavacova et al. 2012). Simultaneously, valproic acid was administered in drinking water at a dose of 100 mg/1 kg body weight/day continuously for 14 days. Animals from placebo groups received drinking water without valproic acid.

On day 14 of the treatments, rats from each group were subjected to behavioral testing in the forced swim test to evaluate depression-like behavior. Behavioral tests were conducted during the light phase of the day, between 9.00 and 11.00 h. The rats were individually placed in a glass cylindrical tank filled with tap water (23±1°C). The testing session lasted 15 min and was videotaped by camera positioned in front of the tank. Rats behavior was scored for the last 5 min of the 15 min session (Hlavacova et al. 2012). The percentage of time which the animal spent immobile was rated as depression-like behavior (Hlavacova et al. 2018). In addition, time which animal spent struggling and swimming was also measured.

\* E-mail: katarina.buzgoova@savba.sk

© European Pharmaceutical Journal

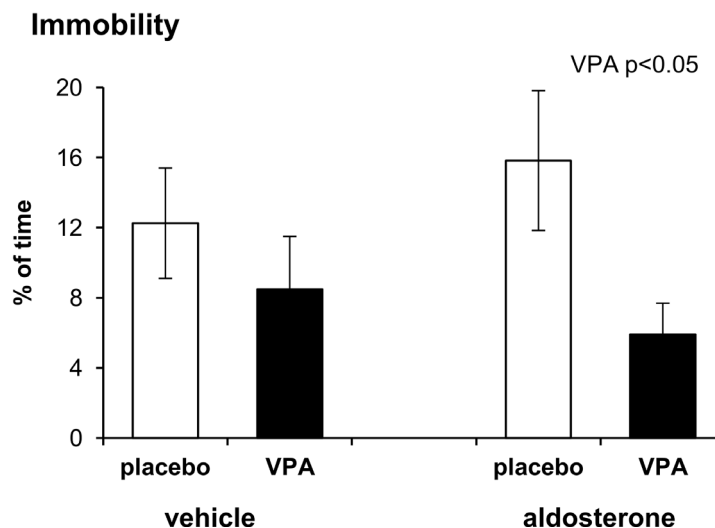


Figure 1. Time spent in immobility in forced swimming test in rats simultaneously treated with valproic acid and aldosterone. The results are expressed as means  $\pm$  SEM. Overall level of significance was defined as  $p < 0.05$ .

## RESULTS

The data were checked for the normality of distribution using the Shapiro–Wilk test and were analyzed by two-way analysis of variance (ANOVA) for factors valproic acid (valproic acid and placebo groups) and aldosterone (aldosterone and vehicle groups).

Statistical analysis of data obtained from the forced swim test showed a significant main effect of valproic acid treatment ( $F(1,34) = 5.05$ ,  $p < 0.05$ ) on immobility time. Valproic-acid-treated rats spent significantly shorter time immobile compared to rats treated with placebo (Fig. 1). The animals treated with aldosterone spent longer time in immobility, but the difference did not reach significance. No significant main effects of valproic acid and aldosterone treatments or their interaction were observed in struggling and swimming behaviors (data not shown).

## DISCUSSION

The present findings show antidepressant effect of sub-chronic treatment with valproic acid in aldosterone model of depression. The valproic acid is clinically used in the treatment of bipolar disorder and there are signals of its efficacy in bipolar depression (Smith et al. 2010). However, the exact experimental evidence of antidepressant effects of valproic acid is limited and contradictory.

The dose of valproic acid used in the present study was 100 mg/kg/day. The research group of Qiu and colleagues (2014; 2015) reported antidepressant-like effects of valproic acid treatment via intragastric gavage at a dose of 300 mg/kg/day in rats exposed to chronic unpredictable stress model of

depression. On the other hand, the same dose of valproic acid injected intraperitoneally to mice increased the immobility in the forced swim test, indicating its depressogenic effects (Lima et al. 2017). That study revealed antidepressant effects of lower dose of valproic acid, namely, 30 and 100 mg/kg. The dose of valproic acid selected in the present study was observed to be effective in the inhibition of histone deacetylase (Bredy and Barad, 2008; Heinrichs et al. 2013) and changes in epigenetic mechanisms have been associated with the pathophysiology of depression.

Unlike our previous results (Hlavacova et al. 2012), the time spent in immobility only tended to be higher in aldosterone-treated rats. One reason for this discrepancy could be the use of Sprague-Dawley and not Wistar strain of rats in the present experiments. Another cause of the difference could be the cessation of the production of the aldosterone substance used previously by the chemical company and the need to purchase aldosterone from another company.

In conclusion, the present study provides evidence on antidepressant effects of valproic acid using a classical behavioral approach for testing the efficacy of antidepressant drug in animal models. It may be related to the epigenetic modulations induced by the same dose of valproic acid described recently (Buzgoova et al. 2019).

## ACKNOWLEDGMENTS

The study was supported by the grant of Slovak Research and Development Agency under the contract No. APVV-15-0388 and VEGA 2/0042/19.

## References

- [1] Bredy TW, Barad M. The histone deacetylase inhibitor valproic acid enhances acquisition, extinction, and reconsolidation of conditioned fear. *Learn Mem.* 2008; 15(1):39-45.
- [2] Heinrichs SC, Leite-Morris KA, Rasmusson AM, Kaplan GB. Repeated valproate treatment facilitates fear extinction under specific stimulus conditions. *Neurosci Lett.* 2013; 552:108-13.
- [3] Hlavacova N, Jezova D. Chronic treatment with the mineralocorticoid hormone aldosterone results in increased anxiety-like behavior. *Horm Behav.* 2008; 54(1):90-7.
- [4] Hlavacova N, Li Y, Pehrson A, Sanchez C, Bermudez I, Csanova A, Jezova D, Franklin M. Effects of vortioxetine on biomarkers associated with glutamatergic activity in an SSRI insensitive model of depression in female rats. *Prog Neuropsychopharmacol Biol Psychiatry.* 2018; 82:332-338.
- [5] Hlavacova N, Wes PD, Ondrejckova M, Flynn ME, Poundstone PK, Babic S, Murck H, Jezova D. Subchronic treatment with aldosterone induces depression-like behaviours and gene expression changes relevant to major depressive disorder. *Int J Neuropsychopharmacol.* 2012;15(2):247-65.
- [6] Lima IVA, Almeida-Santos AF, Ferreira-Vieira TH, Aguiar DC, Ribeiro FM, Campos AC, de Oliveira ACP. Antidepressant-like effect of valproic acid-Possible involvement of PI3K/Akt mTOR pathway. *Behav Brain Res.* 2017; 329:166-171.
- [7] Pistovcakova J, Dostalek M, Sulcova A, Jezova D. Tiagabine treatment is associated with neurochemical, immune and behavioural alterations in the olfactory bulbectomized rat model of depression. *Pharmacopsychiatry.* 2008; 41(2):54-9.
- [8] Qiu HM, Yang JX, Jiang XH, Hu XY, Liu D, Zhou QX. Enhancing tyrosine hydroxylase and tryptophan hydroxylase expression and improving oxidative stress involved in the antidepressant effect of sodium valproate on rats undergoing chronic unpredicted stress. *Neuroreport.* 2015; 26(18):1145-50.
- [9] Qiu HM, Yang JX, Liu D, Fei HZ, Hu XY, Zhou QX. Antidepressive effect of sodium valproate involving suppression of corticotropin-releasing factor expression and elevation of BDNF expression in rats exposed to chronic unpredicted stress. *Neuroreport.* 2014; 25(4):205-10.
- [10] Smith LA, Cornelius VR, Azorin JM, Perugi G, Vieta E, Young AH, Bowden CL. Valproate for the treatment of acute bipolar depression: systematic review and meta-analysis. *J Affect Disord.* 2010; 122(1-2):1-9.
- [11] Buzgoova K, Graban J, Balagova L, Hlavacova N, Jezova D. Brain derived neurotrophic factor expression and DNA methylation in response to subchronic valproic acid and/or aldosterone treatment. *Croat Med J.* 2019 (in press).

# Formulation and evaluation of new oxycodone extended release multiple unit pellet system

Original Paper

Husár Š.<sup>1,2</sup>✉, Sýkorová M.<sup>1</sup>, Rumlová K.<sup>1</sup>, Chomaničová K.<sup>1</sup>, Vladovičová B.<sup>2</sup>

<sup>1</sup>Comenius University in Bratislava,  
Faculty of Pharmacy, Department  
of Pharmaceutical chemistry, Slovak Republic  
<sup>2</sup>Saneca Pharmaceuticals a.s.,  
Hlohovec, Slovak Republic

Received 6 March, 2019, accepted 16 August, 2019

**Abstract** The goal of the present study is to prepare a stable, multiple-unit, extended-release dosage form containing oxycodone pellets coated with aqueous ethylcellulose (EC) dispersion, Surelease E-7-19050. The application of 18% w/w of EC leads to the similar drug release with the hydrophobic, non-swelling, matrix reference product containing 20 mg of oxycodone. Increasing the compression force to 9 kN and including more than 50% w/w of oxycodone pellets into the formulation resulted in faster drug release, indicating the damaging to the EC film coating. The physical appearance of the final formulation, assay of oxycodone, moisture content, and dissolution data over the stability period showed that the multiple-unit pellet system (MUPS) is efficient for the production of highly stable product.

**Keywords** Opioids – Oxycodone – Dissolution – Extended release – Pellets

## INTRODUCTION

Coated pellets are frequently used for oral, controlled-release, drug delivery. The recent trends indicate that multiparticulate drug delivery systems are especially suitable for achieving controlled- or delayed-release oral formulations with low risk of dose dumping, flexibility of blending to attain different release patterns, as well as reproducible and short gastric residence time (Dey et al., 2008). Controlled-release drug delivery systems provide a uniform concentration at absorption site, maintain plasma concentration within a therapeutic range, reduce the frequency of administration, and minimize the side effects. It is also important to avoid dose dumping after the oral administration of ER dosage forms, especially for drugs that possess the characteristics of a higher solubility, higher dose, or a fatal side effect (Uros et al., 2014). Furthermore, an alcohol-induced dose dumping effect in oral ER dosage forms has gained increased attention in the recent years (Jedinger et al., 2014).

Compaction of multiparticulates, commonly called MUPS (abbreviation for multiple-unit pellet system), is one of the

most recent and challenging technologies that combine the advantages of both tablets and pellet-filled capsules in one dosage form. The multiparticulates spread uniformly throughout the gastrointestinal tract, resulting in less variable bioavailability and a reduced risk of local irritation. Various drug release profiles can be obtained by simply mixing pellets with different release characteristics or incompatible drugs can be easily separated (Dashevsky et al., 2004).

Oxycodone hydrochloride is a semisynthetic opioid agonist that provides effective relief for moderate to severe pain in cancer and postoperative patients. The pharmacokinetic and steady-state pharmacodynamic studies with immediate-release (IR) oxycodone have shown it to be well tolerated, with adverse effects similar to those of other opioids. The bioavailability of oral oxycodone in humans is 60% (range: 50–87%). The terminal elimination half-life is independent of dose, with modest interindividual differences (Fukui et al., 2017).

Ethylcellulose (EC) has been widely used as a barrier membrane or binder to prepare pharmaceutical, oral,

\* E-mail: husar.stefan26@gmail.com

© European Pharmaceutical Journal

Table 1. Formulation of oxycodone MUPS tablets F1–F3 (weights in mg/tablet)

Process step	Material	Formulation code		
		F1	F2	F3
Oxycodone drug layered pellets	Oxycodone hydrochloride	20.0	20.0	20.0
	Hypromellose (Methocel E5)	1.2	1.2	1.2
	Polysorbate 80	1.2	1.2	1.2
	Talc	0.5	0.5	0.5
	Sugar spheres with a diameter of 355–425 $\mu\text{m}$	50.0	50.0	50.0
Release modifying polymer	Surelease clear E-7-19050*	11.7* (7.3 mg EC)	21.0* (13.1 mg EC)	30.4* (19.0 mg EC)
Compression into MUPS	Microcrystalline cellulose (Comprecel M102)	124.1	137.5	150.8
	Magnesium stearate	2.2	2.4	2.6
	Silica dioxide	1.1	1.2	1.3
<b>MUPS tablet weight in mg</b>		<b>212.0</b>	<b>235.0</b>	<b>258.0</b>

\* Surelease clear E-7-19050 contains 62.4% w/w of EC. EC, ethylcellulose.

modified-release dosage forms. The aqueous dispersion of EC, for example, Surelease, has been used to manufacture modified-release multiparticulates for filling into capsules and single-unit tablets or soft-gel capsules through film-coating applications. In addition, the use of aqueous EC dispersion as a release retardant binder for the manufacture of inert matrices has been reported. Surelease<sup>®</sup> enhanced the compaction characteristics of the drug, and the drug was released from those inert porous matrices by diffusion (Rajabi-Siahboomi & Farrell, 2008).

## MATERIALS AND METHODS

### Materials

The materials used in this study were oxycodone hydrochloride (Saneca Pharmaceuticals, Slovakia), sugar spheres with a diameter of 355–425  $\mu\text{m}$  (Hanns G. Werner, Germany), talc (Luzenac, China), hypromellose (HPMC, Methocel E5, Dow Chemicals, GB), polysorbate 80 (Centralchem, Slovakia), Surelease clear E-7-19050 (Colorcon, USA), microcrystalline cellulose (Comprecel M102, Mingtai, China), silica dioxide (Grace GmbH, GB), and magnesium stearate (Faci SPA, Italia).

## METHODS

### Preparation of opiate pellets

The spraying of water dispersion method was chosen to prepare the opioid analgesic pellets. The required quantities of hypromellose and polysorbate 80 were dispersed in water, purified to prepare binding suspension, and mixed until clear solution is achieved. Oxycodone HCl powder was then added

to the dispersion and mixed for another 45 min. The required quantity of Talc was added at the end of oxycodone dispersion preparation and mixed for 20 min. Required amount of sugar spheres with a diameter of 355–425  $\mu\text{m}$  was loaded into a fluidized bed coater Glatt GPCG-2 equipped with a 3.0-L Wurster container, air distribution plate type A, and filter bags with a porosity of below 20  $\mu\text{m}$  (Glatt GmbH, Germany) and preheated to a product temperature of 34–36°C. The layering conditions were given as follows: batch size, 400 g; inlet air temperature, 45°C; product temperature, 33°C; air flow, 120  $\text{m}^3/\text{h}$ ; nozzle diameter, 1.2 mm; atomizing air pressure, 1.5 bar; spray rate, 5 g/min; final drying at 40°C for 20 min.

### Coating of drug-layered pellets

The oxycodone drug-layered pellets were coated with aqueous water dispersion of Surelease E-7-19050 (15% w/w solid content) using the fluidized bed coater Glatt GPCG-2 (Glatt GmbH, Germany) and preheated to a product temperature of 36–48°C. Three different quantities of Surelease E-7-19050 were applied onto oxycodone pellets (formulations F1–F3, Table 1). The layering conditions were given as follows: batch size, 400 g; inlet air temperature, 50°C; product temperature, 35°C; air flow, 140  $\text{m}^3/\text{h}$ ; nozzle diameter, 1.2 mm; atomizing air pressure, 1.5 bar; spray rate, 8 g/min; final drying at 45°C for 30 min.

### Compression of coated pellets

The composition of MUPS tablets F1–F3 is presented in Table 1. Coated pellets were mixed in a slow speed blender RV1 (Kovymont, Slovakia) for 15 min at 13 rpm with different amounts of microcrystalline cellulose (Comprecel M102).

Table 2. Formulation of oxycodone MUPS tablets F4–F6 (weights in mg/tablet)

Process step	Material	Formulation code		
		F4	F5	F6
Oxycodone drug layered pellets	Oxycodone hydrochloride	20.0	20.0	20.0
	Hypromellose (Methocel E5)	1.2	1.2	1.2
	Polysorbate 80	1.2	1.2	1.2
	Talc	0.5	0.5	0.5
	Sugar spheres with a diameter of 355–425 $\mu\text{m}$	50.0	50.0	50.0
Release modifying polymer	Surelease clear E-7-19050*	21.0* (13.1 mg EC)	21.0* (13.1 mg EC)	21.0* (13.1 mg EC)
Compression into MUPS	Microcrystalline cellulose (Comprecel M102)	214.4	91.3	38.1
	Magnesium stearate	3.1	1.9	1.3
	Silica dioxide	1.6	0.9	0.7
<b>MUPS tablet weight in mg</b>		<b>313.0</b>	<b>188.0</b>	<b>134.0</b>

\* Surelease clear E-7-19050 contains 62.4% w/w of EC. EC, ethylcellulose.

After that 1.0% of magnesium stearate and 0.5% of silica dioxide were added as a lubricant/glidant (Table 2) and mixed in the slow speed blender RV1 for 5 min at 13 rpm. The tablets were compressed on a rotary tablet press Pressima AX8 (IMA Pharma, Italy) with different compression forces; the composition and tablet weight of formulations F1–F6 are presented in Tables 1 and 2. The hardness of tablets was tested using a hardness tester Sotax Tester 8M (Sotax AG, Switzerland), and the disintegration of 6 MUPS tablets in water (temperature 35–39°C) was performed using a disintegration tester Sotax DT2 (Sotax AG, Switzerland). The friability of 6.5g of MUPS tablets was tested using a Sotax friability tester (Sotax AG, Switzerland) and evaluated after 100 rotations of the drum. The physical characteristics of MUPS formulations F1–F6 are reported in Table 3.

### In vitro dissolution study

The drug release from the coated and compressed pellets was investigated using a paddle apparatus Sotax AT7 Smart (Sotax AG, Switzerland) in 900 mL of 0.1N HCl at 75 rpm at  $37 \pm 0.5^\circ\text{C}$ ,  $n = 6$ . Samples were withdrawn at predetermined time points (sample volume: 1.5 mL) and measured using UV spectrophotometer (Cary 50 UV-VIS spectrophotometer, Agilent technologies) at 230 nm.

### Tablets bulk stability testing

The final formulation of oxycodone MUPS tablets was set for stability study in double PE bags with a desiccant placed between them and closed in a nontransparent plastic container for 3 months at a relative temperature (RT) and relative humidity (RH) conditions in 3 different stability

chambers SC-12 Plus (REMI Laboratory Instruments, India): 25°C/60%, 30°C/65%, and 40°C/75%. After each month, dissolution, appearance, assay, and LOD (halogen analyser Mettler Toledo HF63, 10 min at 105°C, 5-g samples of crushed tablets) were performed and evaluated.

## RESULTS AND DISCUSSION

Compaction of multiparticulates, commonly called MUPS, is one of the most recent and challenging technologies that combine the advantages of both tablets and pellet-filled capsules in one dosage form. Ideally, the compacted pellets should not fuse into a nondisintegrating matrix during compression and should disintegrate rapidly into individual pellets in gastrointestinal fluids. Importantly, the drug release should not be affected by the compaction process and the polymer coating must be able to resist to the compression force; it can deform, but it should not rupture (Bhad et al., 2010). Most studies on the compression of pellets with EC revealed damage to the coating layer with a loss of the extended-release properties. The mechanical properties of the particular Surelease E-7-19050 polymer coating were determined in order to investigate its suitability for the coating of oxycodone pellets, which are intended to be compressed into tablets.

Figure 1 shows drug release profiles of MUPS compressed using oxycodone coated pellets with different concentration of retarding agent Surelease E-7-19050: 10% w/w (referring to the active oxycodone pellets, see composition in Table 1) of EC (EC, Formulation F1), 18% w/w of EC (F2), and 26% w/w of EC (F3). The formulations F1–F3 were compressed at the same main compression force of 4.5 kN. The dissolution profiles are compared with the commercially available reference

Table 3. Physical characteristics of oxycodone MUPS tablets F1–F6

Formulation code	Average weight [mg], <i>n</i> = 20	Hardness [N], <i>n</i> = 10	Friability [25 rpm, 4 min, %], <i>n</i> = 3	Disintegration [s], <i>n</i> = 6
F1	212.2 ± 2.9	51 ± 5.4	0.51 ± 0.08	31 ± 5.8
F2	235.2 ± 2.7	52 ± 6.3	0.47 ± 0.10	24 ± 7.5
F3	258.8 ± 3.6	54 ± 5.8	0.56 ± 0.06	42 ± 4.2
F4	313.0 ± 2.4	76 ± 5.0	0.50 ± 0.07	35 ± 2.8
F5	188.6 ± 2.2	41 ± 4.2	0.35 ± 0.06	161 ± 12.1
F6	134.7 ± 2.9	43 ± 3.6	0.28 ± 0.04	987 ± 9.9
F4 (3 kN)	313.6 ± 3.8	38 ± 4.1	0.91 ± 0.06	24 ± 1.8
F4 (6 kN)	314.2 ± 2.1	54 ± 3.0	0.65 ± 0.02	124 ± 8.2
F4 (9 kN)	313.4 ± 1.2	78 ± 2.6	0.04 ± 0.01	997 ± 13.4

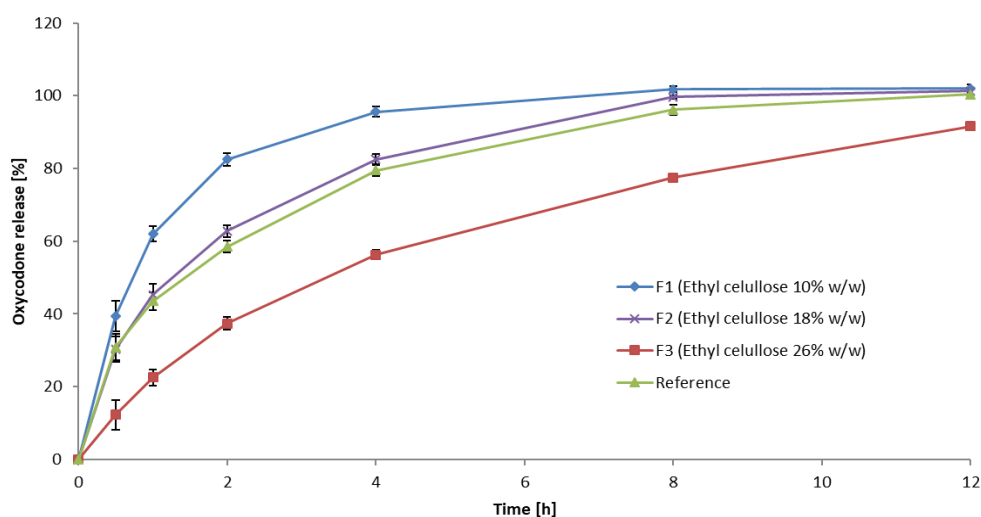


Figure 1. Influence of Ethyl cellulose content on oxycodone drug release from MUPS tablets F1-F3

product, Targin® (Mundipharma, Austria), containing 20 mg of oxycodone hydrochloride in a hydrophobic, non-swellable matrix tablets. As it can be seen, the release decreased with increasing EC content and the similar dissolution profile (similarity factor  $f_2 = 84$ ) was achieved with formulation F2 containing 18% w/w of EC (Surelease E-7-19050). Following this observation, the effect of filler/pellet content was further investigated with this concentration of EC.

Three formulations, F4, F5, and F6 (containing 18% w/w of EC, see composition in Table 2), were prepared with different oxycodone pellet content, 30%, 50% and 70% w/w, mixed with extragranular excipients and compressed at the same main compression force of 4.5 kN. The oxycodone release from compressed pellets was significantly faster compared with that from the original pellets coated with 18% of EC as shown in Figure 2. This could be explained by the weak mechanical properties of EC films, which ruptured during

compression. It has been reported that plastically deforming excipients are more effective in protecting the coated pellets during compression; therefore, the microcrystalline cellulose (Comprecel M102) was selected to provide a better protective effect to the oxycodone-coated pellets. Figure 2 shows that increasing the protective excipient to 70% w/w (30% pellet content, formulation F4) minimized the damage to the compressed drug pellets, with the  $f_2$  between compressed and uncompressed pellets being 61. Values for  $f_2$  (similarity factor) between 50 and 100 indicate that the two profiles are similar (Vetchý et al., 2014). Compressing coated pellets with 30% of protective excipient (formulation F6) resulted in the loss of their extended-release properties. This is explained by the lower yield pressure of the MCC filler that absorbs the energy of compaction and preferentially deforms under pressure, thus protecting the pellets. A higher level of the cushioning excipient also reduces the number of oxycodone

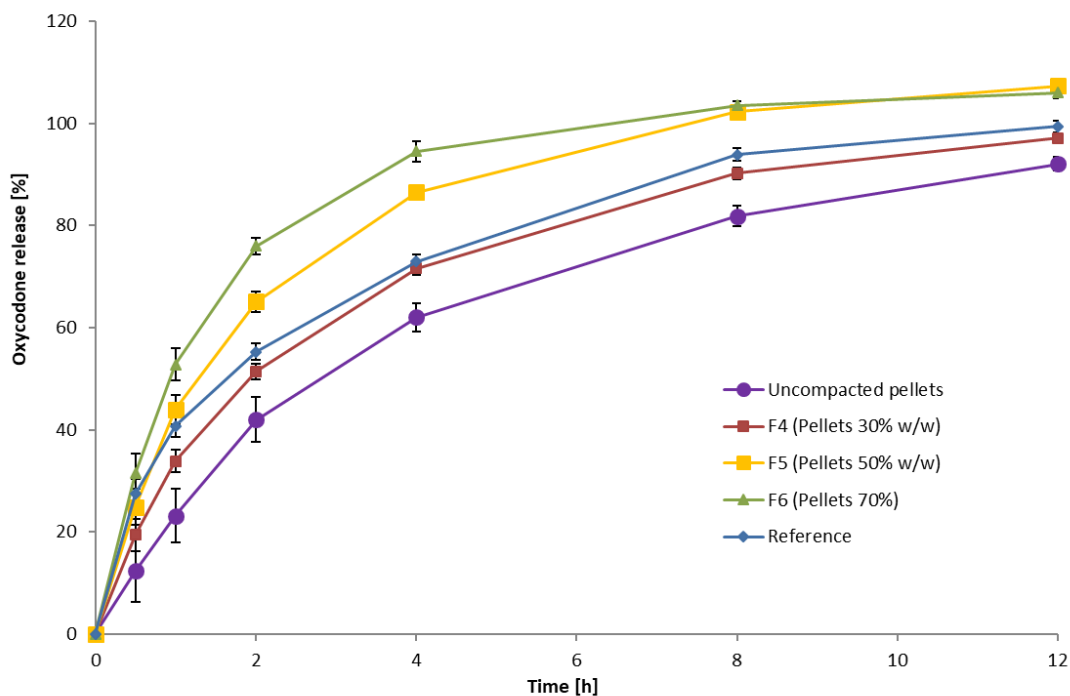


Figure 2. Influence of proportion of coated pellets on oxycodone drug release from MUPS tablets F4-F6

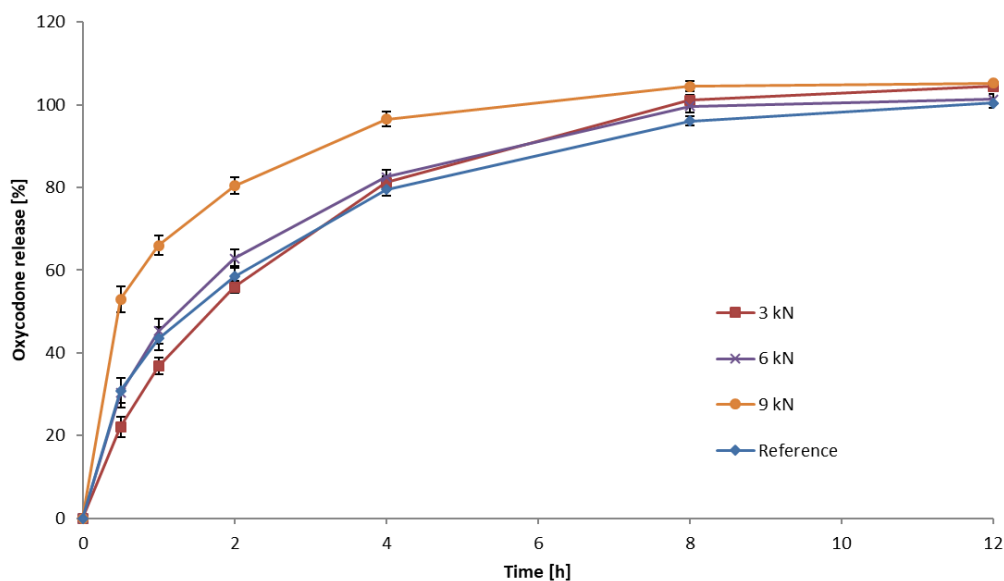


Figure 3. Influence of compression force on oxycodone drug release from MUPS tablets containing 30% w/w proportion of coated pellets

pellets coming in direct contact with each other or with the punch surface during the compression cycle, which can cause pellets to rupture (Al-Hashimi et al., 2018).

Figure 3 shows drug release profile of MUPS compressed at different compression forces using 30% w/w oxycodone pellets content in the formulation. Increasing compression force resulted in faster drug release, indicating the damaging to the EC film coating. The  $f_2$  values for tablets compressed at

a compression force of 3 and 6 kN were 71 and 62, respectively, compared with the matrix reference tablets, Targin. Increasing the tablet compression force to 9 kN leads to MUPS tablets of greater strength; however, an increase in tablet disintegration time to more than 15 min was also observed (Table 3). Higher disintegration time could be attributed to a lower penetration of the disintegration test media into the tablet because of the creation of undesirable matrix structure.

Table 4. Stability data\* of oxycodone MUPS tablets at different time intervals in three different conditions (formulation F4)

Parameters	Initial	25°C/60% RH			30°C/65% RH			40°C/75% RH		
		1M	2M	3M	1M	2M	3M	1M	2M	3M
Assay %	98.7	98.4	98.0	97.7	98.2	98.4	98.0	97.4	97.0	97.2
Appearance (white to off-white, round, biconvex tablets)	Comply	Comply	Comply	Comply	Comply	Comply	Comply	Comply	Comply	Slightly yellowish
Loss on drying %	2.8	3.5	3.8	3.8	3.8	3.8	3.9	4.0	4.2	4.4
Q8	85.91	84.24	84.65	82.17	82.01	82.53	79.85	83.08	81.24	78.66
$t_{50\%}$	2.14	1.98	2.02	1.89	2.01	2.14	1.80	1.99	1.96	1.78
$t_{80\%}$	6.30	6.14	6.28	6.02	6.24	6.34	5.98	6.27	6.24	5.90
$r^2$	0.995	0.990	0.997	0.989	0.991	0.994	0.994	0.984	0.986	0.994
$k$	2.362	2.512	2.378	2.156	2.318	2.305	2.224	1.214	1.105	1.064
$n$	0.656	0.641	0.652	0.671	0.661	0.663	0.658	0.726	0.741	0.735

\* $Q_8$  indicates percentage of oxycodone drug release at 8 h;  $t_{50\%}$  time required for 50% drug release;  $t_{80\%}$  time required for 80% drug release;  $r^2$ , correlation coefficient;  $k$ , release rate constant;  $n$ , diffusion exponent; M, month.

MUPS tablets of the formulation F4 (18% EC, 30% oxycodone pellets content) compressed at 6 kN were set for the stability for 3 months in three different stability chambers. The appearance of MUPS tablets were found to be unchanged even at the end of 3 months in all stability conditions except 40°C/75%RH, where the color of tablets becomes slightly yellowish, which is negligible. The color change might be related to the excipients, as after 3 months at 40°C/75%RH, the assay of oxycodone was found 97.2%, which is close to the initial value (Table 4). The LOD value was increased slightly from its initial value in all stability conditions (Table 4). No significant change in the assay of oxycodone was observed from the storage conditions (Table 4), which reflects that the formulated MUPS tablets are stable. In each month, the dissolution of oxycodone MUPS tablets was performed for the samples stored in three different conditions. The  $t_{50\%}$ ,  $t_{80\%}$ ,  $Q_8$ , release rate constant ( $k$ ), and diffusion exponent ( $n$ ) at different time intervals showed no major difference over the stability period (Table 4). The calculation was performed based on the following equations:

$$t_{50\%} = (0.5/k)^{1/n}$$

$$t_{80\%} = (0.8/k)^{1/n}$$

where  $k$  is the release rate constant and  $n$  is the diffusion exponent. The values of  $k$  and  $n$  were determined graphically from the following equation (Siepmann & Peppas, 2001):

$$Qt/Q_{\infty} = k \cdot tn$$

where  $Qt/Q_{\infty}$  is the fraction of drug released at time  $t$ ,

$$\log (Qt/Q_{\infty}) = \log k + n \cdot \log t.$$

To study release kinetics, a graph is plotted between log cumulative percentage of drug release ( $\log (Qt/Q_{\infty})$ ) versus log time ( $\log t$ ).

## CONCLUSION

Oxycodone pellets coated with aqueous EC dispersion (Surelease E-7-19050) were incorporated into a multiple-unit pellet system providing consistent drug release profiles. Inclusion of 70% cushioning plastically deforming excipient microcrystalline cellulose (Comprecel M102) into the MUPS tablets and application of compression force between 3 and 6 kN resulted in similar dissolution of active substance in comparison with reference matrix tablets. The physical and chemical parameters of the oxycodone MUPS tablets were found consistent over the stability period. The results generated in this study showed that the selected excipients and manufacturing process is suitable to design a new, stable, oxycodone, MUPS, extended-release formulation.

## ACKNOWLEDGMENT

The study was supported by the Ministry of Education, Science, Research and Sport of the Slovak Republic within project No. Req-00357-0001 „Research and development of active pharmaceutical ingredients by stereoselective processes including development of finished dosage forms.“

## References

---

- [1] Dey NS, Majumdar S, Rao MEB. Multiparticulate drug delivery systems for controlled release. *Trop J Pharm Res.* 2008; 7: 1067-1075.
- [2] Uros K, Sasa B, Igor L et al. Determining the polymer threshold amount for achieving robust drug release from HPMC and HPC matrix tablets containing a high dose BCS class 1 model drug: in vitro and in vivo studies. *AAPS PharmSciTech.* 2014; 16: 398-406.
- [3] Jedinger N, Khinast J, Roblegg E et al. The design of controlled release formulations resistant to alcohol induced dose dumping-a review. *Eur J Pharm Biopharm.* 2014; 87: 217-226.
- [4] Dashevsky A, Koller K, Bodmeier R. Compression of pellets coated with various aqueous polymer dispersions. *Int J Pharm.* 2004; 279: 19-26.
- [5] Fukui S, Yano H, Yada S, Mikkaichi T, Minami H. Design and evaluation of an extended release matrix tablet formulation, the combination of Hypromellose acetate succinate and hydroxypropylcellulose. *Asian J Pharm Sci.* 2017; 12: 149-156.
- [6] Rajabi SAR, Farrel TP. Aqueous polymeric coatings for pharmaceutical dosage forms. Eds McGinity J.W. and Fetton LA; 2008.
- [7] Bhad ME, Abdul S, Jaiswal SB, Chandewar AV, Jain JM, Sakarkar M. *Int J PharmTechRes.* 2010; 2: 847-855.
- [8] Vetchý D, Kopecká M, Vetchá M, Franc A. Modely in vitro-in vivo vo vývoji liečiv. *Chem Listy.* 2014; 108: 32-39.
- [9] Al-Hashimi N, Begg N, Alany RG, Hassanin H, Elshaer A. Oral modified release multiple unit particulate systems: Compressed pellets, microparticles and nanoparticles. *Pharmaceutics.* 2018; 10 (1-23).
- [10] Siepmann J., Peppas NA. Modeling of drug release from delivery systems based on hydroxypropyl methylcellulose (HPMC). *Adv Drug Delivery Rev.* 2001; 48: 139-157.

# *In Vitro* Pro-Glycative Effects of Resveratrol and Caffeic Acid

Original research article/Review

Kurin E.✉, Mučaji P., Nagy M.

*Department of Pharmacognosy and Botany, Faculty of  
Pharmacy, Comenius University in Bratislava,  
Bratislava, Slovak Republic*

Received 8 February, 2019, accepted 20 March, 2019

**Abstract** Resveratrol and caffeic acid belong to plant polyphenols and are known for their antioxidant effects. The aim of our research was to study their impact on Maillard reaction. This one occurs when the reducing saccharides react with amino groups of biomolecules including proteins, alter their protein conformation and transform to the variety of advanced glycation end products (AGEs). AGEs exhibit browning and generate fluorescence. There exist expectations that this oxidative protein glycosylation could be prevented by antioxidants. In this study, we incubated bovine serum albumin (BSA) with glucose for 7 days at 37°C and measured characteristic fluorescence and UV absorbance of the formed AGEs. Surprisingly, resveratrol and caffeic acid enhanced transformation of BSA to glycation products, which was confirmed either when cupric Cu(II) or ferric Fe(III) ions in nanomolar concentration were added to the system as pro-oxidant agent.

**Keywords** Protein glycation – BSA – AGEs – caffeic acid – resveratrol

## INTRODUCTION

Polyphenols belong to a large and heterogeneous group of phytochemicals. They are present in food such as tea, coffee, wine, cereal grains, vegetables and fruits. The structural diversity of polyphenols extends from simple monophenolic substances (*e.g.*, *p*-hydroxycinnamic acid) to large polymeric macromolecules like proanthocyanidins and ellagitannins (Hanhineva, 2010). Recently, polyphenolic compounds have shown their biological activities linking to human health benefits, such as antioxidant, cardioprotective, anticancer, antiinflammatory, antiaging and antimicrobial properties (Xia et al., 2010, Pascual-Teresa et al., 2010, Kurin et al. 2012a). Resveratrol possesses some of these effects. There is growing evidence that resveratrol can prevent or delay the onset of cancer, heart disease, ischemic and chemically induced injuries, diabetes, pathological inflammation and viral infection (Baur & Sinclair, 2006, Kurin et al, 2013). Caffeic acid has been studied due to its antibacterial, antifungal, antiviral and antiproliferative properties (Matus, 2010). Both, resveratrol and caffeic acid are known as antioxidant agents (Wang et al., 1999, Kurin et al. 2012b). Well-known antioxidant effect of both molecules is connected with the protection from reactive oxygen species

(ROS). ROS are continuously produced during normal physiological events; there should be a balance between the generation and inactivation of ROS by the functional antioxidant system in an organism. ROS are overproduced under pathological conditions and the result is an oxidative stress, which leads to different oxidative modifications of cellular membranes or intracellular molecules (Gülçin, 2006). However, the same polyphenols can act as pro-oxidant under certain experimental conditions, for example, depending on the concentration, or source of free radicals (Alarcón De La Lastra & Villegas, 2007) and particularly in the presence of transition metal ions such as iron or copper (Bhat et al., 2007). Resveratrol can act as a pro-oxidant of DNA through reduction of ADP-Fe(III) (Miura et al., 2000) and also by switching to pro-oxidant in the presence of Cu(II) by the ROS generation (Alarcón De La Lastra & Villegas, 2007, Hadi et al., 2010). Similar effects were observed for caffeic acid as well (Bhat et al., 2007, Fan et al., 2009). Caffeic acid accelerated LDL oxidation rate in the propagation phase, which means that it exerts pro-oxidant activities in free radical chain reactions such as lipid peroxidation (Yamanaka et al., 1997).

\* E-mail: elena.kurin@uniba.sk  
© European Pharmaceutical Journal

Oxidation of polyphenols produces  $O_2$ ,  $H_2O_2$  and a complex mixture of semiquinones and quinones, which are potentially cytotoxic (Halliwell, 2008). Formation of pro-oxidant molecules has been observed in model systems during the early phases of Maillard browning (López-Galilea et al., 2006). Highly reactive radicals are formed in the early stages of the Maillard reaction just prior to the Amadori rearrangement and their disappearance is accompanied by a gradual development of browning (Nicoli, 1999). Reducing saccharides react with amino groups of biomolecules including proteins, lipids, and nucleic acids during Maillard reaction to form Schiff bases. These ones in turn undergo a transformation to the variety of AGEs (Fatima, 2008). Increasing protein glycation and the gradual build-up of AGEs in body tissues caused by hyperglycaemia play an important role in the pathogenesis of diabetic complications (Ahmed, 2005). In this study, we incubated bovine serum albumin (BSA) with glucose and measured characteristic fluorescence and UV/VIS absorbance of the created AGEs. Effects of resveratrol and caffeic acid were examined in this system with or without the presence of cupric or ferric ions as known pro-oxidant agents.

## MATERIAL AND METHODS

### Incubation of BSA with glucose

The reaction was carried out under the conditions as reported by Morimitsu et al. (1995) with some modifications. The reaction mixture was made of 250 mg D-(+)-glucose (ACS reagent, Sigma-Aldrich, China) and 25 mg bovine serum albumin (pH 7,  $\geq 98\%$ , Sigma-Aldrich, USA) in 2.5 ml sodium phosphate buffer (PBS, 67 mM, pH 7.2) containing  $Na_2HPO_4 \times 12 H_2O$  and  $NaH_2PO_4 \times 2 H_2O$  (p.a., Centralchem, Slovakia). Mixture was incubated at 37°C for 7 days with or without the tested compound, diluted with distilled water in 2.5 ml. Samples (100  $\mu$ M): caffeic acid (CA,  $\geq 98\%$ , Sigma-Aldrich, USA) and resveratrol (Re,  $\geq 99\%$ , Sigma-Aldrich, USA) were used with aminoguanidin (AG,  $\geq 98\%$ , Sigma-Aldrich, USA) as a positive control. Cupric ions ( $CuSO_4 \times 5 H_2O$ , Lachema, Czech Republic) or ferric ions ( $FeSO_4 \times 7 H_2O$ , Lachema, Czech Republic) (3.906 nM) were added to another tested group and were incubated in the same way.

### Fluorescence measurement

The formation of fluorescent AGEs was assessed by characteristic fluorescence of the glycated BSA and was measured at 370 nm excitation wavelength and 440 nm emission one according Wu et al. (2009) using Tecan Infinite M200 (Tecan AG, Austria) microplate reader and 96-well Nunc PP black (0.5 ml, round bottom) microplates. The value (%) of glycation inhibition by different concentrations of the tested polyphenols was calculated as follows:  $[1 - (\text{fluorescence of the test group}/\text{fluorescence of the control group})] \times 100$ . All measurements were done in quadruplicate.

### UV absorbance measurement

Browning of the samples of different concentration were recorded by their absorbance in 96-well Greiner UV-Star microplates (Greiner-Bio One GmbH, Germany) with Tecan Infinite M200 microplate reader (Tecan AG, Austria) at 420 nm according to Morales & Jiménez-Pérez (2001). All the measurements were done in quadruplicate.

### Statistical analysis

All the data were expressed as mean  $\pm$  SD. Differences between the groups were examined for statistical significance using the Student's *t*-test. A *p*-value less than 0.05 was considered as significant.

## RESULTS AND DISCUSSION

It is now well recognized that the reaction of reducing saccharides with proteins can cause marked alterations in protein conformation. Several investigators have shown that reaction of saccharides and dialdehydes with protein can also lead to the formation of structures showing strong emission between 400 and 500 nm, when excited at a wavelength of 370 nm (Fatima et al., 2008, Plaza et al. 2010). This method is different from the fluorescence spectroscopy of BSA excited at 295 nm and emission collected between 260 and 400 nm, where intrinsic fluorescence of albumin are observed (Dufour & Dangles, 2005).

Fig. 1 shows the fluorescence spectra of BSA solutions in the absence and presence of glucose in PBS at pH 7.2 and 370 nm excitation wavelength. We observed only a small increase in the BSA fluorescence intensity in the presence of glucose as compared to the untreated sample.

However, after 7 days of incubation with glucose, fluorescence intensity was measured at 370 nm excitation and 440 nm emission wavelengths. A significant increase of relative fluorescence (BSA fluorescence =  $7\ 399.75 \pm 850.43$  vs. BSA fluorescence treated with glucose =  $19\ 055.00 \pm 1\ 135.85$ ,  $p < 0.001$ ) was observed. This can be caused by new fluorophore formation (Fatima et al., 2008). Protein glycation initiated by a nucleophilic addition reaction between a free amino group of a protein and a carbonyl group of a reducing saccharide forms a reversible Schiff base. This reaction can occur over a period of hours, and once formed, the labile Schiff base rearranges to a more stable ketoamine or Amadori product. It needs a period of days to be formed and then it is practically irreversible. Glycated proteins can undergo further reactions giving rise to AGEs. AGEs exhibit browning and generate fluorescence.

There exist expectations that whereas the protein glycosylation is an oxidative reaction, antioxidants should be able to prevent this reaction. Study of Asgary describes an inhibition of haemoglobin glycation by quercetin, rutin and kaempferol (Asgary et al., 1999). Urios measured inhibition

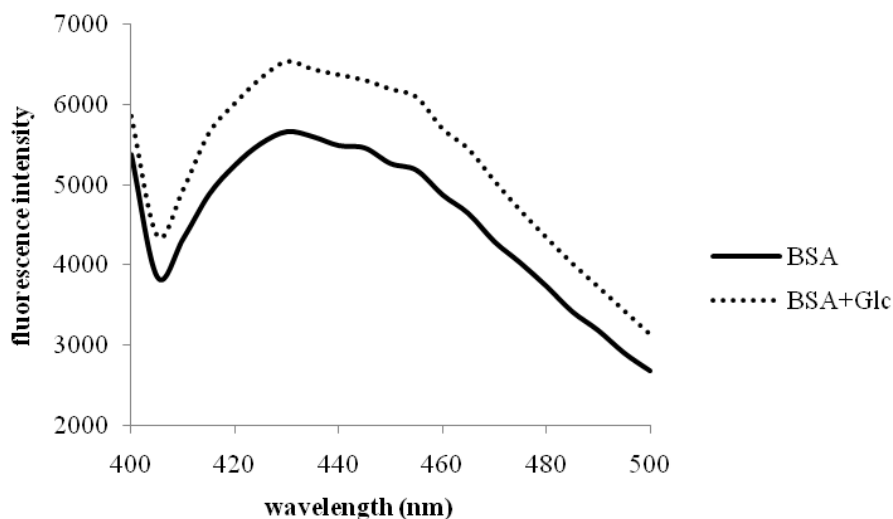


Figure 1. Fluorescence spectra of BSA solutions in the absence (—) and presence (.....) of glucose in PBS pH 7.2, without incubation,  $\lambda_{\text{exc}} = 370 \text{ nm}$ ,  $\lambda_{\text{em}} = 440 \text{ nm}$ .

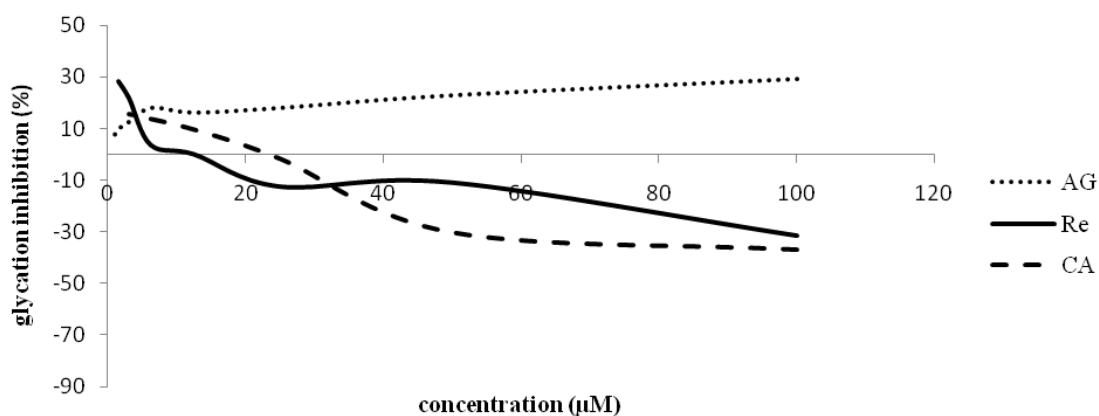


Figure 2. Glycation inhibition (%) of  $100 \mu\text{M}$  samples (AG – aminoguanidin, CA – caffeic acid, Re – resveratrol) after 7 days incubation with BSA and glucose at  $37 \text{ }^\circ\text{C}$ ,  $\lambda_{\text{exc}} = 370 \text{ nm}$ ,  $\lambda_{\text{em}} = 440 \text{ nm}$ .

effects of some monomeric and oligomeric flavonoids on pentosidine formation in collagen incubated with glucose (Urios et al., 2007). Morimitsu tested methanol extracts of 34 types of spices for the inhibitory activity of the AGEs formation, and even though most of these were inhibiting, some of them accelerated the formation of AGEs (i.e., mustard, tarragon, cinnamon, cardamom, cumin, coriander, celery) (Morimitsu et al., 1995).

Fig. 2 shows the results of 7 days of incubation of BSA with glucose in the presence of resveratrol, caffeic acid and aminoguanidine, respectively. Aminoguanidine, which acts as a nucleophilic scavenger by blocking the first step in the glycation (Lunceford & Gugliucci, 2005), was used as a positive control. Surprisingly, resveratrol and caffeic acid enhanced the transformation of BSA to glycation-like products in concentration dependent manner.

Many polyphenols (flavonoids, caffeic acid) possess the ability to reduce transition metal ions, and consequently, to act as pro-oxidants (Simić et al., 2007). It was also

described that Cu(II)-induced pro-oxidant activity of phenolics proceeds *via* intra- and inter-molecular electron transfer reactions accompanying ROS formation, and a copper complexation followed by an oxidation of resveratrol analogues (e.g., 3,4-dihydroxystilbene) ended up with quinone production (Apak et al., 2007). As shown in the Fig. 3, the combination of polyphenols with metals leads to the concentration dependent formation of BSA glycated/transformed products. Only the combination of ferric ions with resveratrol results in a slight inhibition of the glycation. The increase in proglycative (= pro-oxidative) activity of phenolics in the presence of Fe(III) or Cu(II) is primarily associated with their ability to reduce metal ions. Subsequently, Fe(III) and Cu(II) can be re-oxidized in Fenton-type reactions leading to the production of hydroxyl radical and other ROS. The antioxidant/pro-oxidant activities of phenolics are determined by many factors: the concentration and nature of transition metal ion(s) and the concentration and pH of phenolics (Apak et al., 2007).

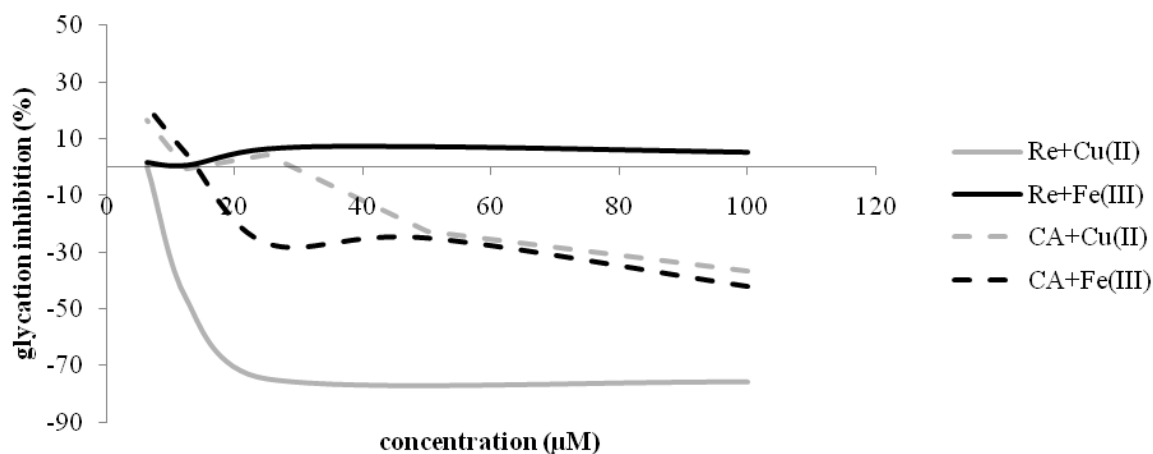


Figure 3. Glycation inhibition (%) of polyphenols at 100  $\mu\text{M}$  (CA – caffeic acid, Re – resveratrol) with metal catalyst Cu(II) or Fe(III) (3.906 nM) after 7 days incubation with BSA and glucose at 37 °C,  $\lambda_{\text{exc}} = 370 \text{ nm}$ ,  $\lambda_{\text{em}} = 440 \text{ nm}$ .

The Maillard reaction produces a variety of intermediate products and the final brown pigments (Lertittikul et al., 2007). Intensity of brown colour is often used as an indicator of the extent of the reaction. It symbolizes an advanced stage of the Maillard reaction (Plaza et al., 2010). Because of the variety and the complexity of Maillard reaction products, it is usually admitted to classify them into early (or precursors), advanced and final products. Following this classification, the intensity of non-enzymatic browning was generally based on the changes in absorbance at 294–297 nm, 320–350 nm and 420–450 nm, respectively.

Cu(II) or Fe(III) ions were used as a catalyst for pro-oxidant action of the polyphenols in the presence of protein and glucose. As Fig. 4 shows, we observed an absorbance increase of samples of BSA + glucose and resveratrol (100  $\mu\text{M}$ ) or caffeic acid (100  $\mu\text{M}$ ) when incubated with ferric ions. Only caffeic acid with cupric ions did not show any impressive changes in the *in vitro* glycation model. An increased absorbance in the 340–360 nm regions should correspond to the formation of heterocyclic derivatives and intermediate water-soluble compounds (reductones, amino-reductones or pre-melanoidins). Conversely, absorbance values at 420 nm should correspond to the formation of brown pigments or melanoidins (Billaud et al., 2004).

The absorbance increase at 420 nm is used as an indicator for the browning development in the final stage of the browning reaction. As Fig. 5 and Fig. 6 show, we observed an absorbance increase in the reaction mixture of BSA depending on the concentration of polyphenols and the presence of metals after 7 days of incubation. Fluorescent compounds – AGEs – are also possible precursors of brown pigments. The higher concentration of saccharide used, the higher the increase in browning was found (Billaud et al., 2005). We observed, at a stable concentration of glucose and varying concentration of polyphenols, a higher content of resveratrol or caffeic acid in the presence of pro-oxidant metal ions led to a higher increase

in browning. Thus, we can postulate that the presence of brown pigments are the Maillard reaction products in the reaction mixtures.

Results of fluorescence and absorbance measurements indicated that the Maillard reaction had progressed to advanced stages in the amino acid–glucose reaction. However, coloured and fluorescent compounds need not be identical and fluorogens may be precursors of brown pigments showing a shorter induction period (Morales & Jiménez-Pérez, 2001).

In our work, using fluorescence measurement of AGEs, we observed that resveratrol and caffeic acid incubated with glucose and BSA accelerated formation of AGEs after 7 days at 37°C. The nanomolar presence of Cu(II) confirmed the pro-glycative effects of resveratrol and caffeic acid. Presence of Fe(III) with caffeic acid increased the formation of AGEs, but there was observed slight inhibition of the glycation with resveratrol. The observed pro-glycative effects of polyphenols can be based on the pro-oxidant activity of these. Resveratrol undergoes oxidation in the presence of Cu(II). The oxidative product of resveratrol is a dimer, which might be formed by dimerization of resveratrol phenoxyl radical as a result of the reductive activation of molecular oxygen (Alarcón De La Lastra & Villegas, 2007). Caffeic acid could dissociate to form a phenoxide, which chelates Cu(II) ions as bidentate ligand and undergoes intramolecular electron transfer to form an *o*-hydroxyphenoxyl radical (semiquinone radical). The radical intermediate was also proven by the formation of the caffeic acid dimer (furofuran bislacton) in the presence of Cu(II) ions (Fan et al., 2009). Pro-oxidant action of plant polyphenols may be an important mechanism of their anti-cancer or apoptosis-inducing properties (Hadi et al., 2010), and therefore, our results can be useful for the next research of their exact mechanism of action. However, in multicomponent mixtures, the risk of the pro-oxidative and pro-glycative effect is present, when phenolics are combined with even

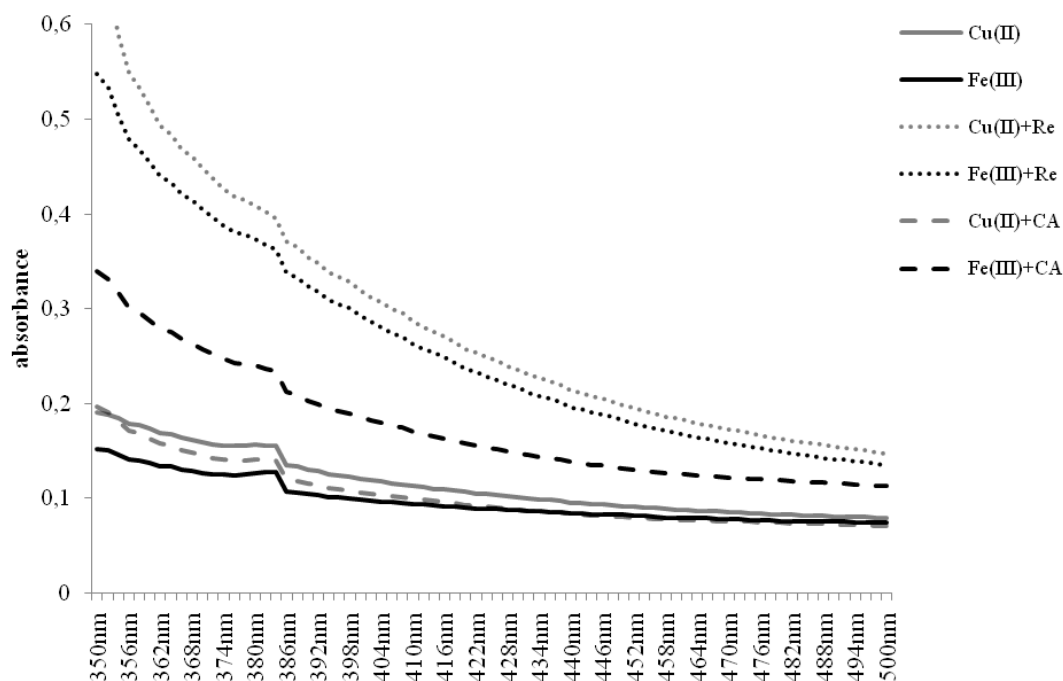


Figure 4. Absorbance of polyphenols (CA – caffeic acid, 100  $\mu$ M, Re – resveratrol, 100  $\mu$ M) with metal catalyst Cu(II) or Fe(III), always 3.906 nM, after 7 days incubation with BSA and glucose at 37  $^{\circ}$ C.

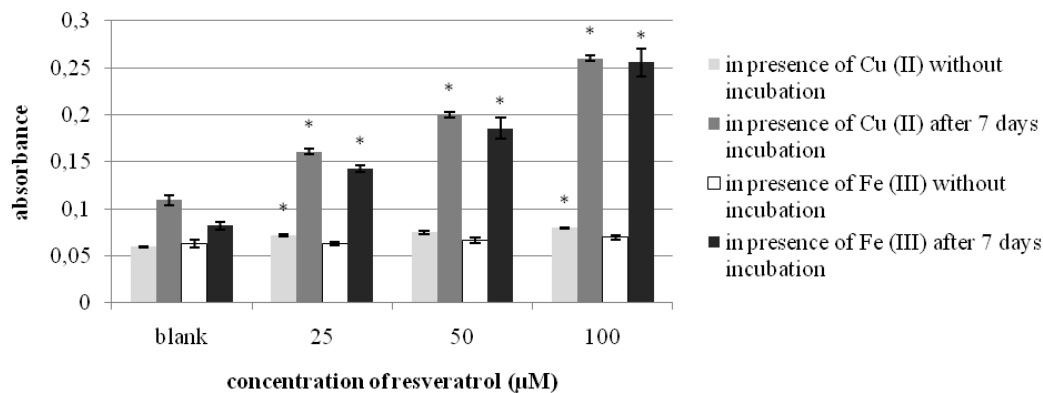


Figure 5. Absorbance of resveratrol (100  $\mu$ M) at 420 nm with metal catalyst Cu(II) or Fe(III), always 3.906 nM, without or after 7 days incubation with BSA and glucose at 37  $^{\circ}$ C. \* $p$  < 0.05 (error bars = mean  $\pm$  SD).

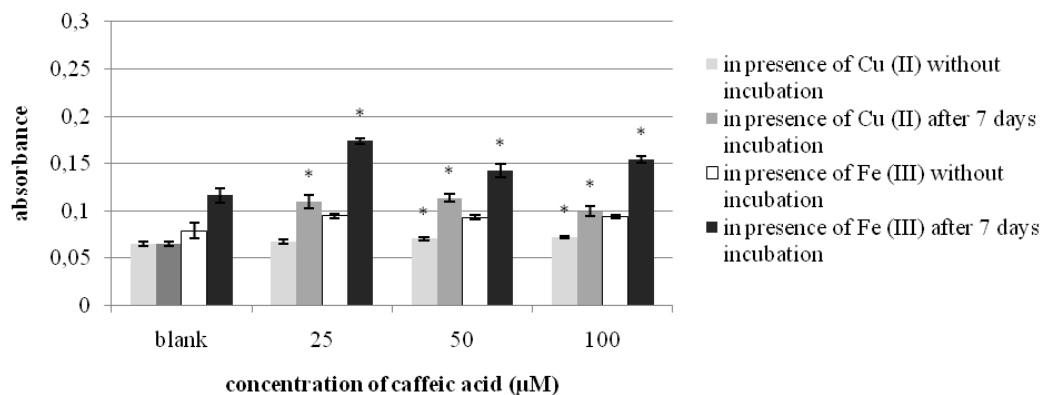


Figure 6. Absorbance of caffeic acid (100  $\mu$ M) at 420 nm with metal catalyst Cu(II) or Fe(III), always 3.906 nM, without or after 7 days incubation with BSA and glucose at 37  $^{\circ}$ C. \* $p$  < 0.05 (error bars = mean  $\pm$  SD).

nanomolar concentration of transition metal ions. This should be considered when multiminerall food supplements with natural substances are made.

## CONCLUSION

In conclusion, resveratrol and caffeic acid are well known antioxidants. However, in certain conditions, they can act as pro-oxidants and trigger pro-glycative action in the presence of glucose and amino acid. We found out that resveratrol and caffeic acid alone, as well as in the nanomolar presence of Cu(II) or Fe(III) ions, when incubated with glucose and BSA after 7 days, can initiate Maillard reaction and accelerate

the formation of AGEs. We confirmed this by fluorescence measurements of AGEs, which act as a fluorophore, and by specific absorbance increase following the browning development. Whereas glycation can negatively alter protein activity, folding or degradation, it is important to research the conditions, which leads to the pathological formation of AGEs.

## ACKNOWLEDGMENTS

This work was supported by the Slovak Ministry of Education grant number VEGA 1/029/16, VEGA 1/0359/18 and ITMS 26240120023 project.

## References

- [1] Ahmed N. Advanced glycation endproducts—role in pathology of diabetic complications. *Diabetes Res Clin Pract.* 2005;67:3–21.
- [2] Alarcón De La Lastra C, Villegas I. Resveratrol as an antioxidant and pro-oxidant agent: Mechanisms and clinical implications. *Biochem Soc Trans.* 2007; 35:1156–1160.
- [3] Apak R, Güçlü K, Demirata B, et al. Comparative evaluation of various total antioxidant capacity assays applied to phenolic compounds with the CUPRAC assay. *Molecules.* 2007;12:1496–1547.
- [4] Asgary S, Naderi G, Sarrafzadegan N, et al. Anti-oxidant effect of flavonoids on hemoglobin glycosylation. *Pharm Acta Helv.* 1999;73:223–226.
- [5] Baur JA, Sinclair DA. Therapeutic potential of resveratrol: The in vivo evidence. *Nat Rev Drug Discovery.* 2006;5:493–506.
- [6] Benjakul S, Lertittikul W, Bauer F. Antioxidant activity of Maillard reaction products from a porcine plasma protein–sugar model system. *Food Chem.* 2005;93:189–196.
- [7] Bhat SH, Azmi AS, Hadi SM. Prooxidant DNA breakage induced by caffeic acid in human peripheral lymphocytes: Involvement of endogenous copper and a putative mechanism for anticancer properties. *Toxicol Appl Pharmacol.* 2007;218:249–255.
- [8] Billaud C, Maraschin C, Nicolas J. Inhibition of polyphenoloxidase from apple by Maillard reaction products prepared from glucose or fructose with L-cysteine under various conditions of pH and temperature. *Lebensm Wiss u Technol.* 2004;37:69–78.
- [9] Dufour C, Dangles O. Flavonoid–serum albumin complexation: determination of binding constants and binding sites by fluorescence spectroscopy. *Biochim Biophys Acta.* 2005;1721:164–173.
- [10] Fan GJ, Jin XL, Qian YP, et al. Hydroxycinnamic acids as DNA-cleaving agents in the presence of Cu II ions: Mechanism, structure-activity relationship, and biological implications. *Chem Eur J.* 2009;15:12889–12899.
- [11] Fatima S, Jairajpuri DS, Saleemuddin M. A procedure for the rapid screening of Maillard reaction inhibitors. *J Biochem Biophys.* 2008;70:958–965.
- [12] Gülçin I. Antioxidant activity of caffeic acid (3,4-dihydroxycinnamic acid). *Toxicology.* 2006;217:213–220.
- [13] Hadi SM, Ullah MF, Azmi AS, et al. Resveratrol mobilizes endogenous copper in human peripheral lymphocytes leading to oxidative DNA breakage: A putative mechanism for chemoprevention of cancer. *Pharm Res.* 2010;27:979–988.
- [14] Halliwell B. Are polyphenols antioxidants or pro-oxidants? What do we learn from cell culture and in vivo studies? *Arch Biochem Biophys.* 2008;476:107–112.
- [15] Hanhineva K, Törrönen R, Bondia-Pons I, et al. Impact of dietary polyphenols on carbohydrate metabolism. *Int J Mol Sci.* 2010;11:1365–1402.
- [16] Kurin E, Atanasov AG, Donath O, Heiss EH, Dirsch VM, Nagy M. Synergy study of the inhibitory potential of red wine polyphenols on vascular smooth muscle cell proliferation. 2012a;78:772–778.
- [17] Kurin E, Mučaji P, Nagy M. In vitro antioxidant activities of three red wine polyphenols and their mixtures: an interaction. *Molecules.* 2012b;17:14336–14348.
- [18] Kurin E, Fakhrudin N, Nagy M. eNOS Promoter Activation by Red Wine Polyphenols: an Interaction Study
- [19] *Acta Fac Pharm Univ Comen.* 2013;60:27–33.
- [20] Lertittikul W, Benjakul S, Tanaka M. Characteristics and antioxidative activity of Maillard reaction products from a porcine plasma protein–glucose model system as influenced by pH. *Food Chem.* 2007;100:669–677.
- [21] López-Galilea I, Andueza S, Di Leonardo I, De Peña MP, Cid C. Influence of torrefacto roast on antioxidant and pro-oxidant activity of coffee. *Food Chem.* 2006;94:75–80.
- [22] Lunceford N, Gugliucci A. Ilex paraguariensis extracts inhibit AGE formation more efficiently than green tea. *Fitoterapia.* 2005;76:419–427.
- [23] Matus MH, Domínguez Z, Salas-Reyes M, Hernández J, Cruz-Sánchez S. Conformational study of caffeic acid derivatives. *J Mol Struct. Theochem.* 2010;953:175–181.
- [24] Miura T, Muraoka S, Ikeda N, Watanabe M, Fujimoto Y. Antioxidative and prooxidative action of stilbene derivatives. *Basic Clin Pharmacol Toxicol.* 2000;86:203–208.
- [25] Morales FJ, Jiménez-Pérez S. Free radical scavenging capacity of Maillard reaction products as related to colour and fluorescence. *Food Chem.* 2001;72:119–125.

- [26] Morimitsu Y, Yoshida K, Esaki S, Hirota A, Protein glycation inhibitors from thyme (*Thymus vulgaris*). *Biosci Biotechnol.* 1995;59:2018–2021.
- [27] Nicoli MC, Anese M, Parpinel M. Influence of processing on the antioxidant properties of fruit and vegetables. *Trends Food Sci Tech.* 1999;10:94–100.
- [28] Pascual-Teresa S, Moreno DA, García-Viguera C. Flavanols and anthocyanins in cardiovascular health. A review of current evidence. *Int J Mol Sci.* 2010;11:1679–1703.
- [29] Plaza M, Amigo-Benavent M, del Castillo MD, Ibáñez E, Herrero M. Neof ormation of antioxidants in glycation model systems treated under subcritical water extraction conditions. *Food Res. Int.* 2010;43:1123–1129.
- [30] Simić A, Manojlović D, Šegan D, Todorović M. Electrochemical behavior and antioxidant and prooxidant activity of natural phenolics. *Molecules.* 2007;12:2327–2340.
- [31] Urios P, Grigorova-Borsos AM, Sternberg M. Flavonoids inhibit the formation of the cross-linking AGE pentosidine in collagen incubated with glucose, according to their structure. *Eur J Nutr.* 2007;46:139–146.
- [32] Wang M, Jin Y, Ho CT. Evaluation of resveratrol derivatives as potential antioxidants and identification of a reaction product of resveratrol and 2,2-diphenyl-1-picrylhydrazyl radical. *J Agric Food Chem.* 1999;47:3974–3977.
- [33] Wu JW, Hsieh CL, Wang HY, Chen HY. Inhibitory effects of guava (*Psidium guajava* L.) leaf extracts and its active compounds on the glycation process of protein. *Food Chem.* 2009;113:78–84.
- [34] Xia EQ, Deng GF, Guo YJ, Li HB. Biological activities of polyphenols from grapes. *Int J Mol Sci.* 2010;11: 622–646.
- [35] Yamanaka N, Oda O, Nagao S. Prooxidant activity of caffeic acid, dietary non-flavonoid phenolic acid, on Cu<sup>2+</sup>-induced low density lipoprotein oxidation. *FEBS Lett.* 1997;405:186–190.

# Dual Loading Of Primaquine And Chloroquine Into Liposome

Original Paper

Miatmoko A.✉, Salim H. R., Zahro S. M., Annuryanti F., Sari R., Hendradi E.

Universitas Airlangga  
Surabaya, East Java, Indonesia

Received 22 January, 2019, accepted 1 October, 2019

**Abstract** Primaquine (PQ) has long been recognized as the only effective drug in the treatment of hepatic stage malaria. However, severe toxicity limits its therapeutical application. Combining PQ with chloroquine (CQ) has been reported as enhancing the former's efficacy, while simultaneously reducing its toxicity. In this study, the optimal conditions for encapsulating PQ-CQ in liposome, including incubation time, temperature and drug to lipid ratio, were identified. Furthermore, the effect of the loading combination of these two drugs on liposomal characteristics and the drug released from liposome was evaluated. Liposome is composed of HSPC, cholesterol and DSPE-mPEG<sub>2000</sub> at a molar ratio of 55:40:5 and the drugs were loaded by means of the transmembrane pH gradient method. The particle size,  $\zeta$ -potential and drug encapsulation efficiency were subsequently evaluated. The results showed that all liposome was produced with a similar particle size and  $\zeta$ -potential. PQ and CQ could be optimally loaded into liposome by incubating the mixtures at 60°C for 20 minutes at a respective drug to lipid ratio of 1:3 for PQ and CQ. However, compared to single drug loading, dual-loading of PQ+CQ into liposome resulted in lower drug encapsulation and slower drug release. In conclusion, PQ and CQ can be jointly loaded into liposome with differing profiles of encapsulation and drug release.

**Keywords** Dual loading – primaquine – chloroquine – liposome – release

## INTRODUCTION

Globally, malaria ranks fourth on a scale of life-threatening infectious diseases (Mishra et al., 2017). Shortly after being bitten by a Plasmodium-infected female Anopheles mosquito, the sporozoite accumulated in its salivary glands enters the liver leading to the hepatic phase of malarial infection. This stage is very important since it represents the starting point of erythrocytic-stage malaria and fatal cerebral malaria (Prudêncio et al., 2006). In addition, the latent phase of hypnozoites in the liver often found in *Plasmodium ovale* and *Plasmodium vivax* infection can cause relapses in about 50–80% of malaria sufferers (Chu and White, 2016).

Primaquine (PQ), recognized as the primary treatment for the hepatic phase of malaria (Longley et al., 2016), is an antimalarial pro-drug compound belonging to the 8-aminoquinoline group that actively works against sporozoites, hypnozoites, asexual phases and gametocytes through inhibition of the metabolic activity of mitochondrial parasites and the production of reactive metabolites, which are toxic to cells (Chu and White, 2016; Marcsisin et al., 2016). PQ constitutes a drug with a short half-life, which is rapidly

metabolized by the liver into a carboxylic acid derivative ultimately excreted in the urine. In order to treat malarial infection and prevent relapse, PQ must be administered for a period of 14 days (Karyana et al., 2016). However, although it demonstrates proven efficacy against hepatic phase malaria, PQ can cause methemoglobinemia and hemolysis in patients presenting glucose-6-phosphate dehydrogenase (G6PD) deficiency (Kedar et al., 2014; Marcsisin et al., 2016; Recht et al., 2015). Furthermore, prolonged drug therapy can also induce abdominal cramps, nausea and vomiting (Jong and Nothdurft, 2001). Such side effects can potentially undermine the adherence of patients to the prescribed drug regime resulting in low PQ levels in the blood. It has been known that low doses administered in the cases of high parasitemia can induce drug resistance, which represents a significant problem in the control program relating to malaria (Gonzalez-Ceron et al., 2015).

It has been previously reported that the administering of a single dose of PQ combined with chloroquine (CQ) constitutes an effective method of treating malaria (Gonzalez-Ceron et

\* E-mail: andang-m@ff.unair.ac.id

© European Pharmaceutical Journal

al., 2015). CQ is a 4-aminoquinoline compound frequently employed in managing the erythrocytic stage of malaria (World Health Organization, 2015). The combination of administering CQ tablets for three consecutive days and PQ tablets for 14 days proved effective in treating erythrocytic phase malarial infection and preventing its reoccurrence (Gonzalez-Ceron et al., 2015; World Health Organization, 2015). In addition, the specific metabolite interaction between PQ and CQ reduced the toxicity of the former without compromising its efficacy against parasites (Fasinu et al., 2016). This study demonstrates that CQ can inhibit PQ metabolism by means of CYP2D6, thus reducing the formation of active metabolites, which are toxic to erythrocytes.

Developing an effective anti-malarial treatment, especially one countering hepatic phase infection, which could involve the use of liposome to deliver PQ and CQ is important. Through the encapsulating of a combination of PQ and CQ in liposome, PQ will prove effective in treating acute infections caused by sporozoites and/or malaria relapse during the latent phase of hypnozoites in the liver, while the CQ loaded in liposomes can provide prophylactic therapy for erythrocytic phase infection. During hepatic phase infection, sporozoites are known to specifically attack hepatocytes, rather than other non-parenchymal cells present in the liver. Therefore, the specific form of delivery intended for hepatocytes will prove useful in enhancing the efficacy and decreasing the toxicity of PQ and CQ during the treatment of malaria.

Liposome constitutes a vesicular formation consisting of a phospholipid bilayer surrounding an inner water phase, which provides optimal protection for drugs against diffusion and external factors (Kohli et al., 2014). Liposome with a particle size within a 125–175 nm range can concentrate densely in hepatic tissue because of the presence of an intercellular gap or fenestrae within endothelial cells in the liver sinusoid (Baratta et al., 2009). Moreover, PEGylation of liposome can minimize drug clearance from the body and produce drugs that circulate for extended periods in the bloodstream (Barenholz, 2012). Therefore, the drug will largely accumulate in hepatocytes.

The use of liposome as a carrier for PQ and CQ has been widely reported (Qiu et al., 2008; Stela Santos-Magalhães and Carla Furtado Mosqueira, 2009; Stensrud et al., 2000), while, in contrast, no previous research on its application to a combination of both drugs has been conducted. Consequently, in this study, a dual drug loading of PQ and CQ in liposome was prepared. However, it has been reported that PQ interacts strongly with the polar headgroup region of dimyristoylphosphatidylcholine (DMPC) in the membrane bilayer forming the space intercalation between the lipids (Basso et al., 2011). Turning to the results, perturbation in the lipid order occurred, which increased the fluidity of the liposomal membrane. CQ has been reported to rigidify the dipalmitoylphosphatidylcholine (DPPC) liposomal membrane by increasing molecular packing in the lipid (Ghosh et al., 1995). This observation is supported by that

of another study incorporating the use of Amodiaquine, a 4-aminoquinoline drug similar in structure to CQ, as the drug model. Amodiaquine demonstrated electrostatic and hydrophobic interactions with DPPC in the headgroup region of the liposomal bilayer, thus increasing the lipid order (Barroso et al., 2015). These contradictory effects of PQ and CQ addition may affect their dual loading and the release of liposome.

It is generally accepted that, in order to achieve high drug accumulation in the target tissue, the drug should be stably encapsulated in liposome during distribution throughout the entire body, either by the use of a sturdy bilayer membrane (Barenholz, 2012; Kokkona et al., 2000) or the formation of drug aggregates in the intraliposomal phase (Barenholz, 2012; Lasic et al., 1992; Miatmoko et al., 2017). This study was aimed to determine the effect of the loading combination of PQ+CQ compared to a single drug, on the physicochemical characteristics and rate of release of PQ and CQ from liposome. PQ and CQ were loaded into liposome consisting of lipid with high rigidity, which was hydrogenated soy phosphatidylcholine (HSPC). It was found that dual loading PQ with CQ affected drug encapsulation efficiency and drug release from liposome.

## MATERIALS AND METHODS

### Materials

For the purposes of this study, primaquine bisphosphate (PQ) was purchased from Sigma-Aldrich Inc. (Rehovot, Israel), while chloroquine diphosphate (CQ) was a product of Sigma-Aldrich® (Gyeonggi-do, South Korea). Hydrogenated soya phosphatidylcholine (HSPC) and methoxy-(polyethylene-glycol)-distearylphosphatidyl-ethanolamine (mPEG-DSPE, PEG mean molecular weight, 2000) were obtained from NOF Inc. (Tokyo, Japan). The cholesterol constituted a product of Wako Pure Chemical Industries Inc. (Osaka, Japan). Potassium dihydrogen phosphate ( $\text{KH}_2\text{PO}_4$ ) and disodium hydrogen phosphate ( $\text{Na}_2\text{HPO}_4$ ) were both products of Merck® (Darmstadt, Germany), while Sephadex® G-50 was obtained from Sigma-Aldrich Inc. (Steinheim, Germany). The organic solvents, that is, chloroform and methanol, were products of Merck® (Darmstadt, Germany). Deionized water (Otsuka Inc., Lawang, Indonesia) was used as water solvent. All other chemicals and reagents were of the highest quality available.

### Determination of optimal incubation for preparation of liposome

Liposome containing a single drug was generated by using CQ as a drug model to determine optimal conditions for drug loading. Liposome was prepared in accordance with the thin-film method (Miatmoko et al., 2016) at a molar ratio of 55:45:5 for HSPC, cholesterol and DSPE-mPEG<sub>2000</sub>, respectively. Each lipid compound was dissolved in chloroform before

Table 1: Formulation of liposome loading combination of PQ and CQ

Component	Formulation				
	P1C0	P0C1	P1C1	P1C3	P1C5
PQ	1.00 mg	-	1.66 mg	0.83 mg	0.55 mg
CQ	-	3.33 mg	1.66 mg	2.48 mg	2.78 mg
HSPC	5.94 mg	5.94 mg	5.94 mg	5.94 mg	5.94 mg
DSPE-mPEG <sub>2000</sub>	1.94 mg	1.94 mg	1.94 mg	1.94 mg	1.94 mg
Cholesterol	2.13 mg	2.13 mg	2.13 mg	2.13 mg	2.13 mg

**Note:**

P1C0, weight ratio of PQ:total lipid (1:10); P0C1, weight ratio of CQ:total lipid (1:3); P1C1, weight ratio of PQ:CQ:total lipid (0.5:0.5:3); P1C3, weight ratio of PQ:CQ:total lipid (0.25:0.75:3); P1C5, weight ratio of PQ:CQ:total lipid (0.17:0.83:3)

appropriate quantities were inserted into a round bottom flask. The chloroform was then completely removed by means of a vacuum rotary evaporator in a water bath (Buchi Rotavapor R-3, Flawil, Switzerland) at 60°C, leading to the formation of a thin dry film in the bottom of the flask. This layer was hydrated with citrate buffer at pH 5.0. In order to prepare homogenous liposome suspension, the mixture was vortexed and subjected to sonication in a waterbath sonicator of approximately 15 minutes' duration. The mixture was passed through a polycarbonate membrane with a pore size of 100 nm by means of an extruder (Avanti<sup>®</sup>, Alabaster, Alabama, US) in order to obtain a homogenous liposome particle size.

The drug loading was conducted by transmembrane pH gradient method, which involved eluting the liposome through a Sephadex<sup>®</sup> G-50 column with phosphate buffer saline (PBS) at pH 7.4. The CQ solution in aquadest was then added at a drug-lipid ratio of 1:5. The drug-liposome mixtures were incubated at specific temperatures, which were 50°C and 60°C, for various incubation periods of 10, 20 and 30 minutes.

### Determination of optimal drug to lipid ratios for the preparation of liposome

In order to determine the optimal drug to lipid ratio for the preparation of liposome, the PQ or CQ was loaded as a single drug component of the liposome. The drug loading was completed by transmembrane pH gradient method, which involved eluting liposome hydrated with citrate buffer pH 5.0 through a Sephadex<sup>®</sup> G-50 column with phosphate buffer saline (PBS) at pH 7.4. The PQ or CQ solution in aquadest was subsequently added at a pre-determined drug-lipid ratio of 1:3, 1:5 or 1:10. The drug-liposome mixtures were incubated at 60°C for 20 minutes. Separation of the liposomal drug from the free drug was achieved by eluting the mixture through a Sephadex<sup>®</sup> G-50 column with PBS at pH 7.4.

The concentration of entrapped PQ or CQ was measured with a UV Spectrophotometer (Shimadzu, Kyoto, Japan) at  $\lambda = 282$  nm or  $\lambda = 330$  nm after lysing with methanol (50% v/v). The encapsulation efficiency was calculated as follows:

$$\text{Percentage of drug loading} = \frac{\text{amount of drug entrapped within liposome}}{\text{total amount of drug}} \times 100\%$$

### Preparation of a liposome loading combination of PQ and CQ

Preparation of a liposome loading combination of PQ and CQ involved processing the lipid components in the manner described above. In order to prepare control liposome containing the drugs, PQ and CQ was added at respective drug:lipid weight ratios of 1:10 and 1:3, while for the liposome loading combination of PQ and CQ, the drugs were added at a weight ratio of 1:3 for total PQ+CQ and lipid, respectively, at a composition shown in Table 1. During the drug loading, the drug-liposome mixtures was incubated at 60°C for 20 minutes.

The entrapped PQ and CQ concentrations were measured with a UV Spectrophotometer (Shimadzu, Kyoto, Japan) using a derivative order 1 method at  $\lambda = 280$  nm or  $\lambda = 346$  nm (data unpublished) for PQ and CQ respectively after lysing the liposomal vesicle with methanol (50% v/v).

### Determination of particle size and $\zeta$ -potential of liposome

In order to determine the particle size and  $\zeta$ -potential of liposome, the sample was diluted appropriately with deionized water. The average particle size and  $\zeta$ -potential of the liposomes were then measured using a cumulative method and electrophoretic mobility with a light scattering photometer (Delsa<sup>™</sup> Nano C Particle Analyzer, Beckman Coulter Inc., Indianapolis, US) at 25°C.

### In vitro drug released from liposome

The *in vitro* study of PQ and CQ released from liposome was conducted by placing a liposome sample in dialysis tubing Spectra Por<sup>®</sup>7 with a molecular weight cut-off (MWCO) of 3,500 (Spectrum Laboratories, Inc., Rancho Dominguez, CA, USA). The dialysis media consisted of 50 mL of PBS at pH 7.4. The study was performed through continuous agitation at a

Table 2: Characteristics of liposome loading CQ prepared at different temperature and period of incubation with drug loaded at a weight ratio of 1:5 for drug and total lipid, respectively

Incubation temperature	Period of incubation	Particle size (nm) <sup>1)</sup>	Polydispersity Index/PDI <sup>1)</sup>	ζ-Potential (mV) <sup>1)</sup>	Entrapment efficiency (%) <sup>1)</sup>
50°C	10 minutes	121.0 ± 6.5	0.30 ± 0.07	-11.3 ± 4.8	17.9 ± 3.2
	20 minutes	123.1 ± 7.5	0.35 ± 0.11	- 5.6 ± 2.0	21.5 ± 4.6
	30 minutes	126.2 ± 14.6	0.27 ± 0.05	-10.9 ± 6.1	15.0 ± 1.9
60°C	10 minutes	122.9 ± 21.4	0.31 ± 0.04	-16.9 ± 3.7	17.5 ± 2.1
	20 minutes	123.4 ± 19.2	0.32 ± 0.08	-23.5 ± 12.2	18.2 ± 2.2
	30 minutes	140.8 ± 30.5	0.26 ± 0.11	-19.8 ± 5.0	16.5 ± 2.8

<sup>1)</sup> Each value represents the mean ± S.D. (n = 3).

speed of 400 rpm in a water bath at 37°C.

At determined sampling points, approximately 2 mL of aliquots were drawn from the media and replaced with the same volume of PBS at pH 7.4. The PQ and CQ concentration was measured spectrophotometrically using a derivative order 1 method at  $\lambda = 280$  nm or  $\lambda = 346$  nm for PQ or CQ respectively. Dilution correction factor was used to calculate the cumulative amount of drug released (Aronson, 1993).

### Statistical analysis

The data existed in triplicate and was presented as the mean ± S.D. The statistical analysis consisted of a one-way ANOVA followed by an LSD post-hoc test, which were performed to determine the significance of the difference. A *P* value less than 0.05 was considered to be statistically significant.

## RESULTS AND DISCUSSION

The characteristics of liposomes are significantly influenced by several factors, including: length of the incubation period, temperature during the incubation period and drug-to-lipid ratio (Qiu et al., 2008). Moreover, the quantity of drug released by liposomes depends predominantly on the physicochemical properties of liposome membrane and its encapsulated drugs (Liang, 2010). In this study, liposomes were prepared for the loading of PQ and CQ. Dual loading these drugs affected both encapsulation and the properties of drug release.

The loading of PQ and CQ into liposome involved remote loading of a drug with a pH gradient using citrate buffer pH 5.0 as the intraliposomal phase and PBS pH 7.4 as the outer phase. The first step was to evaluate the effect of temperature and the incubation period by using CQ as a drug model, since – during clinical therapy – it will be at a higher dose than PQ (World Health Organization, 2015), thus limiting the drug loading capacity of liposome. PQ has different properties to CQ (Qiu et al., 2008; Stensrud et al., 2000), thereby probably resulting in contrasting optimal loading conditions. However, these were undetermined by this study. As shown in Table 2, all liposomes were produced with a similar particle size of approximately 100–150 nm, with a slightly negative charge

of  $\zeta$ - and potential of approximately -15 mV. There was no significant difference in particle size or  $\zeta$ -potential due to the same components of liposome, that is, HSPC, DSPE-mPEG<sub>2000</sub> and cholesterol (Qiu et al., 2008; Yadav et al., 2011). Moreover, the implementation of this transmembrane pH gradient method meant that only approximately 17–22% of the CQ could be loaded into the liposome. There were no significant differences in the encapsulation efficiency of liposome CQ because of the use of varying temperatures in different incubation periods, as shown in Table 2. For further experiments, the incubation of a drug mixture with liposome will be performed at 60°C for 20 minutes, regarded as the highest transition temperature ( $T_m$ ) of liposome component, which is HSPC, at 55°C (Chen et al., 2013). However, it can be seen that the encapsulation efficiency of CQ at a drug:lipid ratio of 1:5 was low.

The optimal drug-to-lipid ratio for the entrapment of PQ and CQ in liposome was determined. A previous study reported that CQ was loaded into liposome at a drug-to-lipid mass ratio of 1:80 (Qiu et al., 2008), while PQ was loaded at one of 1:14 (Stensrud et al., 2000). It proved unfeasible to achieve an efficient drug loading at a very low drug-to-lipid ratio. The optimum ratio of 1:5 adopted by other studies of liposome prepared by using the transmembrane pH gradient (Miatmoko et al., 2017) was modified to drug-to-lipid ratios of 1:10 and 1:5. Decreasing the drug-to-lipid ratio enhanced the encapsulation efficiency of PQ in liposome. Compared to liposome PQ prepared at a drug-to-lipid ratio of 1:10, PQ1-L10 demonstrated the highest encapsulation efficiency of 66.4%, as shown in Table 3. In contrast, CQ could be optimally loaded at a high drug-to-lipid ratio of 1:3 (CQ1-L3) with an encapsulation efficiency of 60.1%. It has been reported that the intravesicular loading capacity of liposome is limited and the significant addition of drugs will reduce the pH gradient between the intra- and extravesicular phases, thus reducing drug loading (Qiu et al., 2008). CQ will be protonated into two basic ionization states since it has pKa values of 8.10 and 9.94 (Qiu et al., 2008). On the other hand, PQ is an amphiphatic drug with pKa values of 3.2 and 10.4 (Stensrud et al., 2000). Therefore, it produced a different profile of drug loading in the same transmembrane pH gradient condition due to contrasting amounts of ionized and unionized drug fractions.

Table 3: Characteristics of liposome loading single PQ or CQ prepared by loading drugs at 60°C for 20 minutes

Drug Component	Formulation	Particle size (nm) <sup>1)</sup>	Polydispersity Index/PDI <sup>1)</sup>	ζ-Potential (mV) <sup>1)</sup>	Entrapment efficiency (%) <sup>1)</sup>
PQ	PQ1-L3	175.8 ± 27.1	0.52 ± 0.33	-16.8 ± 5.2	40.0 ± 3.3
	PQ1-L5	162.1 ± 31.3	0.57 ± 0.25	-19.6 ± 5.4	48.5 ± 3.1
	PQ1-L10	163.8 ± 41.4	0.34 ± 0.05	-17.8 ± 3.9	66.4 ± 8.2
CQ	CQ1-L3	149.1 ± 27.4	0.21 ± 0.02	-22.7 ± 5.3	60.1 ± 7.9
	CQ1-L5	123.4 ± 19.2	0.32 ± 0.08	-23.5 ± 12.2	21.5 ± 4.6
	CQ1-L10	153.1 ± 23.1	0.15 ± 0.04	-22.2 ± 7.9	21.3 ± 9.2

<sup>1)</sup> Each value represents the mean ± S.D. (n = 3).

PQ, primaquine; CQ, chloroquine; L, total lipid of liposome; PQ1-L3, one part of primaquine to 3 parts of total lipid of liposome (w/w)

Based on these results, a 20-minute incubation at 60°C and PQ-to-lipid ratio of 1:10 and CQ to-lipid ratio of 1:3 (w/w) were selected for loading drugs into liposome in further experiments.

In order to prepare a liposome loading combination of PQ and CQ, the liposome was added to PQ and CQ solution at a determined drug weight:lipid ratio, namely; 0.5:0.5:3; 0.25:0.75:3 and 0.13:0.87:3 for PQ:CQ:total lipid, as shown in Table 1. All liposomes were produced with particle sizes ranging from 100 to 175 nm as shown in Fig. 1A with a polydispersity index of approximately 0.20–0.40 (Fig. 1B). These liposomes had slightly negative ζ-potential charges of -9.7 to -22.7 mV (Fig. 1C). Compared to single drug-loaded liposome, combining PQ and CQ into liposome resulted in lower drug encapsulation efficiency (Fig. 1D). The addition of CQ into liposome affected PQ encapsulation, which stood at 72% for the single drug-loaded PQ liposome (P1C0) and 6% for dual drug-loaded liposome (P1C1). Moreover, PQ also influenced liposomal encapsulation of CQ. Compared to single-loaded CQ liposome (P0C1), dual drug loaded-liposome had a lower CQ loading, 56% and 31% for P0C1 and P1C1 liposome, respectively. The PQ-CQ ratio also played an important role in determining liposomal drug encapsulation, which decreases the proportion of CQ to PQ. This resulted in lower encapsulation of PQ as achieved in P1C1 liposome. In contrast, increasing the proportion of CQ to PQ did not produce significant differences in CQ encapsulation. Although these two drugs were encapsulated within an aqueous intraliposomal compartment of the same volume, the addition of PQ and CQ probably affected the permeability of the bilayer during incubation in a contradictory manner. This produced a different optimal drug-to-lipid ratio required for the achieving of impressive encapsulation efficiency. In liposome, drugs can be encapsulated within the hydrophobic bilayer or the hydrophilic aqueous phase, or may interact with the polar headgroup region of the lipid bilayer. The encapsulation efficiency is affected by many factors such as bilayer fluidity (Kulkarni et al., 1995). It has been reported that the positively charged amine of PQ interacts with the polar headgroup region of phosphatidylcholine/PC. In contrast, its quinolone ring indicates Van der Waals interaction with the hydrocarbon core of lipids resulting in fluidizing effects

within and perturbation to the bilayer membrane (Basso et al., 2011). On the other hand, the positively charged amine of CQ has been reported as interacting with negative phosphate groups of phosphatidylcholine and producing rigidification of the liposomal membrane (Barroso et al., 2015; Ghosh et al., 1995). However, although dual loading produced low drug encapsulation, PQ could be delivered together with CQ, which may play an important role in drug metabolism in hepatocytes improving therapeutical efficacy of PQ as well as reducing its toxicity.

The *in vitro* drug released from liposomes was evaluated by immersing liposomes in PBS at pH 7.4 (Fig. 2). The results showed that both PQ and CQ were released more gradually from dual drug-loaded (P1C1) liposome than from P1C0 and P0C1 liposomes. Approximately 63% of the initial dose of PQ was released from P1C0 liposome over a period of 48 hours, while this figure fell to 44% in the presence of CQ encapsulated in P1C1 liposome. CQ displays a similar profile of liposomal drug release indicating an approximate 50% reduction in the drug released by the P1C1 liposome compared to the single CQ-loaded liposome (P0C1 liposome). These results indicate that the liposome loading combination of PQ and CQ produced slower drug release than single drug-loaded liposome, suggesting that the CQ may produce powerful rigidifying effects on the liposomal bilayer since it contains more numerous drug molecules entrapped within the liposome than does PQ. It would be advantageous to avoid premature PQ release during systemic circulation before the liposome enters the hepatocytes. On the other hand, slow release of CQ would also be important for the prophylactic effect on the erythrocytic stage development.

The dual drug loading of PQ and CQ into liposome, which was composed of HSPC, cholesterol and DSPE-mPEG<sub>2000</sub>, greatly influenced drug encapsulation efficiency and drug release. It is important to produce high drug loading and tailor delivery for deliberate release of the drug in an appropriate manner in order to achieve high accumulation in liver tissue for treatment of hepatic stage malaria. However, further investigation is still required to evaluate PQ interaction with the liposomal membrane in the presence of CQ, pharmacokinetic profiles and activity for further exploration of dual-loaded PQ+CQ liposome as part of malaria therapy.

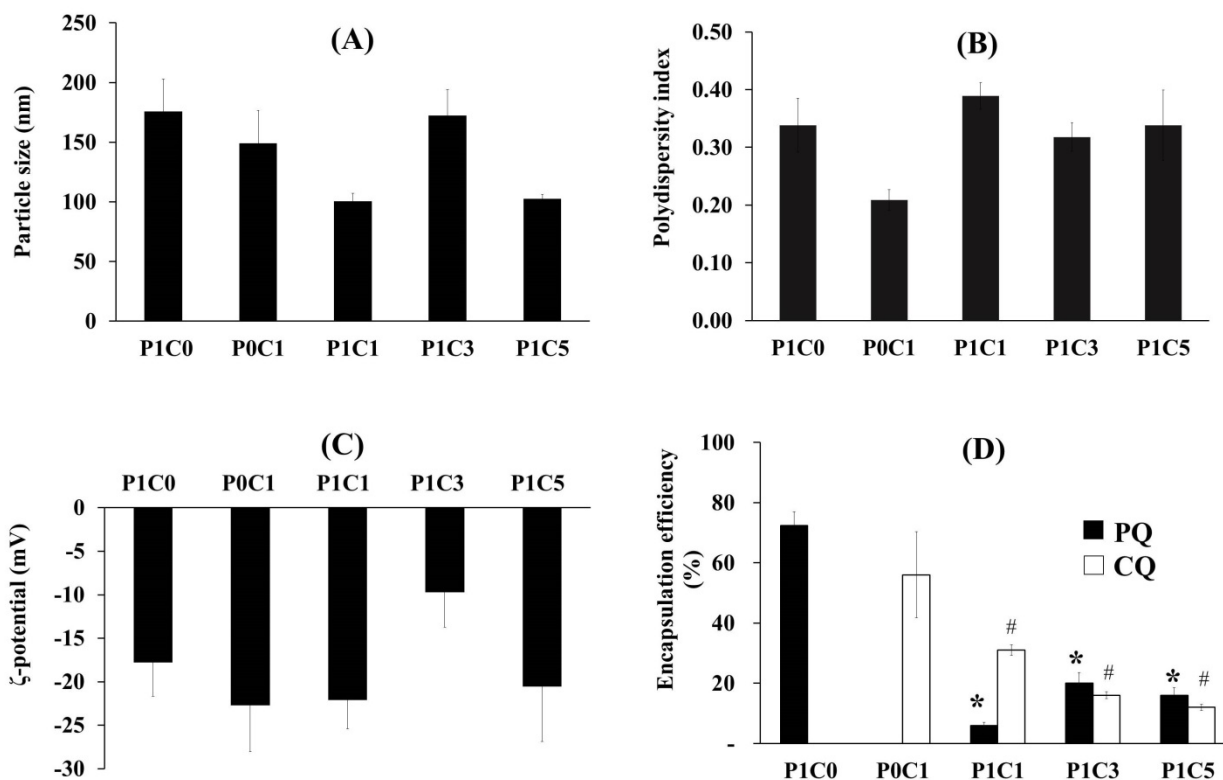


Figure 1: The characteristics of (A) particle size, (B) polydispersity index, (C)  $\zeta$ -potential, (D) encapsulation efficiency of liposome encapsulating PQ (black), CQ (white) and the combination of PQ+CQ loaded by incubating the mixtures at 60°C for 20 minutes. Each value represents mean  $\pm$  S.D. (n=3). \*P < 0.05 compared with P1C0. #P < 0.05 compared with P0C1.

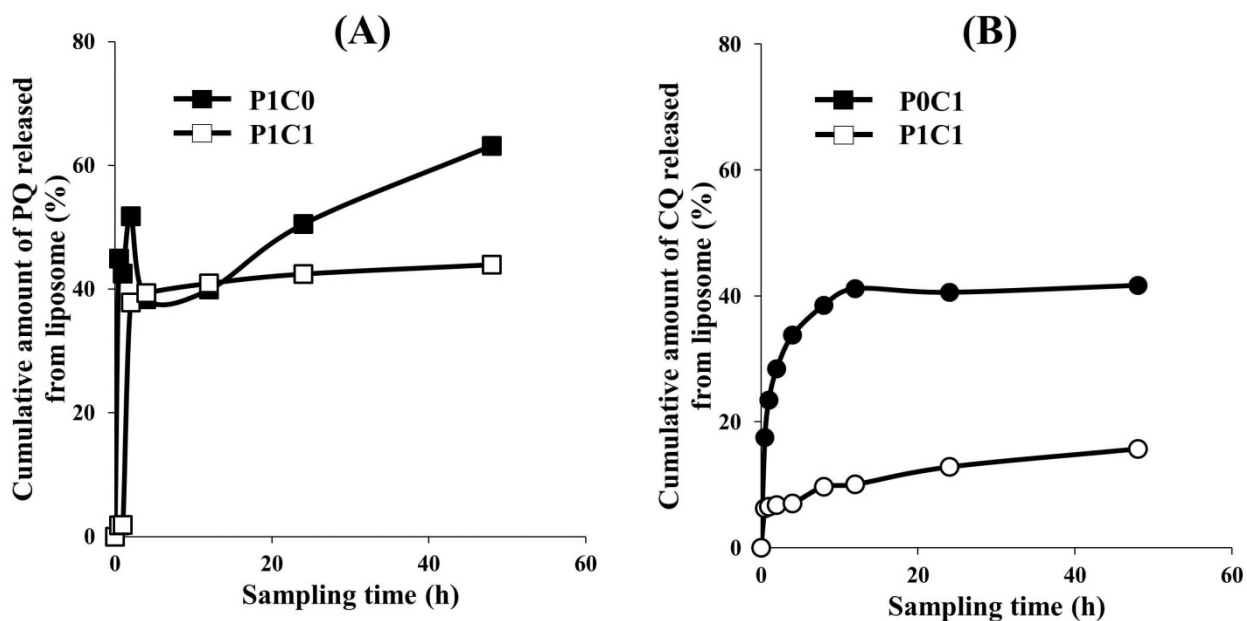


Figure 2: Profiles of release of (A) PQ and (B) CQ from single drug-loaded liposome (P0C1 and P1C0) and dual drug-loaded liposome (P1C1) in phosphate-buffered saline (PBS), pH 7.4 at 37°C.

## CONCLUSIONS

In this study, liposomal containing dual drug loading, which consisted of PQ and CQ, was prepared and subsequently evaluated for drug loading and *in vitro* drug release. Nano-sized particles, high encapsulation for the PQ+CQ combination and slow drug release were achieved by combined loading PQ and CQ at 1:1 weight ratio. This finding suggested that dual PQ+CQ-loaded liposome could potentially be used for comprehensive malaria therapy involving hepatic and erythrocytic stage malaria.

## ACKNOWLEDGEMENTS

This research was supported by a Preliminary Research on Excellence in Higher Education Institutions (Penelitian Dasar Unggulan Perguruan Tinggi, PDUPT) Grant No. 200/UN3.14/LT/2018 provided by the Ministry of Research, Science, and Technology of the Republic of Indonesia.

## CONFLICTS OF INTEREST

The authors declare no conflict of interest or financial interests such as grants, employment, gifts, stock holdings, honoraria, consultancies, expert testimony, patents and royalties, in any product or service mentioned in this article.

## References

- [1] Aronson, H.. Correction Factor for Dissolution Profile Calculations. *J. Pharm. Sc.* 1993;82:3549.
- [2] Baratta, J.L., Ngo, A., Lopez, B., Kasabwalla, N., Kenneth, J., Robertson, R.T. Cellular organization of normal mouse liver: A histological, quantitative immunocytochemical, and fine structural analysis. *Histochem Cell Bio.* 2009;131:713–726.
- [3] Barenholz, Y. Doxil®-The first FDA-approved nano-drug: Lessons learned. *J. Control. Release.* 2012;160:117–134.
- [4] Barroso, R.P., Basso, L.G.M., Costa-Filho, A.J. Interactions of the antimalarial amodiaquine with lipid model membranes. *Chem. Phys. Lipids.* 2015;186:68–78.
- [5] Basso, L.G.M., Rodrigues, R.Z., Naal, R.M.Z.G., Costa-Filho, A.J. Effects of the antimalarial drug primaquine on the dynamic structure of lipid model membranes. *Biochim. Biophys. Acta - Biomembr.* 2011;1808:55–64.
- [6] Chen, J., Cheng, D., Li, J., Wang, Y., Guo, J., Chen, Z., Cai, B., Yang, T. Influence of lipid composition on the phase transition temperature of liposomes composed of both DPPC and HSPC. *Drug Dev. Ind. Pharm.* 2013;39:197–204.
- [7] Chu, C.S., White, N.J. Management of relapsing *Plasmodium vivax* malaria. *Expert Rev. Anti. Infect. Ther.* 2016;14:885–900.
- [8] Fasinu, P.S., Tekwani, B.L., Avula, B., Chaurasiya, N.D., Nanayakkara, N.P.D., Wang, Y.-H., Khan, I.A., Walker, L.A. Pathway-specific inhibition of primaquine metabolism by chloroquine/quinine. *Malar. J.* 2016;15:466.
- [9] Ghosh, A.K., Basu, R., Nandy, P. Lipid perturbation of liposomal membrane of dipalmitoyl phosphatidylcholine by chloroquine sulphate - a fluorescence anisotropic study. *Colloids Surfaces B Biointerfaces.* 1995;4:1–4.
- [10] Gonzalez-Ceron, L., Rodriguez, M.H., Sandoval, M.A., Santillan, F., Galindo-Virgen, S., Betanzos, A.F., Rosales, A.F., Palomeque, O.L. Effectiveness of combined chloroquine and primaquine treatment in 14 days versus intermittent single dose regimen, in an open, non-randomized, clinical trial, to eliminate *Plasmodium vivax* in southern Mexico. *Malar. J.* 2015;14:426.
- [11] Jong, E.C., Nothdurft, H.D. Current drugs for antimalarial chemoprophylaxis: a review of efficacy and safety. *J. Trav. Med.* 2001;8:48–56.
- [12] Karyana, M., Devine, A., Kenangalem, E., Burdarm, L., Poespoprodjo, J.R., Vemuri, R., Anstey, N.M., Tjitra, E., Price, R.N., Yeung, S. Treatment-seeking behaviour and associated costs for malaria in Papua, Indonesia. *Malar. J.* 2016;15:536.
- [13] Kedar, P., Warang, P., Sanyal, S., Devendra, R., Ghosh, K., Colah, R. Primaquine-induced severe methemoglobinemia developed during treatment of *Plasmodium vivax* malarial infection in an Indian family associated with a novel mutation (p.Agr57Trp) in the CYB5R3 gene. *Clin. Chim. Acta* 2014;437:103–105.
- [14] Kohli, A.G., Kierstead, P.H., Venditto, V.J., Walsh, C.L., Szoka, F.C. Designer lipids for drug delivery: From heads to tails. *J. Control. Release.* 2014;190:274–287.
- [15] Kokkona, M., Kallinteri, P., Fatouros, D., Antimisiaris, S.G. Stability of SUV liposomes in the presence of cholate salts and pancreatic lipases: effect of lipid composition. *Eur. J. Pharm. Sci.* 2000;9:245–252.
- [16] Kulkarni, S.B., Betageri, G. V, Singh, M. Factors affecting microencapsulation of drugs in liposomes. *J. Microencapsul.* 1995;12:229–246.
- [17] Lasic, D.D., Frederik, P.M., Stuart, M.C., Barenholz, Y., McIntosh, T.J. Gelation of liposome interior. A novel method for drug encapsulation. *FEBS Lett.* 1992;312:255–258.
- [18] Liang, Y. Drug Release and Pharmacokinetic Properties of Liposomal DB-67 [Theses]. University of Kentucky ;2010.

- [19] Longley, R.J., Sriporote, P., Chobson, P., Saeseu, T., Sukasem, C., Phuanukoonnon, S., Nguitragee, W., Mueller, I., Sattabongkot, J. High Efficacy of Primaquine Treatment for *Plasmodium vivax* in Western Thailand. *Am. J. Trop. Med. Hyg.* 2016;95:1086–1089.
- [20] Marcsisin, S.R., Reichard, G., Pybus, B.S. Primaquine pharmacology in the context of CYP 2D6 pharmacogenomics: Current state of the art. *Pharmacol. Ther.* 2016;161:1–10.
- [21] Miatmoko, A., Kawano, K., Yoda, H., Yonemochi, E., Hattori, Y. Tumor delivery of liposomal doxorubicin prepared with poly-L-glutamic acid as a drug-trapping agent. *J. Liposome Res.* 2017;27:99–107.
- [22] Miatmoko, A., Kawano, K., Yonemochi, E., Hattori, Y. Evaluation of Cisplatin-Loaded Polymeric Micelles and Hybrid Nanoparticles Containing Poly ( Ethylene Oxide ) -Block- Poly ( Methacrylic Acid ) on Tumor Delivery. *Pharmacology & Pharmacy.* 2016;7:1–8.
- [23] Mishra, M., Mishra, V.K., Kashaw, V., Iyer, A.K., Kashaw, S.K. Comprehensive review on various strategies for antimalarial drug discovery. *Eur. J. Med. Chem.* 2017;125:1300–1320.
- [24] Prudêncio, M., Rodriguez, A., Mota, M.M. The silent path to thousands of merozoites: the *Plasmodium* liver stage. *Nat. Rev. Microbiol.* 2006;4:849–56.
- [25] Qiu, L., Jing, N., Jin, Y. Preparation and in vitro evaluation of liposomal chloroquine diphosphate loaded by a transmembrane pH-gradient method. *Int. J. Pharm.* 2008;361:56–63.
- [26] Recht, J., White, N.J., Ashley, E., Safety of 8-Aminoquinoline Antimalarial Medicines. Geneva: World Health Organization, 2015.
- [27] Stela Santos-Magalhães, N., Carla Furtado Mosqueira, V. Nanotechnology applied to the treatment of malaria. *Adv. Drug Deliv. Rev.* 2009;62:560–575.
- [28] Stensrud, G., Sande, S.A., Kristensen, S., Smistad, G. Formulation and characterisation of primaquine loaded liposomes prepared by a pH gradient using experimental design. *Int. J. Pharm.* 2000;198:213–228.
- [29] World Health Organization. Guidelines for the treatment of malaria, Third Edit. ed. Geneva: World Health Organization, 2015.
- [30] Yadav, A. V., Murthy, M.S., Shete, A.S., Sakhare, S. Stability aspects of liposomes. *Indian J. Pharm. Educ. Res.* 2011;45:402–413.

# Evaluation of analgesic and anti-inflammatory activities of ethanolic extract of *Cordia sebestena* L.

Original Paper

Sunaryo H.<sup>1,3</sup>, Siska S.<sup>1,3,✉</sup>, Hanani E.<sup>2,3</sup>, Anindita RS.<sup>3</sup>, Yanti N.<sup>3</sup>, Lisa<sup>3</sup>

<sup>1</sup>Department of Pharmacology, Universitas Muhammadiyah Prof. Dr HAMKA, Jl. Delima II/IV Klender, Jakarta 13460, Indonesia

<sup>2</sup>Department of Pharmaceutical Biology, Universitas Muhammadiyah Prof. Dr HAMKA, Jl. Delima II/IV Klender, Jakarta 13460, Indonesia

<sup>3</sup>Faculty of Pharmacy and Sciences, Universitas Muhammadiyah Prof. Dr HAMKA, Jl. Delima II/IV Klender, Jakarta 13460, Indonesia

Received 27 May, 2019, accepted 16 October, 2019

**Abstract** Trees and shrubs of the genus *Cordia* are widely distributed in the warmer regions, including Indonesia. The aim of this study was to evaluate the analgesic and anti-inflammatory properties of the ethanolic extract of plant leaves in Wistar albino rats. The analgesic activity was evaluated using the hot plate method and acetic acid-induced writhing, and the anti-inflammatory activity was determined using carrageenan-induced paw oedema. The results showed that the *Cordia sebestena* ethanol extract (100, 200 and 400 mg/kg) exhibited significant analgesic effects in a dose-dependent manner in the two pain models tested. The extract also exhibited significant anti-inflammatory effects in the carrageenan-induced inflammation test. The data obtained support the traditional folklore therapeutic claim about its analgesic and anti-inflammatory properties. Nonetheless, further scientific investigation is required to establish its analgesic and anti-inflammatory properties in other experimental models and clinical settings.

**Keywords** analgesic – anti-inflammatory – carrageenan – *Cordia sebestena* – hot plate – writhing

## INTRODUCTION

*Cordia sebestena* L. belongs to the Boraginaceae family, a native plant from the Bahamas to the tip of northern South America, which has been erroneously listed as a Florida native (Osho et al., 2015). *C. sebestena* L. is an evergreen tree, also known as the Geiger tree, Kou Haole (means a 'foreign plant') in Hawaiian and as 'Geiger' in Indonesia. The plant can grow up to 10 m tall and cultivated largely in tropical and subtropical areas, where it is widely distributed due to its extensive use in landscaping. The flowers are dark orange in colour, appear as clusters at branch tips, throughout the year, especially in June–July and have a pleasant fragrance. The fruits are oval shaped and green and white in colour (Atolani et al., 2014). This plant originated in Hawaii and has been used as traditional medicine. In Nigeria, *C. sebestena* is used in traditional medicine for the treatment of gastrointestinal disorders (Osho et al., 2015).

Preliminary phytochemical screening of the flowers, stem bark and fruit was done by some researchers (Adeosun et al., 2012, 2013; Dai et al., 2013). Osho et al. (2015) mention that the ethyl acetate extract of the leaf indicates the presence of a mixture of non-polar aliphatic and aromatic compounds and polar hydroxyl aliphatic and aromatic compounds. However, the chemical composition of the analgesic and anti-inflammatory activities of the leave extract of *C. sebestena* have not been studied to date. The isolation of the pure compounds of the bioactivity of individual compounds of the leaf extract will give much information about the medicinal values of this plant.

The *C. sebestena* ethyl acetate leaf extract has been shown to have antibacterial activity against *Bacillus cereus* and *Staphylococcus aureus*, as well as a relatively low toxicity profile in the liver of rats (Osho et al., 2015). The ethanolic

\* E-mail: siska@uhamka.ac.id

© European Pharmaceutical Journal

extract of the whole plant of *C. sebestena* possesses significant hepatoprotective activity (Chandana et al., 2014), while *C. sebestena* root has anti-inflammatory and analgesic activities (Trivedi et al., 2017). The leaves of the plant possess anti-hyperglycemic properties in streptozotocin-induced diabetes, and it is hypolipidemic and a potent antioxidant (Sarithchandiran and Gnanavel, 2013). The essential oil of *C. sebestena* stem bark obtained through hydrodistillation was analysed using GC-MS, identifying a total of 19 compounds, including aliphatic hydrocarbons (72.73%) and cyclic hydrocarbons (13.89%). The essential oil is a potent antioxidant *in vitro* (Adeosun et al., 2013). Sebestenoids A–D (1–4) were isolated from bioassay-guided fractionation prepared from the *C. sebestena* fruit extract (Dai et al., 2013). The chloroform, ethyl acetate and methanol extract of *C. sebestena* root showed significant anti-inflammatory and analgesic activities at both dose levels of 100 and 200 mg/kg (Trivedi et al., 2017).

This study investigated the analgesic and anti-inflammatory activities of an ethanolic extract of *C. sebestena* L. cultivated in Indonesia. Analgesic activity was assessed using a hot plate method, acetic acid-induced writhing and formalin-induced paw licking. Anti-inflammatory activity was determined using carrageenan-induced rat paw oedema.

## MATERIALS AND METHODS

### Plant materials

Fresh leaves of *C. sebestena* in the flowering stage were collected in September 2018 from the Universitas Muhammadiyah Prof. Dr HAMKA regional, East Jakarta, Indonesia. The leaves were identified and authenticated taxonomically as Herbarium Bogoriense, Bogor, Indonesia. A voucher specimen was deposited at the Pharmacognosy laboratory, Universitas Muhammadiyah Prof. Dr HAMKA as a record. The plant material was dried in the shade and ground to a coarse powder.

### Preparation of ethanol extract

The dried powder (2 kg) was subjected to repeated extraction by maceration at room temperature with petroleum ether (60–80°C) as a solvent for 2 days. The plant material was separated by filtration. The marc was dried and extracted continuously (two times, 2 days) with 1.5 L of dichloromethane (DCM; Merck, Germany) and filtered. The final marc was extracted with ethanol 70% (Brataco, Indonesia) and concentrated by a vacuum evaporator (under reduced pressure). The percentage yield of the ethanol extract was 8.88% w/w. The final 70% ethanol *C. sebestena* leaves extract (CSE) was used to evaluate the analgesic and anti-inflammatory activities.

### Animals

Healthy male Wistar albino rats aged 8–9 weeks and weighing 180–200 g were obtained from the animal house, Faculty of

Veterinary, Bogor Agriculture Institute, Bogor. They were acclimatised to the laboratory conditions for 10 days before the studies, maintained in normal conditions and fed with standard pellet and water *ad libitum*. The room temperature was maintained at 25±1°C, and the animals were kept under a 12 h light and dark cycle. The experimental protocol was approved by the Institutional Animal Ethical Committee of Universitas Prof. Dr HAMKA, Reg. no. 08/18.09/003. For all pharmacology experiments (analgesic, anti-inflammatory), male Wistar albino rats were used and divided into five groups of five animals each: Group I was the control group, Group II was the standard group treated with a standard drug (tramadol, Kimia Farma, Indonesia), Groups III, IV and V were treated with CSE at a dose of 100, 200 and 400 mg/kg orally, respectively, for 5 days. The extract and standard drug were given once a day between 08:00 and 09:00.

## Analgesic screening

### Hot plate method

The hot plate method was modified from those described by Ojewole (2006). Group I served as the control group and was orally administered 2 mL of 0.5% carboxymethyl cellulose (CMC) sodium (Na) suspension; Group II was treated with the standard drug tramadol (5.14 mg/kg) and Groups III, IV and V were treated with CSE at a dose of 100, 200 and 400 mg/kg, respectively. All test samples were prepared by suspending in 0.5% CMC Na solution immediately before the start of the experiments. The animals were in a fasting condition for 12 h before starting the experiments. Rats were placed on a hot plate maintained at 55±1°C. The responses were recorded in the form of jumping or licking of the paws, with the reaction time recorded at 15, 30, 45 and 60 min intervals after the administration of the treatments. A cut-off time of 30 s was selected to avoid tissue damage. Inhibition of hot plate paw-licking responses was expressed as the percentage of the maximal possible effect (% MPE), calculated as:

$$\%MPE = T_a - T_b / T_b \times 100,$$

where  $T_a$  and  $T_b$  represent the hot plate paw-licking latencies after and before the administration of test drug or vehicle, respectively.

### Writhing method

The method described in Koster et al. (1959) was used. In this method, pain-causing acetic acid was injected in the peritoneal cavity, which induced writhing (abdominal pain and constrictions). Group I (the control group) was treated with 2 mL of 0.5% CMC Na suspension; Group II was treated with the standard drug acetylsalicylic acid intraperitoneal injection (i.p) given 15 min before i.p. injection of 0.75% acetic acid solution (Merck, Germany) and Groups III, IV and V were

Table 1: Analgesic effects of CSE as determined by the hot plate method in rats

Treatment	Dose (mg/kg)	Time after drug administration				
		0 min	15 min	30 min	45 min	60 min
Control	---	2.32±1.36	2.56±0.97	2.26±1.11	2.40±1.00	1.66±0.61
Tramadol	5.14	2.54±0.69	3.58±2.28	3.44±1.74	3.94±1.98	3.94±1.79 <sup>b</sup> (57.87)
CSE	100	5.00±1.17	4.96±1.75 <sup>a</sup>	3.80±2.81	2.70±0.89	3.34±2.13 <sup>b</sup> (50.30)
CSE	200	3.20±1.09	5.16±2.02 <sup>a</sup>	4.24±0.66	4.40±0.74	3.98±1.60 <sup>b</sup> (58.29)
CSE	400	3.64±1.21	5.52±1.98 <sup>a</sup>	4.20±2.44	5.46±2.95	3.94±1.00 <sup>b</sup> (57.87)

The latency for licking of the hind paw or jumping off from the surface was expressed as mean±SEM, (n=5).

Values in brackets denote percentage of maximum possible effect (MPE) of the latency for licking of the hind paw or jumping off. CSE, *C. sebestena* ethanol extract.

<sup>a</sup>p<0.05 compared with the control.

<sup>b</sup>p<0.05 compared with the control group.

treated orally with CSE at doses of 100, 200 and 400 mg/kg, respectively. Afterwards, the abdominal writhing was counted for 15, 30, 45 and 60 min, and the rate of inhibition of writhing was determined. The number of writhing and stretching was observed, recorded and expressed as percentage inhibition. The effectiveness of the treatment was evaluated by the decrease in the number of writhes compared with the control group. The percentage of inhibition of the number of writhing episodes was calculated as:

$$\% \text{inhibition rate} = (V - V_t) / V \times 100\%,$$

where 'V' is the average number of stretching of control per group and 'V<sub>t</sub>' is the average number of stretching of test per group.

### Anti-inflammatory screening

#### Carrageenan test

Acute anti-inflammatory activity was evaluated by carrageenan-induced rat paw oedema as previously described by Turner et al. (1965). Male Wistar albino rats (150–200 g) maintained under environmental conditions had free access to standard diet and were fasted for 10 h before starting the experiments. Group I (the negative control group) was treated with 2 mL of 0.5% CMC Na suspension and diclofenac Na (Kimia Farma, Indonesia) 5 mg/kg was used as a standard control. The CSE (100, 200 and 400 mg/kg) was administered to Groups III, IV and V. The treatment of Groups I, II, III, IV and V were given 30 min before carrageenan injection. At 30 min after sample administration, oedema was induced by injecting 0.1 mL of 1% λ-carrageenan in sterile saline into the subplantar surface of the right hind paw. The paw volume was measured using a micrometre screw gauge at 0, 1, 2, 3 and 4 h after carrageenan injection and compared with the

standard treated group. The anti-inflammatory effect was expressed as percentage inhibition of oedema:

$$\text{Percentage inhibition} = (V_t - V) / V_t \times 100,$$

where V is the volume of control and V<sub>t</sub> is the volume of the test.

### Statistical analysis

The experimental data were expressed as mean±SEM. Data were analysed by one-way analysis of variance followed by Tukey, and the significance of the difference between means was determined when the values of p<0.05 were considered significant.

## RESULTS AND DISCUSSION

Two different analgesic testing methods were employed to identify possible peripheral and central effects of the test substance. In this study, the analgesic reactivity to thermal stimuli in rats was assessed using the hot plate test, which is a sensitive acute pain test for detecting opiate analgesia. The hot plate test is a simple and sensitive method for studying analgesic and hyperanalgesic reactions in rats. Using the hot plate test, it was shown that oral administration of the ethanolic extract (100, 200 and 400 mg/kg) significantly prolonged the reaction time 15 min after treatment compared with the corresponding control groups (Table 1), and these effects were dose independent.

The analgesic effects of 100, 200 and 400 mg/kg of CSE were investigated. Table 1 presents the analgesic activity of the ethanol extract assessed using the hot plate. Tramadol showed no statistically significant increase in the reaction time, but there were significant differences in the thermal

Table 2. Analgesic activity of CSE determined by the writhing test method

Treatment	Dose (mg/kg)	Reaction time (min)			
		15	30	45 (%inhibition)	60 (% inhibition)
Control	---	68.6±10.64	59.0±7.91	56.2±6.87	39.0±5.95
Acetosal	5.14	29.4±1.34	23.8±3.70	20.6±2.51 (63.35)	14.4±2.96(63.07)
CSE	100	38.6±7.02	36.6±12.17	36.0±14.31(35.94)	31.2±10.89(20.00) <sup>a</sup>
CSE	200	32.6±7.02	31.0±4.41	29.0±3.74 (48.40)	25.4±2.61 (34.87) <sup>a</sup>
CSE	400	33.2±4.86	29.0±4.94	27.8±1.48 (50.53)	22.2±5.93(43.08) <sup>a</sup>

The data were expressed as mean±SEM, (n=5). Values in brackets denote the percentage of inhibition rate of the number of writhing.

CSE, *C. sebestena* ethanol extract.

<sup>a</sup>p<0.05 compared with the positive group.

Table 3: Anti-inflammatory effects of CSE assessed by the carrageenan-induced rat paw oedema method CSE, *C. sebestena* ethanol extract

Treatment	Dose (mg/kg)	Volume of hind paw (mm)				
		0 h	1 h	2 h	3 h	4 h
Control	---	7.73±6.02	13.18±0.72	23.68±7.52	25.68±1.91	20.56 ±0.65
Diclofenac sodium	5	5.25±0.56	10.01±6.56	16.57±7.90	19.37±9.39 (72.90)	14.74±7.90 (64.38) <sup>a</sup>
CSE	100	6.26±0.58	11.89±0.68	23.51±0.92	24.78±9.39 (74.74)	16.86±7.90 (61.32) <sup>a</sup>
CSE	200	5.31±1.00	10.02±6.56	14.88±6.23	21.45±8.80 (75.24)	16.18±1.18 (67.18) <sup>a</sup>
CSE	400	5.53±0.85	12.36±5.89	18.51±0.68	23.69±0.93 (76.66)	16.46±6.30 (66.40) <sup>a</sup>

The values of paw oedema were expressed as mean±SEM, n=5. Values in brackets denote inhibition percentage of the oedema paw volume.

<sup>a</sup>p<0.05 compared with the positive group.

stimulus observed in rats treated with the different doses of CSE compared with normal saline (negative control) throughout the 60 min.

From Table 1, it is clear that oral administration of 100, 200 and 400 mg/kg of CSE significantly prolonged the reaction time 15 min after treatment in comparison with the control groups. Although the extracts appeared to induce higher analgesic activity in most cases, there was no consistent pattern of activity among the three extracts, that is, the effects were not dose dependent. The oral administration of ethanol extract of *C. sebestena* (100, 200 and 400 mg/kg) significantly attenuated hot plate thermal stimulation.

In this study, the analgesic activity was evaluated through the hot plate and writhing assay in rats, whereas anti-inflammatory activity was assessed via carrageenan-induced paw oedema in rats. Tissue damage or injury is associated with pain and inflammation. Analgesics can act on the peripheral or central nervous system. Peripherally acting analgesics act by blocking the generation of impulses of chemoreceptors at the site of pain, while centrally acting analgesics not only raise

the pain threshold but also alter the physiological response to pain, suppressing animal anxiety and apprehension (Kumar et al., 2014).

The results presented in Table 2 show that 100, 200 and 400 mg/kg of CSE exhibited significant (p<0.05) inhibition of the writhing compared with the standard drug (acetosal, 5.14 mg/kg i.p). Indeed, CSE exerted a dose-dependent decrease in abdominal constriction in rats stimulated with 1% acetic acid solution. At 60 min, the number of writhing of all extracts decreased significantly compared with the control. The oral administration of ethanol extract (100, 200 and 400 mg/kg) significantly attenuated the number of writhing in the writhing test method.

The acetic acid-induced writhing method is not only simple and reliable but also affords rapid evaluation of peripheral analgesic action. In this experiment, the animals react with characteristic stretching behaviour, which is called writhing. The abdominal constriction is related to the sensitisation of nociceptive receptors to prostaglandins (Victoria et al., 2012). In this model, pain is generated indirectly via endogenous

mediators, such as bradykinin, serotonin, histamine, substance P and PGs which all act by stimulation of peripheral nociceptive neurons (Garcia, 2004). The ethanolic extract (100, 200 and 400 mg/kg) administered orally significantly inhibited the acetic acid-induced writhing in rats.

In the carrageenan-induced oedema test, a maximum oedema paw volume of  $25.68 \pm 1.91$  and  $20.56 \pm 0.65$  mm (Table 3) was observed in the control rats, 3 and 4 h after the carrageenan injection. Administration of CSE (100, 200 and 400 mg/kg) significantly ( $p < 0.05$ ) inhibited the development of paw swelling at 4 h after carrageenan injection. All doses of CSE were potent and produced anti-inflammatory effects similar to diclofenac Na.

The oral administration of CSE (100, 200 and 400 mg/kg) significantly attenuated the volume of carrageenan-induced oedema similar to diclofenac Na, indicating that the ethanolic extract of *C. sebestena* leaves possesses anti-inflammatory activity.

This result has a similar effect to the previous research (Trivedi et al., 2017). It could be the phytochemical composition of the root that attributed the analgesic and anti-inflammatory properties the same as in the leaves. In this experiment, we did not explore the phytochemical components and could not find the reference of active ingredients from *C. sebestena* leaves that attributed the analgesic and anti-inflammatory properties.

Inflammation is a pathophysiological response of living tissue to injury that leads to the local accumulation of plasmatic fluid and blood cells. There are various components to an inflammatory reaction, such as oedema formation, leukocyte infiltration and granuloma formation that can contribute to the associated symptoms and tissue injury. Inflammation types are acute and chronic. The initial cardinal signs of inflammation include redness, heat, swelling, pain and loss of

function (Trivedi et al., 2015, 2017). The carrageenan-induced oedema method has been commonly used as an experimental animal model for acute inflammation. This model is mainly mediated by histamine, serotonin and increased synthesis of prostaglandins in the damaged tissue, followed by prostaglandin release mediated by bradykinin, leukotrienes and polymorphonuclear cells (Kaushik, 2012). In this study, oral treatment with all the CSE doses significantly inhibited the paw oedema, suggesting that the anti-inflammatory actions of the ethanol extracts are related to inhibition of one or more intracellular signalling pathways involved with these mediator effects.

## CONCLUSION

The present study demonstrated that the ethanol extract from *C. sebestena* leaves (100, 200 and 400 mg/kg) possess significant potential to inhibit pain and suppress inflammation. The increase in dose is proportional to an increase in effect. However, further studies should be conducted to ensure efficacy and safety. The experiments could explore the fractions of the extract for further pharmacological and toxicological characterisation.

## CONFLICTS OF INTEREST

The authors declare that they have no competing interests.

## ACKNOWLEDGEMENT

All authors are grateful to the Dean of Faculty of Pharmacy and Sciences, Universitas Muhammadiyah Prof. Dr HAMKA Jakarta Indonesia, for providing necessary facilities and support to carry out the research work.

## References

- [1] Adeosun CB, Olaseinde S, Opeifa AO, Atolani O, Essential oil from the stem bark of *Cordia sebestena* scavenges free radicals. *J. of Acute Medicine*. 2013;(3): 138-141.
- [2] Atolani O, Kayode OO, Adeniyi O and Adeosun CB. In vitro antioxidant potential of fatty acids obtained by direct transmethylation from fresh *Cordia sebestena* flowers. *Annals of Tropical Research*. 2014; 36(2): 104-114.
- [3] Chandana R, Basini J, Reddy VJS., Hepatoprotective and antioxidant effect of *Cordia sebestena* in animal model. *International J. of Pharmacology & Toxicology*. 2014;4(3): 181-189.
- [4] Dai J, Sorribs A, Yoshida WY, Williams PG., Sebestenoids A-D, BACE1 inhibitors from *Cordia sebestena*. *J. of Phytochemistry*. 2013; 71 (17-18): 2168-2173.
- [5] Garcia MD, Fernandez MA, Alvarez A, Saenz MT., Antinociceptive and anti-inflammatory effect of the aqueous extract from leaves of *Pimenta racemosa* var. *ozua* (Mirtaceae). *J. Ethnopharmacol*. 2004; (91): 69-73.
- [6] Kaushik D, Kumar A, Kaushik P, Rana AC., Analgesic and anti-inflammatory activity of *Pinus roxburghii* Sarg. *Advances in Pharmacological Sciences*. 2012; 1-6.
- [7] Koster R, Andersons M, DeBeer E., Acetic acid analgesic screening. *Federation Proceeding*. 1959;(18): 418-420.
- [8] Kumar CNS, Das A, Ray AGR., Anti-inflammatory activity of *Sapindus laurifolius* leaf extract in wistar rats. *J. of Medicinal Plants Studies*. 2014; 2 (1): 1-5.
- [9] Ojewole JAQ., Analgesic, anti-inflammatory and hypoglycaemic effects of ethanol extract of *Zingiber officinale* (Roscoe.) Rhizomes (Zingiberaceae) in mice and rats. *Phytother. Res*. 2006; (20): 764-772.
- [10] Osho A, Otuechere CA, Adeosun CB, Oluwagbemi T and Atolani O. Phytochemical, sub-acute toxicity, and antibacterial evaluation of *Cordia sebestena* leaf extracts. *J Basic Clin Physiol Pharmacol*. 2015: 1-8.
- [11] Sarathchandiran I and Gnanavel M., Investigation on hypoglycemic, antioxidant and hypolipidemic activity of ethanolic leaf extract of *Cordia sebestena* in Streptozotocin –

- induced diabetic rat. *International J. of Research in Pharmaceutical Sciences*. 2013; 4 (3): 336-343.
- [12] Trivedi MH, Ramana KV, and Rao CV., Anti-inflammatory and analgesic activities of *Cordia monoica* Roxb. Stem. *World J. of Pharmacy and Pharmaceutical Sciences*. 2017; 6 (9): 1530 -1536.
- [13] Trivedi MH, Ramana KV, Rao CV., Evaluation of antiinflammatory and analgesic activities of *Cordia sebestena* L. Roots. *Indo American J. of Pharm. Research*. 2015;5(08): 2765-2768.
- [14] Turner RA., Screening Methods in Pharmacology. Academic Press Inc, London. 1965; 152.
- [15] Victoria SH, Das S, Lalhlenmawia H, Phucho L, and Shantabi L., Study of analgesic, antipyretic and anti-inflammatory activities of the leaves of *Thunbergia coccinea* Wall. *International Multidisciplinary Research J*. 2012; 2 (2): 83-88.

# Chronopharmacology of high blood pressure—a critical review of clinical evidence

Original Paper

Potucek P.<sup>✉</sup>, Klimas J.

Faculty of Pharmacy, Comenius University, Department  
Pharmacology and Toxicology, Comenius University  
Bratislava, Odbojarov 10, 832 32 Bratislava, Slovak Republic

Received 3 July, 2019, accepted 26 September, 2019

**Abstract** Physiological functions of cardiovascular system (CVS) are exhibiting circadian patterns regulated by complex system of endogenous factors. Preserving this rhythmicity is important for its normal function, whereas disturbing the synchronization with natural day–night cycle can increase the risk of cardiovascular damage. Cardiovascular pathophysiology also follows cyclic variation; time susceptibility and period with maximum risk associated with elevated blood pressure (BP) can be predicted. Given this rhythmic nature, significant changes in efficacy between morning and evening administration of the drug may occur; appropriate timing of pharmacological intervention in therapy of hypertension may affect the efficacy of the treatment.

**Keywords** *chronopharmacology – blood pressure – circadian rhythm – non-dipping*

## INTRODUCTION

The light–dark cycle is the most prominent rhythm on the earth, and organisms have adapted to this rhythm by the evolution of biological rhythms. Rhythmicity of life processes is one of the key factors for survival by adapting to environmental changes. This also applies to the cardiovascular system (CVS); its rhythmic features are important to synchronize the organ response to external changes (Wu et al., 2011). Conversely, loss of synchronization between the circadian oscillator and external stimuli can cause damage to the cardiovascular organs, and in long term, it can lead to increased morbidity and mortality risk. CVS exhibits distinct 24 hours rhythm within its physiological functions; main features such as blood pressure (BP), cardiac output, and heart rate have a clear and characteristic circadian pattern. Likewise, the pathophysiological mechanisms connected to morbidity and mortality display this rhythm.

Values of BP are not constant throughout the day (Portaluppi et al., 2012). A distinct 24-h rhythm given by cyclic alternation of day and night with subsequent changes in behavior (e.g., physical activity and mental stress) and circadian rhythm of endogenous factors can be observed. The rhythm character is largely due to the dominance of the sympathetic nervous system with high levels of circulating noradrenaline,

adrenaline, and catecholamines in the first hours after waking. Renin-angiotensin-aldosterone hormone system (RAAS) also plays an important role contributing to the composite rhythm of BP with plasma concentrations of renin activity, angiotensin-converting enzyme (ACE), angiotensin I and II, and aldosterone all of them peaking in the morning before awakening. Conversely, comparatively lower BP during sleep is a result of predominance of parasympathetic action over the sympathetic nervous system, lower RAAS concentration, and maximum vasodilator levels—atrial natriuretic peptide and nitric oxide (Hermida et al., 2011). In organisms with reversed day–night activities, that is, nocturnal animals, the BP rhythm is opposite, so the highest values occur at night when animals are active and seek food, confirming that the day and night rhythm and differences in mental and physical activities are a key factor affecting the circadian rhythm of BP.

## CHRONOTHERAPY OF HYPERTENSION

The goal of chronotherapy is to achieve maximum drug concentrations in synchrony with the intrinsic circadian rhythm of the disease or symptoms process, thereby increasing the efficacy as well as reducing the adverse effects of treatment.

\* E-mail: petar.potucek@gmail.com

© European Pharmaceutical Journal

Table 1: Administration-time-dependent effect of BP-lowering medications

Medication	Dosage (mg per day)	Treatment times	Study length (weeks)	No. of completed subjects	Comparison of morning vs. evening dosing	Author
Valsartan	160	Awakening bedtime	12	90	Significant reduction in asleep SBP/DBP with evening dosing	Hermida et al., 2003
Olmesartan	20	Awakening bedtime	12	133	Significant reduction in asleep SBP/DBP with evening dosing	Hermida et al., 2009
Telmisartan	80	Awakening bedtime	12	215	Significant reduction in asleep SBP/DBP with evening dosing	Hermida et al., 2007
Lisinopril	20	08:00; 16:00; 22:00	8	40	Significant reduction in early morning SBP/DBP with evening dosing	Macchiarulo et al., 1999
Trandolapril	1	Awakening bedtime	8	30	Significant reduction in 24-h BP mean with evening dosing	Kuroda et al., 2004
Ramipril	5	Awakening bedtime	6	115	Significant reduction in 48-h SBP/DBP mean with evening dosing	Hermida and Ayala, 2009
Spirapril	6	Awakening bedtime	12	165	Significant reduction in asleep SBP/DBP with evening dosing	Hermida et al., 2010
Nifedipine	30	Awakening bedtime	8	180	Significant reduction in 48-h SBP/DBP mean with evening dosing	Hermida et al., 2008
Torasemide	5	Awakening bedtime	6	113	Significant reduction in 48-h SBP/DBP mean with evening dosing	Hermida et al., 2008

This can be achieved by specific drug technologies but often by simply adjusting the time of administration of conventional therapy (Smolensky et al. 2010). Research has shown that the majority of patients with hypertension use BP-lowering medication in the morning; some data refer up to 80% of patients with hypertension taking all antihypertensive drugs in the morning (De La Sierra et al., 2009). In contrary to this practice, a number of randomized clinical trials (RCTs) have demonstrated that appropriate timing of administration of an antihypertensive drug can affect the efficacy and safety of the treatment, so that changes in efficacy between morning and evening drug delivery may be significant for individual drugs.

### Monotherapy

Clinical trials focusing on monotherapy have been performed with all available classes of drugs used in the treatment of hypertension, that is, ACE inhibitors, diuretics,  $\alpha$ -blockers,  $\beta$ -blockers, direct renin inhibitor, angiotensin receptor blockers, and calcium channel blockers (see Table 1). Significant treatment-time differences were confirmed for several classes of antihypertensive drugs. With the RAAS being highly circadian rhythmic, most of the recent and well-designed studies have focused on drugs acting on

this cascade—ACE inhibitors and AT1 blockers—and have indeed shown statistically significant changes in chronic non-dipping nocturnal adjustment when monotherapy was given in the evening and not in the morning (Hermida et al., 2013; Schillaci et al., 2015). The thiazide diuretics have also been shown to have a greater efficacy with evening treatment, being significantly more effective in reducing the incidence of severe cardiovascular events, adjustment of circadian pattern, and reduction of nocturnal BP values (Kasiakogias et al., 2015; Liu et al. 2014). A meta-analysis comparing the results of more than 20 RCTs involving almost 2,000 patients with primary hypertension confirmed that more effective BP control was achieved with evening monotherapy (Zhao et al., 2011).

However, this does not apply to all antihypertensive drugs. Given their long elimination half-life, trials with calcium channel blockers have shown no significant difference between morning and evening administration of majority of the dihydropyridines (amlodipine, isradipine, lacidipine) (Qui et al., 2003; Lemmer, 2006); however, studies with nifedipine have shown reduction of the mean BP values to be significantly better with bedtime dosing (Hermida et al., 2008). Conversely,  $\beta$ -blockers appear to be more effective in morning administration and alter the circadian BP toward a

Table 2: Administration-time-dependent effect of selected BP-lowering medications in combination treatment

Combination treatment	Dosage (mg per day)	Treatment times	Study length (weeks)	No. of completed subjects	Comparison of morning vs. evening dosing	Author
Valsartan/amlodipine (free combination)	160/5-10	06:00–10:00 18:00–22:00	8	463	No difference in mean, asleep, and awake SBP/DBP with evening or morning dosing	Asmar et al., 2011
Valsartan/amlodipine (fixed/free combination)	160/5	Awakening bedtime	12	203	Significant reduction in asleep SBP/DBP and mean SBP with evening dosing	Hermida et al., 2010
Valsartan/HCT (fixed combination)	160/12.5	Awakening bedtime	12	204	Significant reduction in asleep SBP with evening dosing	Hermida et al., 2011
Amlodipine/HCT (fixed combination)	5/25	8:00 22:00	12	80	Significant reduction in mean and asleep SBP/DBP with evening dosing	Zeng et al., 2011
Amlodipine/fosinopril (free combination)	5/10	7:00–8:00 7:00–8:00/ 20:00–21:00	4	40	Significant reduction in asleep SBP/DBP with split evening dosing	Meng et al., 2010
Amlodipine/fosinopril (free combination)	5/10	7:00–8:00 7:00–8:00/ 20:00–21:00	4	40	Significant reduction in asleep SBP/DBP with split evening dosing	Meng et al., 2010

nondipper profile. This can be reasonably expected with the concentration of catecholamines as well as the expression of beta-receptors being lowest during the night, thus owing the administration of  $\beta$ -blockers in the evening lower effect compared with that in the morning (Langner, Lemmer, 1988)

### Fixed combination therapy

Although the treatment of hypertension is usually initiated as monotherapy, in most cases, combination therapy, that is, use of multiple antihypertensive agents simultaneously, is also indicated (Dahlöf, 2009). Therapy with lower doses of two or more drugs is preferable to monotherapy at higher doses with one drug, because better control of BP is achieved along with better tolerability and related patient compliance. Compared with large number of studies investigating difference between morning and evening dosing, studies with combination therapy investigating the chrono-effect are still limited (see Table 2). In these cases, it is assumed that chronopharmacological profiles of each drug might contribute to the dosing-time-dependent influences on the efficacy and safety of combined hypertension medication, with results suggesting evening dosing to be more effective in terms of BP reduction and/or normalization of the circadian rhythm of BP (Potúček, Klimas, 2013). However, interesting observation came from the comparison of two independent studies investigating the chrono-effect of the same combination (amlodipine and valsartan). While significant reduction in asleep BP and mean BP values with evening dosing was proven in one of the studies, no difference between time of administration has been observed in the

other one (Hermida et al., 2010; Asmar et al., 2011). With the study length being the only difference between these two studies, this fact might indicate that the duration of treatment can also influence the chrono-effect. Similar results were also confirmed in preclinical settings (Potucek et al., 2017).

### DISCUSSION

Circadian rhythms at targeted site of action are a primary prerequisite for chronopharmacology. This is confirmed by several experiments showing that the peak pharmacodynamic (PD) effect of drugs does not correlate with the plasma concentration peak, thus suggesting a circadian stage dependency of the drug plasma concentration–antihypertensive effect relationship (Smolensky et al. 2010). However, PD and/or pharmacokinetic (PK) profile of the drug must also be taken into consideration before selecting suitable candidates, because molecules with a longer elimination half-life or slow dissociation from the receptor-binding site are prone to have decreased chronopharmacological effect (Liu et al., 2011).

The appropriate choice of the drug and the timing of its administration must, therefore, respect PK profile of the molecule, but, at the same time, circadian rhythms of body may as well affect the fate of the drug in the body. Gastric emptying, motility, and perfusion are significantly longer in the morning, whereas gastric acid secretion reaches its maximum in the evening. Lipophilic molecules seem to be more prone to circadian rhythms of the body affecting their PK and then hydrophilic one with respect to differences between the maximum plasma concentrations (C<sub>max</sub>) measured after

morning and evening administration (Lemmer et al., 1991; Shiga et al., 1993). However, no significant changes in AUC were observed so far suggesting that circadian changes in the PD of medicines used in chronotherapy of CVS are the result of direct interaction with the target system rather than changes in efficacy because of changes in PK.

Last but not the least; consideration must be also given to the duration of treatment. Short elimination half-life suggests greater drug fluctuations in plasma. In short-term administration, this may also translate to more pronounced differences between morning and evening treatments (Portaluppi et al., 2007), especially when comparing the difference in decreasing the mean BP values. Conversely, once the steady state of drug is reached in the body and the plasma levels of the drug are constant, the chronopharmacological effect may be waning, so the difference between morning and evening doses is less profound. Thus, with respect to the treatment duration, chrono-effect is expected to be more prominent in the beginning rather than after long-term administration. Therefore, chronotherapy might be of clear benefit in settings, where rapid onset of treatment or normalization of BP pattern is needed.

However, it is of important note that significant difference between dosing regimens in terms of dipping prevalence has been observed in long-term treatment even if there was no more effect on the mean 24-h BP values. It is known that loss of the physiological circadian pattern of BP may lead to pathological mechanism associated with increased morbidity and mortality (Ohkubo et al., 2002). Chronically increased BP may even lead to general dysfunctional circadian body rhythms. For all blood pressure profiles with impaired, disturbed, or otherwise deviating rhythmicity compared with

normal diurnal pattern, it was confirmed that there is a clear association with the risk of cardiovascular disease (Takeda, Maemura, 2011). Normotensive non-dippers are exposed to almost the same risk of cardiovascular mortality as hypertensive dippers. It has been also shown that when the diurnal rhythm of BP was normalized, free survival of patients with heart failure has increased, whereas non-dipping is associated with increased incidence of cardiovascular events (Salles et al., 2016). Therefore, normalization of the circadian rhythm of BP is one of the primary targets in the treatment of hypertension. Vast majority of reviewed RCT have shown normalization of the dipping profile and/or changes in asleep BP values when applying chronotherapy, and this fact may have even more clinical impact than the differences in the mean 24-h BP reduction alone.

## CONCLUSION

The results from the RCTs clearly indicate that appropriate timing for dosing of antihypertensive drugs may increase the control of the hypertension; however, consideration must always be given to the circadian rhythm of the targeted site of action, kinetic profile of the drug, and also to the duration of treatment. Although the comparison between morning and evening dosing has not been always translated into significant difference in the decrease in the mean 24-h BP values, normalization of the circadian rhythm of BP has been achieved with appropriate timing of pharmacological intervention. With the later having the clear clinical relevance in terms of decreased CVS morbidity, these data substantiate the need for chronopharmacological approach in clinical settings.

## References

- [1] Asmar R, Gosse P, Quere S, Achouba A. Efficacy of morning and evening dosing of amlodipine/valsartan combination in hypertensive patients uncontrolled by 5 mg of amlodipine. *Blood pressure monitoring*. 2011 Apr 1;16(2):80-6.
- [2] Dahlöf B. Management of cardiovascular risk with RAS inhibitor/CCB combination therapy. *Journal of human hypertension*. 2009 Feb;23(2):77.
- [3] De La Sierra A, Redon J, Banegas JR, Segura J, Parati G, Gorostidi M, de la Cruz JJ, Sobrino J, Llisterri JL, Alonso J, Vinyoles E. Prevalence and factors associated with circadian blood pressure patterns in hypertensive patients. *Hypertension*. 2009 Mar 1;53(3):466-72.
- [4] Hermida RC, Ayala DE, Fernández JR, Portaluppi F, Fabbian F, Smolensky MH. Circadian rhythms in blood pressure regulation and optimization of hypertension treatment with ACE inhibitor and ARB medications. *American journal of hypertension*. 2011 Apr 1;24(4):383-91
- [5] Hermida RC, Ayala DE, Fernández JR, Mojón A, Smolensky MH, Fabbian F, Portaluppi F. Administration-time differences in effects of hypertension medications on ambulatory blood pressure regulation. *Chronobiology international*. 2013 Mar 1;30(1-2):280-314.
- [6] Hermida RC, Ayala DE, Fontao MJ, Mojón A, Fernández JR. Chronotherapy with valsartan/amlodipine fixed combination: improved blood pressure control of essential hypertension with bedtime dosing. *Chronobiology international*. 2010 Jul 1;27(6):1287-303.
- [7] Hermida RC, Ayala DE, Mojón A, Fernández JR. Chronotherapy with nifedipine GITS in hypertensive patients: improved efficacy and safety with bedtime dosing. *American journal of hypertension*. 2008 Aug 1;21(8):948-54.
- [8] Kasiakogias A, Tsioufis C, Thomopoulos C, Andrikou I, Aragiannis D, Dimitriadis K, Tsiachris D, Bilo G, Sideris S, Filis K, Parati G. Evening versus morning dosing of antihypertensive drugs in hypertensive patients with sleep apnoea: a cross-over study. *Journal of hypertension*. 2015 Feb 1;33(2):393-400.
- [9] Langner B, Lemmer B. Circadian changes in the pharmacokinetics and cardiovascular effects of oral propranolol in healthy subjects. *European journal of clinical pharmacology*. 1988 Nov 1;33(6):619-24.

- [10] Lemmer B. The importance of circadian rhythms on drug response in hypertension and coronary heart disease—from mice and man. *Pharmacology & therapeutics*. 2006 Sep 1;111(3):629-51.
- [11] Lemmer B, Nold G, Behne S, Kaiser R. Chronopharmacokinetics and cardiovascular effects of nifedipine. *Chronobiology international*. 1991 Jan 1;8(6):485-94.
- [12] Liu X, Liu X, Huang W, Leo S, Li Y, Liu M, Yuan H. Evening-versus morning-dosing drug therapy for chronic kidney disease patients with hypertension: a systematic review. *Kidney and Blood Pressure Research*. 2014;39(5):427-40.
- [13] Liu Y, Ushijima K, Ohmori M, Takada M, Tateishi M, Ando H, Fujimura A. Chronopharmacology of angiotensin II-receptor blockers in stroke-prone spontaneously hypertensive rats. *Journal of pharmacological sciences*. 2011;1101240507-.
- [14] Ohkubo T, Hozawa A, Yamaguchi J, Kikuya M, Ohmori K, Michimata M, Matsubara M, Hashimoto J, Hoshi H, Araki T, Tsuji I. Prognostic significance of the nocturnal decline in blood pressure in individuals with and without high 24-h blood pressure: the Ohasama study. *Journal of hypertension*. 2002 Nov 1;20(11):2183-9.
- [15] Portaluppi F, Lemmer B. Chronobiology and chronotherapy of ischemic heart disease. *Advanced drug delivery reviews*. 2007 Aug 31;59(9-10):952-65.
- [16] Portaluppi F, Tiseo R, Smolensky MH, Hermida RC, Ayala DE, Fabbian F. Circadian rhythms and cardiovascular health. *Sleep medicine reviews*. 2012 Apr 1;16(2):151-66.
- [17] Potucek P, Klimas J. Chronotherapy of hypertension with combination treatment. *Die Pharmazie-An International Journal of Pharmaceutical Sciences*. 2013 Dec 2;68(12):921-5.
- [18] Potucek P, Radik M, Doka G, Kralova E, Krenek P, Klimas J. mRNA levels of circadian clock components Bmal1 and Per2 alter independently from dosing time-dependent efficacy of combination treatment with valsartan and amlodipine in spontaneously hypertensive rats. *Clinical and Experimental Hypertension*. 2017 Nov 17;39(8):754-63.
- [19] Qiu YG, Chen JZ, Zhu JH, Yao XY. Differential effects of morning or evening dosing of amlodipine on circadian blood pressure and heart rate. *Cardiovascular drugs and therapy*. 2003 Jul 1;17(4):335-41.
- [20] Salles GF, Reboldi G, Fagard RH, Cardoso CR, Pierdomenico SD, Verdecchia P, Eguchi K, Kario K, Hoshida S, Polonia J, de la Sierra A. Prognostic effect of the nocturnal blood pressure fall in hypertensive patients: the ambulatory blood pressure collaboration in patients with hypertension (ABC-H) meta-analysis. *Hypertension*. 2016 Apr;67(4):693-700.
- [21] Schillaci G, Battista F, Settini L, Schillaci L, Pucci G. Antihypertensive drug treatment and circadian blood pressure rhythm: a review of the role of chronotherapy in hypertension. *Current pharmaceutical design*. 2015 Feb 1;21(6):756-72.
- [22] Shiga T, Fujimura A, Tateishi T, Ohashi K, Ebihara A. Differences of chronopharmacokinetic profiles between propranolol and atenolol in hypertensive subjects. *The Journal of Clinical Pharmacology*. 1993 Aug;33(8):756-61.
- [23] Smolensky MH, Hermida RC, Ayala DE, Tiseo R, Portaluppi F. Administration-time-dependent effects of blood pressure-lowering medications: basis for the chronotherapy of hypertension. *Blood pressure monitoring*. 2010 Aug 1;15(4):173-80.
- [24] Takeda N, Maemura K. Circadian clock and cardiovascular disease. *Journal of cardiology*. 2011 May 1;57(3):249-56.
- [25] Wu X, Liu Z, Shi G, Xing L, Wang X, Gu X, Qu Z, Dong Z, Xiong J, Gao X, Zhang C. The circadian clock influences heart performance. *Journal of biological rhythms*. 2011 Oct;26(5):402-11.
- [26] Zhao P, Xu P, Wan C, Wang Z. Evening versus morning dosing regimen drug therapy for hypertension. *Cochrane Database of Systematic Reviews*. 2011(10).

# Tannins, novel inhibitors of the volume regulation and the volume-sensitive anion channel

Original Paper

Tsiferova N.A.<sup>1,2‡</sup>, Khamidova O. J.<sup>1‡</sup>, Amonov A. U.<sup>1,3</sup>, Rakhimova M. B.<sup>1,3</sup>, Rustamova S. I.<sup>1</sup>,  
Kurbannazaova R. Sh.<sup>1,5</sup>, Merzlyak P. G.<sup>1</sup>, Abdulladjanova N. G.<sup>4</sup>, Sabirov R. Z.<sup>1,3✉</sup>

<sup>1</sup>Institute of Biophysics and Biochemistry, National University of Uzbekistan, Tashkent, Uzbekistan

<sup>2</sup>Center for Advanced Technologies, Tashkent, Uzbekistan

<sup>3</sup>Department of Biophysics, National University of Uzbekistan, Tashkent, Uzbekistan

<sup>4</sup>Institute of Bioorganic Chemistry, Academy of Sciences of Uzbekistan, Tashkent, Uzbekistan

<sup>5</sup>Institute of Chemical Technology, Tashkent, Uzbekistan

<sup>‡</sup>These authors contributed equally to this study

Received 19 June, 2019, accepted 16 October, 2019

**Abstract** The volume-sensitive outwardly rectifying anion channel (VSOR) is a key component of volume regulation system critical for cell survival in non-isosmotic conditions. The aim of the present study was to test the effects of four tannin extracts with defined compositions on cell volume regulation and VSOR. Preparation I (98% of hydrolysable tannins isolated from leaves of sumac *Rhus typhina* L.) and Preparation II (100% of hydrolysable tannins isolated from leaves of broadleaf plantain *Plantago major* L.) completely and irreversibly abolished swelling-activated VSOR currents in HCT116 cells. Both preparations profoundly suppressed the volume regulation in thymocytes with half-maximal effects of 40.9 µg/ml and 12.3 µg/ml, respectively. The inhibition was more efficient at lower concentrations but reverted at higher doses due to possible non-specific membrane-permeabilizing activity. Preparations III and IV (54.7% and 54.3% of hydrolysable tannins isolated, respectively, from roots and aboveground parts of Fergana spurge *Euphorbia ferganensis* B.Fedtch) inhibited VSOR activity in a partially reversible manner and suppressed the volume regulation with substantially higher half-maximal doses of 270 and 278 µg/ml, respectively, with no secondary reversion at higher doses. Hydrolysable tannins represent a novel class of VSOR channel inhibitors with the capacity to suppress the cell volume regulation machinery.

**Keywords** Tannins – plant polyphenols – thymocytes – cell volume regulation – volume-sensitive anion channel

This work was supported by the Ministry of Innovative Development of the Republic of Uzbekistan (under the grants FA-A11-T060 and PZ2017092049).

## INTRODUCTION

In order to survive in constantly changing osmotic conditions caused by intensive physiological processes (breathing, food intake, fluid secretion and absorption, filtration and urine formation, etc.) and pathologies (inflammation, edema, trauma, ischemia and hypoxia), living cells developed elaborate volume regulatory mechanisms. The volume-sensitive outwardly rectifying anion channel (VSOR) is a key

component of the cellular volume regulation system and of some other physiological and pathophysiological processes including cell proliferation, migration and apoptosis (Akita & Okada, 2014; Hoffmann et al., 2014; Okada et al., 2009). VSOR is the main pathway for the efflux of anions from swollen cells and, in cooperation with the Ca-activated potassium channels, provides a reduction of the intracellular osmotic pressure during the active phase of volume regulation upon the hypoosmotic stress called the Regulatory Volume Decrease (RVD) (Akita et al., 2011; Akita & Okada, 2014; Delpire & Gagnon, 2018; Hoffmann et al., 2014; Okada et al., 2006; Pedersen et al., 2016). Recent studies have demonstrated that the LRRC8 family proteins constitute the molecular

\* E-mail: zairovich@gmail.com

© European Pharmaceutical Journal

basis of VSOR (Qiu et al., 2014; Voss et al., 2014), structurally organized into a hexameric pore (Deneka et al., 2018; Kasuya et al., 2018; Kefauver et al., 2018). However, pharmacology of this biologically important ion channel remains poorly explored. Thus far, a number of structurally diverse compounds including stilbene derivatives, etacrynic acid analogs and flavonoids have been shown to suppress the activity of VSOR in a voltage-dependent and independent manner (Okada et al., 2019; Xue et al., 2018).

Tannins are structurally heterogeneous polyphenols, which bind to proteins and can trigger their precipitation (Mavlyanov et al., 2001). Tannins are secondary metabolites and constitute a part of the plants' defense system against pathogens and insect's invasion. In addition, these substances exhibit a wide spectrum of biological activities such as antimicrobial (Scalbert, 1991); antioxidant, (Rice-Evans et al., 1995, 1996); anti-inflammatory (Terra et al., 2007; Xue et al., 2018); neuroprotective (Behravan et al., 2014). Tannins, along with other polyphenolic compounds, have been considered to be responsible for the health benefits of red wine and green tea, possibly by inhibiting the activity of the Ca-activated chloride channels (CaCCs) (Namkung et al., 2010). Penta-m-digalloyl-glucose, a hydrolysable tannin extracted from the Chinese gallnut, was demonstrated to inhibit the cystic fibrosis transmembrane conductance regulator protein (CFTR), a chloride channel activated by intracellular cAMP (Wongsamitkul et al., 2010). Tannic acid was shown to inhibit CaCCs formed by TMEM16A and B (Cruz-Rangel et al., 2015; Namkung et al., 2010, 2011) and TMEM16F (Sztejn et al., 2012), which is consistent with an antidiarrhoeic activity of tannin-containing extracts reported earlier (Galvez et al., 1991). Tannic acid also blocks L-type Ca-channels (Zhu et al., 2016) and the maxi-anion channel (Woll et al., 1987). The latter is known to be swelling-activated (Okada et al., 2018, 2019; Sabirov & Merzlyak, 2012; Sabirov et al., 2016), although it operates mostly when cells are metabolically deprived, whereas VSOR is the major contributor to the swelling-activated plasmalemmal conductance at normal intracellular ATP levels. Tannins were never considered as modulators of the cell volume regulation system and its constituent components. Here, we tested four tannin preparations of plant origin on their effects on the cell volume regulation in rat thymocytes and the VSOR channel activity in HCT116 human colon cancer cells.

## MATERIALS AND METHODS

### Substances

The plants were collected from the Tashkent environs during the flowering stage and taxonomically identified by Dr. Gnatchenko E.V. of the Institute of Botany of the Academy of Sciences of Uzbekistan. Preparation of tannin extracts was performed essentially as described previously (Islambekov et al., 1994; Olchowik-Grabarek et al., 2017)

and their composition was determined by a combination of preparative column chromatography (silica gel, polyamide), quantitative paper chromatography and spectral methods as described elsewhere (Abdulladzhanova et al., 2001).

Preparation I was obtained from the leaves of sumac (*Rhus typhina* L.) and contained: 3,6-bis-*O*-di-*O*-galloyl-1,2,4-tri-*O*-galloyl- $\beta$ -D-glucose (74%); 1,2,3,4,6-penta-*O*-galloyl- $\beta$ -D-glucose (10%); 1,4,6-tri-*O*-galloyl- $\beta$ -D-glucose (5%); 2,3-di-*O*-galloyl- $\beta$ -D-glucose (2%); 2-*O*-galloyl- $\beta$ -D-glucose (2%); 3-*O*-galloyl- $\beta$ -D-glucose (2%); 6-*O*-galloyl- $\beta$ -D-glucose (2%); gallic acid (1%); rutin (1%); quercetin (0.5%); kaempferol (0.5%).

Preparation II was obtained from the leaves of broadleaf plantain (*Plantago major* L.) and contained: diester of hexahydroxydiphenoyl-1-(*O*-2-*O*-galloyl- $\beta$ -D-glucopyranosido)-1-(*O*- $\beta$ -D-xylopyranosido) (30.1%); diester of hexahydroxydiphenoyl-1-(*O*- $\beta$ -D-glucopyranosido)-2-(*O*-4-*O*-galloyl- $\beta$ -D-glucopyranosido) (27.9%); quercetin-3-*O*-(2",6"-di-*O*-galloyl-3"-*O*-*p*-coumaroyl)- $\beta$ -D-glucopyranoside (25.4%); kaempferol-3-*O*-(2",3"-di-*O*-galloyl-6"-*O*-coumaroyl)- $\beta$ -D-glucopyranoside (16.6%).

Preparation III was obtained from the roots of Fergana spurge (*Euphorbia ferganensis* B.Fedtsch.) and contained: 1-*O*-galloyl-2,4-valoneoyl-4,6-hexahydroxydiphenoyl- $\beta$ -D-glucose (48%); gallic acid (15%); digallic acid (10%); ellagic acid (9%); terchebin (8%); 2,3-digalloyl- $\beta$ -D-glucose (6.7%); quercetin-3-*O*-rutinoside (2.3%); myricetin (0.8%); iso-myricitrin (0.2%).

Preparation IV was obtained from the aboveground part of Fergana spurge (*Euphorbia humifusa* Willd.) and contained: 1-*O*-galloyl-4,6-hexahydroxydiphenoyl- $\beta$ -D-glucose (35%); quercetin (17%); ellagic acid (10.8%); 3-*O*-galloyl-4,6-hexahydroxydiphenoyl- $\beta$ -D-glucose (8.3%); 1,2,3-tri-*O*-galloyl- $\beta$ -D-glucose (7%); gallic acid (7%); geraniin (2.5%); quercetin-3-*O*-rhamnoside (4%); quercetin-3-*O*-galactoside (3.2%); kaempferol-3-*O*-glucoside (2.7%); 1-*O*-galloyl-6-*O*-bis-galloyl-2,4-valoneoyl- $\beta$ -D-glucose (1.5%); kaempferol (1%).

The tannin preparations were added from concentrated stock solutions in dimethylsulfoxide (DMSO). Final concentration of DMSO did not exceed 0.1%, and at this concentration, the solvent did not significantly affect the records.

### Solutions

The normal Ringer solution contained (mM): 135 NaCl, 5 KCl, 2 CaCl<sub>2</sub>, 1 MgCl<sub>2</sub>, 11 HEPES, 5 glucose (pH 7.4, adjusted with NaOH, 290 mOsm/kg-H<sub>2</sub>O). The H-buffer contained (mM): 5 KCl, 2 CaCl<sub>2</sub>, 1 MgCl<sub>2</sub>, 10 HEPES, 5 glucose (pH 7.4, adjusted with NaOH, 40 mOsm/kg-H<sub>2</sub>O). Hypotonic solutions were prepared by mixing the Ringer solutions with H-buffer in a ratio of 3:4 (vol/vol). The pipette solution for whole-cell experiments contained (in mM): 125 CsCl, 2 CaCl<sub>2</sub>, 1 MgCl<sub>2</sub>, 3 Na<sub>2</sub>ATP, 5 HEPES (pH 7.4 adjusted with CsOH), 10 EGTA, and 50 mannitol (pCa 7.65; 320 mOsm/kg-H<sub>2</sub>O).

## Cells

Human colon tumor cell line, HCT116, was cultured in DMEM supplemented with 10% of fetal bovine serum and antibiotics (100 U/ml penicillin plus 100 mg/ml streptomycin) at 37°C and 5% CO<sub>2</sub>. For patch-clamping, the cells were cultured in suspension under mild stirring during 3–5 h.

All animal experiments were conducted in accordance with the ARRIVE guidelines and approved by the Bioethics Committee of the Institute of Biophysics and Biochemistry. The isolation of thymic lymphocytes (thymocytes) was performed as described previously (Kurbannazarova et al., 2003, 2008, 2011; Sabirov et al., 2013). Briefly, the 6–8 weeks old rats, kept in vivarium on an average diet, were anaesthetized with halothane or diethyl ether and painlessly euthanized by cervical dislocation. The thymi were dissected and carefully washed with an ice-cold normal Ringer solution. The thymi were then minced using fine forceps and passed through a 100 µm-nylon mesh. The suspension was centrifuged at 1000 g for 5 min; the pellet was washed two times with the normal Ringer solution and resuspended in this medium at a cell density of 100 × 10<sup>6</sup> cells/ml. The cell suspension was kept on ice for ≤ 5 h and contained no more than 5% of damaged cells as assayed by trypan blue exclusion.

## Cell Volume Measurements

Cell volume changes under non-isosmotic conditions were recorded by light transmittance measurement as described previously (Kurbannazarova et al., 2003, 2008, 2011). Briefly, 900 ml of the normal Ringer or hypotonic solutions was added to the 1.5 cm<sup>3</sup> glass cuvette thermo stated with a water jacket and equilibrated for 10 min. An aliquot (100 ml) of cell suspension was added to this medium to yield the final cell density of 10 × 10<sup>6</sup> cells/ml. The light transmittance was measured at 610 nm (band-pass filter) using a photometer MKMF-01 (Russia). The output signal was amplified by U5-11 amplifier (Russia), digitized at 100 Hz using a USB sensor interface GO!Link and recorded by Logger Lite software (Vernier, Beaverton, OR).

The parameter *RVD* was calculated using the following equation (1):

$$RVD = (T_{max} - T_{15}) / (T_{max} - T_0) * 100\% \quad (1)$$

where  $T_0$  and  $T_{max}$  are the initial and maximal light transmittances, and  $T_{15}$  is the light transmittance measured 15 minutes after the onset of hypotonic stress.  $RVD = 100$  for complete recovery of the cell volume to the initial level, and  $RVD = 0$  when volume regulation is fully suppressed. Under control conditions,  $RVD$  usually had values of 60–90% depending on the cells condition, osmotic gradient, temperature and other experimental conditions.

## Electrophysiology

Patch electrodes were fabricated from borosilicate glass capillaries using a micropipette puller (PP-830, Narishige, Japan) and had a tip resistance of 3–5 MΩ when filled with pipette solution. Fast and slow capacitive transients were routinely compensated for. For whole-cell recordings, the access resistance did not exceed 10 MΩ and was always compensated for by 80%. Membrane currents were measured with an EPC-9 patch-clamp system (Heka-Electronics, Lambrecht/Pfalz, Germany). The membrane potential was controlled by shifting the pipette potential ( $V_p$ ) and is reported as  $V_p$  for whole-cell recordings. Currents were filtered at 1 kHz and sampled at 5–10 kHz. Data acquisition and analysis were done using Pulse + PulseFit (Heka-Electronics). Liquid junction potentials were calculated using pCLAMP 8.1 (Molecular Devices, Sunnyvale, CA) algorithms and were corrected off-line when appropriate. All experiments were performed at room temperature (23–25 °C).

## Data analysis

The dose-response data were approximated using a Hill equation of the following form:

$$RVD = RVD_{min} + (RVD_{max} - RVD_{min}) / (1 + (C/IC_{50})^h) \quad (2)$$

Here:  $RVD_{min}$  and  $RVD_{max}$  are the minimal and maximal values of  $RVD$ ,  $C$  – concentration of the substance (µg/ml),  $IC_{50}$  – concentration of the substance rendering a half-maximal inhibitory effect (µg/ml),  $h$  – Hill coefficient.

Data were analyzed using Origin 8 (OriginLab Corporation, Northampton, MA, USA). Pooled data are given as means ± SEM of  $n$  observations. Comparisons between the two experimental groups were made using the unpaired two-sample Student's *t*-test. The data of Fig. 3d and 4d were analyzed using both unpaired two-sample (comparison at different voltages) and one-sample (comparison with control) *t*-test. Differences were considered to be statistically significant at  $p < 0.05$ .

## RESULTS

### Tannin preparations inhibit thymocyte volume regulation under hypoosmotic stress

Blockers of VSOR channel are expected to suppress the regulatory volume decrease phase of cellular response to the hypoosmotic stress. In order to test this possibility, we employed the immature thymic lymphocytes which possess fully functional volume regulation machinery (Arrazola et al., 1993; Kurbannazarova et al., 2003; Soler et al., 1993). We have previously shown that thymocytes express the VSOR channels with the same biophysical and pharmacological profile as other cell types, and that VSOR blockers completely abolish

RVD in these cells (Kurbannazarova et al., 2011; Sabirov et al., 2013). Therefore, we supposed that tannin preparations might affect the volume regulation in thymocytes.

In our experiments, thymocytes, when challenged with hypoosmotic stress, first rapidly swelled (passive response) and then gradually restored their volume toward an initial level (active response; Fig. 1a). The parameter RVD as defined by Equation (1) (see Experimental section) ranged from 66% to 93% and averaged at  $79.6 \pm 1.9\%$  ( $n = 17$ ).

When added to the hypoosmotic medium, tannin preparations I and II exhibited a profound suppressive effect on the thymocyte volume regulation (Fig. 1a,b). For preparation I, an inhibition at lower doses was gradually lost as the amount of the added preparation was increased above  $30 \mu\text{g/ml}$  (Fig. 1a,c). Since the maximal swelling also declined at high doses, we supposed that high concentrations of preparation I were detrimental for cellular plasma membrane. A similar biphasic action was also observed for preparation II (Fig. 1b,d). The half-maximal concentrations and Hill coefficients for the inhibiting phase of the dose-response curves (solid circles and solid lines in Fig. 1c,d) were as follows: preparation I ( $IC_{50} = 40.9 \pm 7.2 \mu\text{g/ml}$ ;  $h = 0.96 \pm 0.2$ ) and preparation II ( $IC_{50} = 12.3 \pm 8.1 \mu\text{g/ml}$ ;  $h = 0.59 \pm 0.294$ ).

In contrast to the first two preparations, preparations III and IV did not affect the maximal swelling and did not display the secondary damaging phase on the dose-response curves (Fig. 2). The half-maximal concentrations and Hill coefficients for the inhibiting phase of the dose-response curves (solid circles and solid lines in Fig. 2c,d) were as follows: preparation III ( $IC_{50} = 270 \pm 77 \mu\text{g/ml}$ ;  $h = 0.63 \pm 0.15$ ) and preparation IV ( $IC_{50} = 278 \pm 43 \mu\text{g/ml}$ ;  $h = 0.65 \pm 0.07$ ).

Comparison of the  $IC_{50}$  values suggested that preparations I and II are more efficient inhibitors of the cell volume regulation than preparations III and IV.

### Tannin preparations block the swelling-induced anion conductance

Tannins were never considered as volume-regulated anion channel blockers. In order to test this possibility, we employed direct electrophysiological assessment of the VSOR channel activity in human colorectal cancer HCT116 cells, which have been used recently for molecular identification of the VSOR channel proteins (Qiu et al., 2014; Voss et al., 2014).

In our experiments, we filled the patch-pipettes with slightly hypertonic (by  $\sim 30 \text{ mOsm/kg-H}_2\text{O}$ ) solution to induce cellular swelling as described previously (Kurbannazarova et al., 2011; Sabirov et al., 2013). Upon attaining the *whole-cell* configuration, cells gradually swelled as could be observed visually under phase-contrast microscopy. The cellular swelling was accompanied by a robust activation of the macroscopic currents with outward rectification and inactivation at large depolarizing positive potentials (Fig. 3a,b), a phenotypical landmark of the VSOR anion channel (Okada, 1997).

When preparations I and II were added to the flow chamber at a dose of  $31 \mu\text{g/ml}$  and  $41 \mu\text{g/ml}$ , respectively (at these doses, their effect on RVD was maximal, see Fig. 1c,d), we observed almost instant suppression of the macroscopic currents (Fig. 3a,b). The effect was essentially irreversible. The ionic currents were suppressed at both positive and negative potentials (Fig. 3c,d) suggesting that the channel blockage is voltage-independent. Voltage-independence together with the irreversibility of blockage may indicate a strong, possibly covalent, interaction of the tannins with the channel protein. Preparations III and IV also exhibited suppressive effects on the macroscopic swelling-induced conductance. However, in contrast to the preparations I and II, current inhibition by preparations III and IV was slower (Fig. 4a,b) and partially reversible. The currents in the presence of these preparations were decreased more efficiently at positive potentials (Fig. 4c,d) than at negative voltages. Reversibility of the inhibition together with voltage-dependency may suggest an open-channel blockage mechanism: applied positive voltage drives the negatively charged polyphenolic compounds applied from the extracellular side into the channel lumen.

### DISCUSSION

Thus, we have demonstrated that polyphenolic tannins of plant origin represent a novel class of VSOR channel inhibitors. This activity may contribute to the well-documented beneficial health effects of *polyphenol-rich food* and drink products.

In our experiments, preparations (I and II) were more efficient inhibitors of VSOR and volume regulation system compared to the preparations III and IV. Since preparation II consisted exclusively of hydrolysable tannins, and the content of hydrolysable tannins in preparation I reached 98%, we inferred that hydrolysable tannins represent a novel class of VSOR channel inhibitors. Certainly, the tannin preparations used in these experiments have rather complex composition, and thus, the individual tannins might be more effective and selective modulators of the VSOR chloride channel.

Preparations III and IV contained less overall tannin content (54.7% and 54.3%, respectively) and were less effective. Possibly, other types of polyphenols, which constituted a large part of these preparations may have weakened the inhibitory effects of hydrolysable tannins of preparations III and IV.

It should be noted that 3,6-bis-O-digalloyl-1,2,4-tri-O-galloyl- $\beta$ -D-glucose, which is the major component of Preparation I, was recently shown to form anion-selective channels in lipid bilayers (Borisova et al., 2019). This effect may explain the secondary rising phase on the dose-response curve on the Figure 1a,c, suggesting that these newly formed pores functionally replace the VSOR channel by serving as a pathway for anion efflux. Since Preparation II also displayed a biphasic effect of RVD, one may suppose that some of its

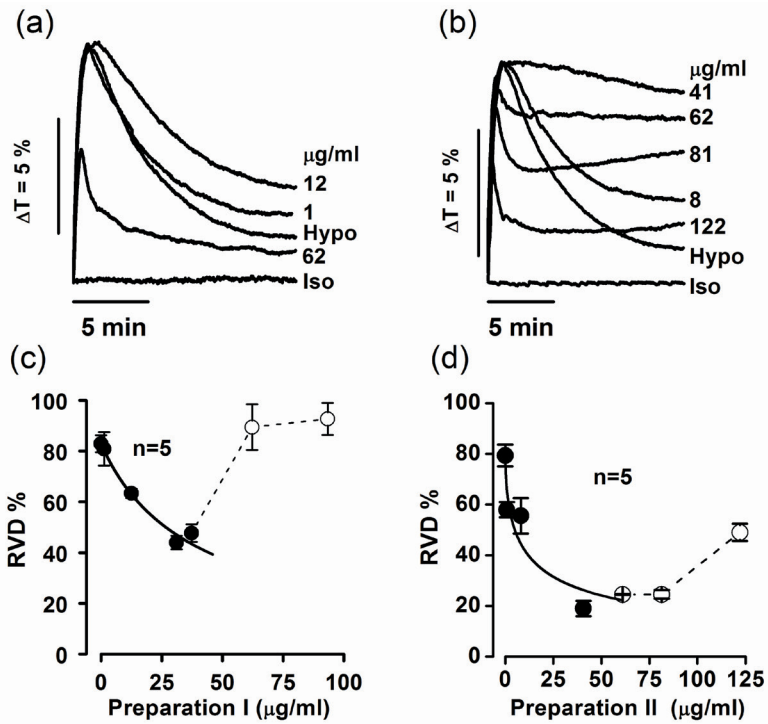


Figure 1: Dose-dependent effects of Preparations I and II on the thymocyte volume regulation under hypoosmotic stress. (a, b) Representative recordings of light transmittance changes. (c, d) Dose-response curves; the solid lines are fits to the equation (2) with half-maximal concentrations and Hill coefficients given in the text.

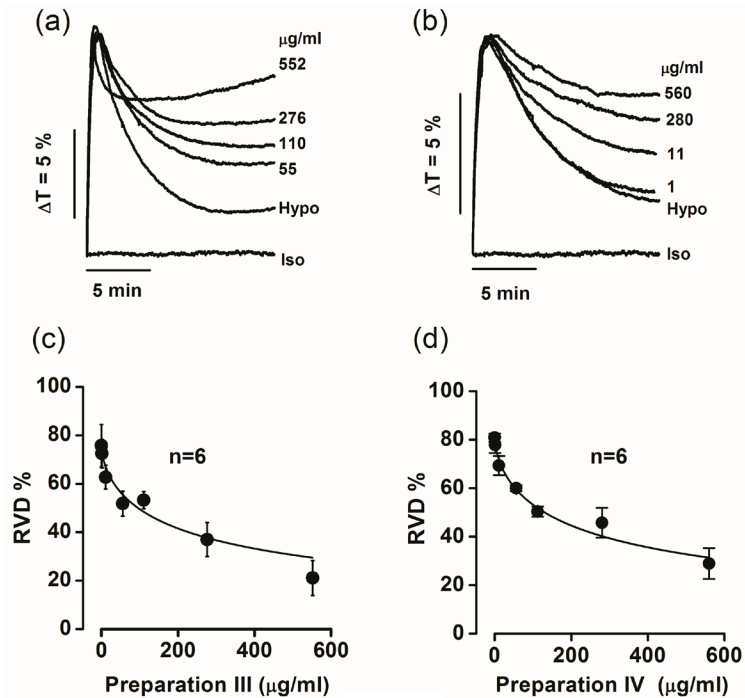


Figure 2: Dose-dependent effects of Preparations III and IV on the thymocyte volume regulation under hypoosmotic stress. (a, b) Representative recordings of light transmittance changes. (c, d) Dose-response curves; the solid lines are fits to the equation (2) with half-maximal concentrations and Hill coefficients given in the text.

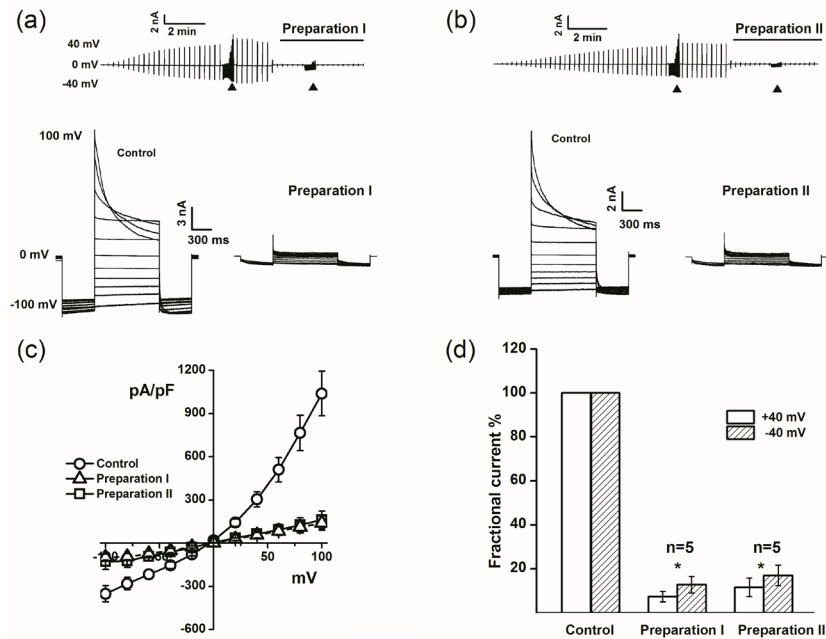


Figure 3: Inhibition of VSOR currents by Preparations I and II. (a, b) The time course of whole-cell current activation in response to cell swelling. Currents were elicited by application of alternating test-pulses from 0 to  $\pm 40$  mV every 15 s. Arrowheads ( $\blacktriangle$ ) denote the time points where the step-pulses from  $-100$  to  $+100$  mV in 20 mV increments were applied to test the voltage-dependence of the macroscopic conductance. (c) Instantaneous current-to-voltage relationships measured at the beginning of test-pulses from recordings similar to those shown in (a) and (b);  $n = 5$  for Preparation I and  $n = 4$  for Preparation II. (d) Fractional currents measured at  $+40$  mV (open bars) and  $-40$  mV (hatched bars). \*Significantly different from control values at  $p < 0.05$ .

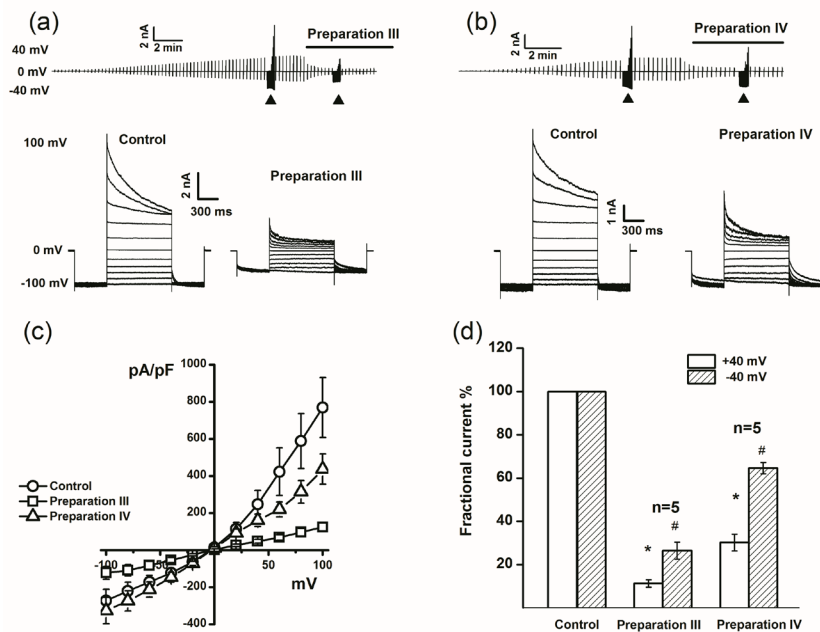


Figure 4: Inhibition of VSOR currents by Preparations III and IV. (a, b) The time course of whole-cell current activation in response to cell swelling. Currents were elicited by the application of alternating test-pulses from  $-100$  to  $+100$  mV in 20 mV increments were applied to test the voltage-dependence of the macroscopic conductance. (c) Instantaneous current-to-voltage relationships measured at the beginning of test-pulses from recordings similar to those shown in (a) and (b);  $n = 5$  for Preparation III and  $n = 4$  for Preparation IV. (d) Fractional currents measured at  $+40$  mV (open bars) and  $-40$  mV (hatched bars). \*Significantly different from control values at  $p < 0.05$ . #Significantly different at  $p < 0.05$  from values measured at negative voltages.

components could also act as pore formers on lipid matrix of the cellular plasma membrane.

What kind of pharmacological effects could be anticipated for VSOR-inhibitory hydrolysable tannins? It is known, that the most effective and selective blocker of VSOR channel, 4-(2-butyl-6,7-dichloro-2-cyclopentyl-indan-1-on-5-yl) oxobutyric acid (DCPIB), exhibits a great beneficial effect in the reversible middle cerebral artery occlusion (rMCAO) model in adult rats (Han et al., 2014; Zhang et al., 2008) and in neonatal mouse hypoxic-ischemic brain injury (Alibrahim et al., 2013; Wong et al., 2018). The drug also protected cardiomyocytes from injury induced by hyperglycemia (Wang et al., 2017). Given the well-known beneficial effects of the tannin-containing plant extracts in cerebral ischemia and stroke (Behravan et al., 2014), our results would suggest

that tannins antagonizing activity of the VSOR anion channel could be beneficial in protecting brain tissues, and possibly, the heart, during ischemic/hypoxic injury.

## ACKNOWLEDGEMENTS

This work was supported by the Ministry of Innovative Development of the Republic of Uzbekistan (under the grants FA-A11-T060 and PZ2017092049).

## CONFLICT OF INTEREST

The authors declare no conflict of interests.

## References

- [1] Abdulladzhanova NG, Mavlyanov SM, Dalimov DN. Phenolic Compounds of *Euphorbia ferganensis* B. Fedtsch. Chem Nat Compd. 2001;37:193–194.
- [2] Akita T, Fedorovich SV, Okada Y. Ca<sup>2+</sup> nanodomain-mediated component of swelling-induced volume-sensitive outwardly rectifying anion current triggered by autocrine action of ATP in mouse astrocytes. Cell Physiol Biochem. 2011;28:1181–1190.
- [3] Akita T, Okada Y. Characteristics and roles of the volume-sensitive outwardly rectifying (VSOR) anion channel in the central nervous system. Neuroscience. 2014;275:211–231.
- [4] Alibrahim A, Zhao LY, Bae CY, et al. Neuroprotective effects of volume-regulated anion channel blocker DCPIB on neonatal hypoxic-ischemic injury. Acta Pharmacol Sin. 2013;34:113–118.
- [5] Arrazola A, Rota R, Hannaert P, Soler A, Garay RP. Cell volume regulation in rat thymocytes. J Physiol. 1993;465:403–414.
- [6] Behravan E, Razavi BM, Hosseinzadeh H. Review of plants and their constituents in the therapy of cerebral ischemia. Phytother Res. 2014;28:1265–1274.
- [7] Borisova MP, Kataev AA, Sivozhelezov VS. Action of tannin on cellular membranes: Novel insights from concerted studies on lipid bilayers and native cells. Biochim Biophys Acta. 2019;1861:1103–1111.
- [8] Cruz-Rangel S, De Jesus-Perez JJ, Contreras-Vite JA, Perez-Cornejo P, Hartzell HC, Arreola J. Gating modes of calcium-activated chloride channels TMEM16A and TMEM16B. J Physiol. 2015;593:5283–5298.
- [9] Delpire E, Gagnon KB. Water Homeostasis and Cell Volume Maintenance and Regulation. Curr Top Membr. 2018;81:3–52.
- [10] Deneka D, Sawicka M, Lam AKM, Paulino C, Dutzler R. Structure of a volume-regulated anion channel of the LRRC8 family. Nature. 2018;558:254–259.
- [11] Galvez J, Zarzuelo A, Crespo ME, et al. Antidiarrhoeic activity of *Sclerocarya birrea* bark extract and its active tannin constituent in rats. Phytother Res. 1991;5:276–278.
- [12] Han Q, Liu S, Li Z, et al. DCPIB, a potent volume-regulated anion channel antagonist, attenuates microglia-mediated inflammatory response and neuronal injury following focal cerebral ischemia. Brain Res. 2014;1542:176–185.
- [13] Hoffmann EK, Holm NB, Lambert IH. Functions of volume-sensitive and calcium-activated chloride channels. IUBMB Life. 2014;66:257–267.
- [14] Islambekov YS, Mavlyanov S, Kamaev FG, Ismailov AI. Phenolic compounds of sumac. Chem Nat Compd. 1994;30:37–39.
- [15] Kasuya G, Nakane T, Yokoyama T, et al. Cryo-EM structures of the human volume-regulated anion channel LRRC8. Nat Struct Mol Biol. 2018;25:797–804.
- [16] Kefauver JM, Saotome K, Dubin AE, et al. Structure of the human volume regulated anion channel. Elife. 2018;7.
- [17] Kurbannazarova RS, Bessonova SV, Okada Y, Sabirov RZ. Swelling-activated anion channels are essential for volume regulation of mouse thymocytes. Int J Mol Sci. 2011;12:9125–9137.
- [18] Kurbannazarova RS, Tashmukhamedov BA, Sabirov RZ. Osmotic water permeability and regulatory volume decrease of rat thymocytes. Gen Physiol Biophys. 2003;22:221–232.
- [19] Kurbannazarova RS, Tashmukhamedov BA, Sabirov RZ. Role of potassium and chlorine channels in the regulation of thymocyte volume in rats. Bull Exp Biol Med. 2008;145:544–547.
- [20] Mavlyanov SM, Islambekov YS, Ismailov AI, Dalimov DN, Abdulladzhanova NG. Vegetable Tanning Agents. Chem Nat Compd. 2001;37:1–24.
- [21] Namkung W, Phuan PW, Verkman AS. TMEM16A inhibitors reveal TMEM16A as a minor component of calcium-activated chloride channel conductance in airway and intestinal epithelial cells. J Biol Chem. 2011;286:2365–2374.
- [22] Namkung W, Thiagarajah JR, Phuan PW, Verkman AS. Inhibition of Ca<sup>2+</sup>-activated Cl<sup>-</sup> channels by gallotannins as a possible molecular basis for health benefits of red wine and green tea. FASEB J. 2010;24:4178–4186.
- [23] Okada Y. Volume expansion-sensing outward-rectifier Cl<sup>-</sup> channel: fresh start to the molecular identity and volume sensor. Am J Physiol. 1997;273:C755–789.
- [24] Okada Y, Okada T, Islam MR, Sabirov RZ. Molecular Identities and ATP Release Activities of Two Types of Volume-Regulatory Anion Channels, VSOR and Maxi-Cl. Curr Top Membr. 2018;81:125–176.

- [25] Okada Y, Okada T, Sato-Numata K, et al. Cell Volume-Activated and Volume-Correlated Anion Channels in Mammalian Cells: Their Biophysical, Molecular, and Pharmacological Properties. *Pharmacol Rev.* 2019;71:49–88.
- [26] Okada Y, Sato K, Toychiev AH, et al. The Puzzles of Volume-Activated Anion Channels. In: *Physiology and Pathology of Chloride Transporters and Channels in the Nervous System*. San Diego: Elsevier; 2009.
- [27] Okada Y, Shimizu T, Maeno E, Tanabe S, Wang X, Takahashi N. Volume-sensitive chloride channels involved in apoptotic volume decrease and cell death. *J Membr Biol.* 2006;209:21–29.
- [27] Olchowik-Grabarek E, Mavlyanov S, Abdullajanova N, Gieniusz R, Zamaraeva M. Specificity of Hydrolysable Tannins from *Rhus typhina* L. to Oxidants in Cell and Cell-Free Models. *Appl Biochem Biotechnol.* 2017;181:495–510.
- [29] Pedersen SF, Okada Y, Nilius B. Biophysics and Physiology of the Volume-Regulated Anion Channel (VRAC)/Volume-Sensitive Outwardly Rectifying Anion Channel (VSOR). *Pflugers Arch.* 2016;468:371–383.
- [30] Qiu Z, Dubin AE, Mathur J, et al. SWELL1, a plasma membrane protein, is an essential component of volume-regulated anion channel. *Cell.* 2014;157:447–458.
- [31] Rice-Evans CA, Miller NJ, Bolwell PG, Bramley PM, Pridham JB. The relative antioxidant activities of plant-derived polyphenolic flavonoids. *Free Radic Res.* 1995;22:375–383.
- [32] Rice-Evans CA, Miller NJ, Paganga G. Structure-antioxidant activity relationships of flavonoids and phenolic acids. *Free Radic Biol Med.* 1996;20:933–956.
- [33] Sabirov RZ, Kurbannazarova RS, Melanova NR, Okada Y. Volume-sensitive anion channels mediate osmosensitive glutathione release from rat thymocytes. *PLoS One.* 2013;8:e55646.
- [34] Sabirov RZ, Merzlyak PG. Plasmalemmal VDAC controversies and maxi-anion channel puzzle. *Biochim Biophys Acta.* 2012;1818:1570–1580.
- [35] Sabirov RZ, Merzlyak PG, Islam MR, Okada T, Okada Y. The properties, functions, and pathophysiology of maxi-anion channels. *Pflugers Arch.* 2016;468:405–420.
- [36] Scalbert A. Antimicrobial properties of tannins. *Phytochemistry.* 1991;30:3875–3883.
- [37] Soler A, Rota R, Hannaert P, Cragoe EJ, Jr., Garay RP. Volume-dependent K<sup>+</sup> and Cl<sup>-</sup> fluxes in rat thymocytes. *J Physiol.* 1993;465:387–401.
- [38] Sztejn K, Schmid E, Nurbaeva MK, et al. Expression and functional significance of the Ca(2+)-activated Cl(-) channel ANO6 in dendritic cells. *Cell Physiol Biochem.* 2012;30:1319–1332.
- [39] Terra X, Valls J, Vitrac X, et al. Grape-seed procyanidins act as antiinflammatory agents in endotoxin-stimulated RAW 264.7 macrophages by inhibiting NFκB signaling pathway. *J Agric Food Chem.* 2007;55:4357–4365.
- [40] Voss FK, Ullrich F, Munch J, et al. Identification of LRRC8 heteromers as an essential component of the volume-regulated anion channel VRAC. *Science.* 2014;344:634–638.
- [41] Wang L, Shen M, Guo X, et al. Volume-sensitive outwardly rectifying chloride channel blockers protect against high glucose-induced apoptosis of cardiomyocytes via autophagy activation. *Sci Rep.* 2017;7:44265.
- [41] Woll KH, Leibowitz MD, Neumcke B, Hille B. A high-conductance anion channel in adult amphibian skeletal muscle. *Pflugers Arch.* 1987;410:632–640.
- [43] Wong R, Abussaud A, Leung JW, et al. Blockade of the swelling-induced chloride current attenuates the mouse neonatal hypoxic-ischemic brain injury in vivo. *Acta Pharmacol Sin.* 2018;39:858–865.
- [44] Wongsamitkul N, Sirianant L, Muanprasat C, Chatsudthipong V. A plant-derived hydrolysable tannin inhibits CFTR chloride channel: a potential treatment of diarrhea. *Pharm Res.* 2010;27:490–497.
- [45] Xue Y, Li H, Zhang Y, et al. Natural and synthetic flavonoids, novel blockers of the volume-regulated anion channels, inhibit endothelial cell proliferation. *Pflugers Arch.* 2018;470:1473–1483.
- [46] Zhang Y, Zhang H, Feustel PJ, Kimelberg HK. DCPIB, a specific inhibitor of volume regulated anion channels (VRACs), reduces infarct size in MCAo and the release of glutamate in the ischemic cortical penumbra. *Exp Neurol.* 2008;210:514–520.
- [46] Zhu F, Chu X, Wang H, et al. New Findings on the Effects of Tannic Acid: Inhibition of L-Type Calcium Channels, Calcium Transient and Contractility in Rat Ventricular Myocytes. *Phytother Res.* 2016;30:510–516.

# Chromatographic Profiles Analysis of Fruits of *Crataegus* L. Genus by High-Performance Thin-Layer Chromatography

Original Paper

Khokhlova K.O.<sup>1✉</sup>, Zdoryk O. A.<sup>1</sup>, Sydora N.V.<sup>1</sup>, Shatrovska V.I.<sup>2</sup><sup>1</sup>National University of Pharmacy, 53, Pushkinska, 61002 Kharkiv, Ukraine<sup>2</sup>Botanical Garden of V.N. Karazin Kharkiv National University, 52, Klochkivska, 61000 Kharkiv, Ukraine

Received 23 April, 2018, accepted 1 October, 2018

**Abstract** It was known that hawthorn - *Crataegus* L. is a polymorphic genus. Two hawthorn species and their hybrids are included in the European Pharmacopoeia, twelve – in Ukrainian pharmacopoeia. Determination of chromatographic profiles of hawthorn fruits species native to Ukraine and other countries that are non-pharmacopoeial, but have sufficient plant raw material base, is essential for quality control of drugs.

**Aim.** To analyze and compare the chromatographic profiles of fruits of 23 *Crataegus* L. species on phenolic compounds, evaluated by means of high-performance thin-layer chromatography procedure (HPTLC), and determine the specific features of chromatographic fingerprints.

**Materials and Methods.** A total of 39 samples of fruits of 23 hawthorn species that are native to Europe, Asia and North America, such as *Crataegus monogyna*, *C. laevigata*/*C. oxyacantha*, *C. leiomonogyna*, *C. curvisepala*, *C. pseudokyrstostyla*, *C. fallacina*, *C. subrotunda*, *C. ambigua*, *C. pentagyna*, *C. sanguinea*, *C. chlorosarca*, *C. almaatensis*, *C. pseudoheterophylla* subsp. *turkestanica*, *C. pinnatifida*, *C. pentagyna* subsp. *pseudomelanocarpa*, *C. punctata*, *C. pringlei*, *C. festiva*, *C. douglasii*, *C. holmesiana*, *C. submollis*, *C. flabellata*, *C. canadensis* were investigated. The analysis has been done following the TLC method from European Pharmacopoeia modified into HPTLC, using automated HPTLC herbal system (CAMAG, Switzerland).

**The results** have shown that chromatographic profiles of phenolic constituents of nine *Crataegus* L. species of Europe, both pharmacopoeial and non-pharmacopoeial, were quite similar, despite the significant morphological distinctions. The chromatographical profiles of three species of Asia were similar to the pharmacopoeial species; three other species looked different and had specific marker zones. In addition, eight *Crataegus* L. species of North America had specific markers helping for discriminative analysis from pharmacopoeial species.

**Conclusion.** The findings could help to identify the possible adulterations and prevent the falsification of finished products. The results will be taken into consideration during revision of the Ukrainian national pharmacopoeial monograph for hawthorn fruits.

**Keywords** Hawthorn – identification – phenolic compounds – high-performance thin-layer chromatography

## INTRODUCTION

Hawthorn berries (*Crataegi fructus*) is the herbal raw material that has been traditionally used for cardiac failure, myocardial weakness, paroxysmal tachycardia, hypertension, arteriosclerosis and Buerger's disease.<sup>[1]</sup> It is widely used in the commerce of Ukraine as bulk, extracts, tinctures and tablets.<sup>[2-4]</sup> The monograph on «hawthorn berries» is included in the European Pharmacopoeia and the State Pharmacopoeia of Ukraine.<sup>[5,6]</sup> According to these monographs, two species such as *Crataegus monogyna* Jacq. and *C. laevigata* (Poir.) DC. (*C. oxyacantha* L.) and their hybrids are allowed to be used as a herbal medicine. The national Ukraine monograph

on Hawthorn fruits<sup>[6]</sup> besides the *C. laevigata*/*C. oxyacantha* and *C. monogyna* includes 10 more other related Hawthorn species. Out of these pharmacopoeial species, there are four, namely *C. monogyna*; *C. laevigata*; *C. pentagyna* Waldst. a Kit. ex Willd.; *C. curvisepala* Lindm., that are native to Ukraine flora, while others are cultivated or can be exported.<sup>[7,8]</sup> Meanwhile, there are great numbers of other non-pharmacopoeial *Crataegus* L. species representative of the flora of Ukraine and other countries that have sufficient herbal raw material base. The identification of its chromatographic profiles is essential for quality control of finished herbal drugs.

\* E-mail: Kateryna\_Khokhlova@Ukr.Net

© European Pharmaceutical Journal

Thus, the **purpose** of this paper was the analysis and comparison of chromatographic profiles of phenolic constituents of fruits of 23 *Crataegus* L. species, growing in Europe, Asia and North America, evaluated by means of high-performance thin-layer chromatography (HPTLC), and the determination of specific distinguishing markers of its fingerprints.

## MATERIALS AND METHODS

### Standards

Hyperoside, batch 33520F, was purchased from USP; rutin, batch A0299493, and chlorogenic acid, batch A0290470, were purchased from EDQM.

### Samples

A total of 39 hawthorn samples of 23 *Crataegus* L. species obtained from Botanical Garden of V.N. Karazin Kharkiv National University, Ukraine and different States and regions, and purchased from the market were investigated in this study. All the samples were properly identified by botanist V.I. Shatrovska, Botanical Garden of V.N. Karazin Kharkiv National University, Ukraine according to the National floristic datasets.<sup>[7-9]</sup> Voucher specimens are deposited at the Herbarium of the Department Technology of Drugs, National University of Pharmacy, Kharkiv, Ukraine. Details and voucher specimen numbers are shown in Table 1.

### Source Of The Method

TLC method for *C. laevigata*/*C. oxyacantha* and *C. monogyna* from European Pharmacopoeia<sup>[5]</sup> was modernized into HPTLC method; 21 other different *Crataegus* L. species, growth worldwide (Table 1), were included in the method.

### Chromatographic Conditions

Analyses were conducted on Merck HPTLC silica gel F<sub>254</sub> (Darmstadt, Germany). The following mobile phase was used: *anhydrous formic acid R*, *water R*, *methyl ethyl ketone R*, *ethyl acetate R* (10:10:30:50). For identification 6 µL of standard solutions and 6 µL of sample solutions were applied to the plate.

### Visualization Of Fingerprints

The multiple detection modes used were white light and 366 nm after derivatization. Plates were heated at 100–105°C for 5 min and derivatized by dipping (speed of 3, t = 0), while still hot in NP/PEG reagents. The plate was evaluated after about 30 min. The NP/PEG reagent was prepared as follows: Solution A: 1.0 g of diphenylborinic acid aminoethylester is dissolved in 100 mL of methanol. Solution B: 10 g of polyethylene glycol 400 is dissolved in 200 mL of dichloromethane.

### Preparation Of Samples And Standards

*The sample solution of different Crataegus L. fruits:* 1.0 g of dried powdered sample was mixed with 10 mL of methanol absolute, sonicated for 10 min and centrifuged or filtered. The supernatant/filtrate was used as the sample solution

*Standard solution A:* 0.25 mg/mL of hyperoside in methanol; 0.35 mg/mL of rutin in methanol.

*Standard solution B:* 2.5 ml of Standard solution A was diluted with 10.0 mL of methanol.

*System suitability solution (SST):* 0.3 mg/mL of chlorogenic acid and 0.25 mg of hyperoside was diluted with 10.0 mL of methanol.

### Instruments And Reagents

*Instruments:* A CAMAG HPTLC system (Muttensz, Switzerland) included a visualizer, an Automatic TLC Sampler 4, an Automatic Developing Chamber 2, and a Scanner 4 controlled by visionCATS software.

*Reagents:* ethyl acetate (purity 99.5%), lot № AO355705, anhydrous formic acid (purity 98%), lot AO343914, were purchased from Acros Organics. Methanol (HPLC Ultra Gradient Grade), lot № 1042801 was purchased from CarlRoth GmbH.

## RESULTS AND DISCUSSION

The taxonomical classification of hawthorn genus is quite diffuse as all *Crataegus* L. species are quite variable and tend to hybridize with each other. For instance, according to the Flora of SSSR,<sup>[9]</sup> Russian and European authors often do not differentiate between *C. kyrtostyla* and *C. monogyna*, despite their significant morphological differences. From the other side, as is evident from Red Flora of URSR,<sup>[7]</sup> *C. kyrtostyla* is a generalized species and includes *C. curvisepala*, *C. pseudokyrtostyla* Klokov, *C. subrotunda* Klokov, *C. fallacina* Klokov.

Most of the identified *Crataegus* L. species used in the analysis conformed to the worldwide accepted database "The Plant list".<sup>[10]</sup> At the same time, some hawthorn species, that according to the national floristic datasets<sup>[7]</sup> have distinctive morphological features (Fig. S1), are listed in "The Plant List"<sup>[10]</sup> as synonyms (*C. oxyacantha*; *C. curvisepala*; *C. pseudokyrtostyla*; *C. subrotunda* are listed as synonym for *C. rhipidophylla* Gand. and *C. leiomonogyna* Klokov is listed as synonym for *C. monogyna*) or have unresolved status (*C. fallacina*, *C. festiva* Sarg.). These findings testify that "The Plant List" classification could be improved.

Despite that it is possible to discriminate different hawthorn species using morphological features when the fruits are intact, it is an analytical challenge for the finished dosage forms. It was established that hawthorn fruits are characterized by its phenolic constituents, in particular, the flavonoid components to which many of the pharmacological

Table 1: Description of the samples analyzed

N	Species	Voucher Spicemens Number	Amount	Growth	Source, Year/Lot	Pharmacopoeia
1	<i>C. laevigata</i> (Poir.) DC./ <i>C. oxyacantha</i> L.	S15232	2	<sup>1</sup> CE, <sup>2</sup> EE	Botanic Garden, Kharkiv, Ukraine, 2015	<sup>7</sup> EPh, <sup>8</sup> SPhU
		S15195			'Likarski roslyny', Kharkiv, Ukraine, 2014	
2	<i>C. monogyna</i> Jacq.	S15231	3	CE, EE	Botanic Garden, Kharkiv, Ukraine, 2015	EPh, SPhU
		S15237			Ireland, 2015	
		S15194			'Fitosvit', Ukraine, 2014	
3	<i>C. leiomonogyna</i> Klokov	S15227	1	CE, EE	Botanic Garden, Kharkiv, Ukraine, 2015	-
4	<i>C. curvisepala</i> Lindm.	S15229	3	CE, EE	Botanic Garden, Kharkiv, Ukraine, 2015	SPhU
		S15202			'Viola', Zaporizhzhia, Ukraine, 01012012	
		S15203			'Likarski roslyny', Kharkiv, Ukraine, 2014	
5	<i>C. pseudokyrstostyla</i> Klokov	S15228	7	CE, EE	Botanic Garden, Kharkiv, Ukraine, 2015	-
		S15197			Kharkiv, Ukraine, 2014	
		S15198			'Ahrofirma', Mykolaiv, Ukraine, 2015	
		S15206			Kharkiv, Ukraine, 2012	
		S15207			'Zdorovia', Kharkiv, Ukraine, BMP-081014	
		S15208			'Ternofarm', Ternopil, Ukraine, P. 415/06.14	
		S15210			'Sumyfitofarmatsiia', Sumy, Ukraine, 6612.Y.1211	
6	<i>C. fallacina</i> Klokov	S15230	1	CE, EE	Botanic Garden, Kharkiv, Ukraine, 2015	-
7	<i>C. subrotunda</i> Klokov	S15205	1	CE, EE	'Chysta flora' Vyshneve, Ukraine, 2014	-
8	<i>C. ambigua</i> C.A.Mey. ex A.K. Becker	S15226	1	CE, EE	Botanic Garden, Kharkiv, Ukraine, 2015	-
9	<i>C. pentagyna</i> Waldst. & Kit. ex Willd.	S15196	1	CE, EE	Kharkiv, Ukraine, 2015	SPhU
10	<i>C. pseudoheterophylla</i> subsp. <i>turkestanica</i> (Pojark.) K.I.Chr.	S15216	2	<sup>3</sup> CA, <sup>4</sup> EA	Botanic Garden, Kharkiv, Ukraine, 2014	-
		S15236			Botanic Garden, Kharkiv, Ukraine, 2015	
11	<i>C. sanguinea</i> Pall.	S15199	3	Siberia, <sup>5</sup> ME	Anapa, Russia, 051014	SPhU
		S15200			Anapa, Russia, 2014	
		S15201			Anapa, Russia, 2015	
12	<i>C. chlorosarca</i> Maxim.	S15235	1	CA, EA	Botanic Garden, Kharkiv, Ukraine, 2015	-
13	<i>C. pentagyna</i> subsp. <i>pseudomelanocarpa</i> (Popov ex Pojark.) K.I.Chr.	S15217	1	CA, EA	Botanic Garden, Kharkiv, Ukraine, 2015	-
14	<i>C. pinnatifida</i> Bunge	S15233	1	CA, EA	Botanic Garden, Kharkiv, Ukraine, 2015	-
15	<i>C. almaatensis</i> Pojark.	S15214	2	CA, EA	Botanic Garden, Kharkiv, Ukraine, 2014	-
		S15215			Botanic Garden, Kharkiv, Ukraine, 2015	

Continued **Table 1: Description of the samples analyzed**

N	Species	Voucher Spicemens Number	Amount	Growth	Source, Year/Lot	Pharmacopoeia
16	<i>C. punctata</i> Jacq.	S15218	1	<sup>6</sup> NA	Botanic Garden, Kharkiv, Ukraine, 2015	-
17	<i>C. pringlei</i> Sarg.	S15219	1	NA	Botanic Garden, Kharkiv, Ukraine, 2015	-
18	<i>C. festiva</i> Sarg.	S15220	2	NA	Botanic Garden, Kharkiv, Ukraine, 2014	-
		S15221			Botanic Garden, Kharkiv, Ukraine, 2015	
19	<i>C. douglasii</i> Lindl.	S15223	1	NA	Botanic Garden, Kharkiv, Ukraine, 2015	-
20	<i>C. holmesiana</i> Ashe	S15224	1	NA	Botanic Garden, Kharkiv, Ukraine, 2015	-
21	<i>C. submollis</i> Sarg.	S15225	1	NA	Botanic Garden, Kharkiv, Ukraine, 2015	-
22	<i>C. flabellata</i> (Bosc ex Spach) K.Koch.	S15234	1	NA	Botanic Garden, Kharkiv, Ukraine, 2015	-
23	<i>C. canadensis</i> Sarg.	S15238	1	NA	Botanic Garden, Kharkiv, Ukraine, 2015	-

<sup>1</sup>CE – Central Europe; <sup>2</sup>EE – East Europe; <sup>3</sup>CA – Central Asia; <sup>4</sup>EA – Eastern Asia; <sup>5</sup>ME – Middle East; <sup>6</sup>NA – North America, <sup>7</sup>EPh – European Pharmacopoeia; <sup>8</sup>SPhU – State Pharmacopoeia of Ukraine.

properties have been attributed.<sup>[1,8,11,12]</sup> Moreover, flavonoids are used for pharmacopoeial standardization of hawthorn fruits. That is why, our investigation included modification of existing TLC method from European Pharmacopoeia into modern and reproducible HPTLC method that can help to detect an adulteration,<sup>[13,14]</sup> the inclusion of new *Crataegus* L. species and comparison of their chromatographic profiles.

For the proposed HPTLC method, the stationary phase, sample and standard preparations, application volume, documentation were modified, and acceptance criteria were set.

The derivatization reagent NP/PEG used in the method for the visualization of results in UV 366 nm allowed us to distinguish phenolic constituents of different *Crataegus* L. species, depending on its structure.<sup>[15]</sup> Thus, the obtained HPTLC fingerprints showed orange-yellow fluorescent (fl) zones due to flavanols: quercetin, myricetin and their glycosides, and yellow-green fl zones due to kaempferol, isoramnetin and their glycosides; orange fl zones due to flavones: luteolin and their glycosides, and yellow-green fl zones due to apigenin and their glycosides; blue fl zones due to phenol carboxylic acids (caffeic acid, chlorogenic acids) and coumarins.

Comparison of HPTLC fingerprints of different samples of 23 *Crataegus* L. species on phenolic constituents is shown in Fig. 1. As we can see in Fig. 1, *Crataegus* L. species, which are widespread in Central and East Europe, both pharmacopoeial and non-pharmacopoeial, such as: *Crataegus monogyna*, *C. laevigata* (*C. oxyacantha*), *C. leiomonogyna*, *C. curvisepala*, *C. pseudokyrstostyla*, *C. fallacina*, *C. subrotunda*, *C. ambigua*

*C.A.Mey. ex A.K. Becker*, *C. pentagyna* Waldst. & Kit. ex Willd., and species, which are widespread in Central and Eastern Asia, such as *C. sanguinea* Pall., *C. chlorosarca* Maxim., *C. almaatensis* Bunge, show quite similar fingerprints without specific discriminative features. Below, the acceptance criteria for these species are proposed.

**Acceptance criteria.** Under UV 366 nm, 30 min after derivatization, the chromatogram of the test solutions shows in the lower part of the chromatogram a very faint or faint yellow or orange fl zone at  $R_f \sim 0.32$ , corresponding to the reference substance rutin. In the middle part of the chromatogram, a faint to equivalent yellow or orange fl zone at  $R_f \sim 0.52$  corresponding to the reference substance hyperoside and another faint yellow or orange fl zone at  $R_f \sim 0.56$  above the position of reference substance hyperoside are present; one or two faint light blue fl zones at  $R_f \sim 0.43$  (chlorogenic acid) and at  $R_f \sim 0.47$  below the zone corresponding to the reference substance hyperoside are present. Close to the solvent front, one or two blue fl zones are seen.

Furthermore, other very faint or faint green fl zone at  $R_f \sim 0.35$  above the zone corresponding to the reference substance rutin (green arrows), light-blue fl zone at  $R_f \sim 0.62$  (blue arrows) and yellow or orange fl zones at  $R_f \sim 0.16$  and  $R_f \sim 0.24$  (yellow arrows) can be present.

Some other non-pharmacopoeial *Crataegus* L. species, which are widespread in Central and Eastern Asia – *C. pseudoheterophylla* subsp. *turkestanica* (Pojark.) K.I.Chr., *C. pinnatifida* Bunge, *C. pentagyna* subsp. *pseudomelanocarpa*



*C. laevigata* (Poir.) DC. /  
*C. oxyacantha* L.



*C. monogyna* Jacq.



*C. leiomonogyna* Klokov



*C. curvisepala* Lindm.



*C. pseudokyrstostyla* Klokov



*C. fallacina* Klokov



*C. ambigua* C.A.Mey. ex A.K.  
Becker



*C. pentagyna* Waldst. & Kit.  
ex Willd.



*C. pentagyna* subsp.  
*pseudomelanocarpa* (Popov  
ex Pojark.) K.I. Chr.



*C. pseudoheterophylla* subsp.  
*turkestanica* (Pojark.)  
K.I. Chr.

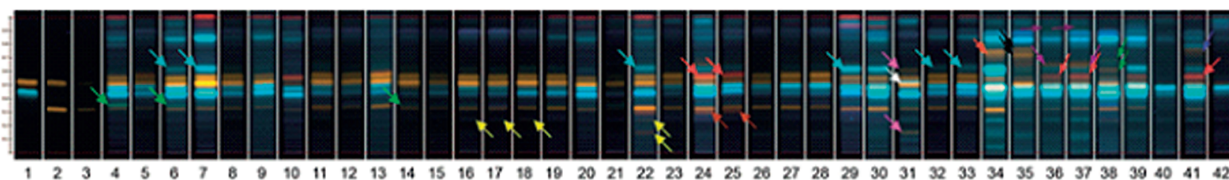


*C. pinnatifida* Bunge



*C. chlorosarca* Maxim.

Figure 1S: Pictures of some *Crataegus* L. species

*C. almaatensis* Pojark.*C. pringlei* Sarg.*C. festiva* Sarg.*C. punctata* Jacq.*C. submollis* Sarg.*C. flabellata* (Bosc ex Spach) K.Koch.Continued Figure 1S: Pictures of some *Crataegus* L. species

**Figure 1. Comparison of HPTLC fingerprints of phenolic compounds of 23 *Crataegus* species. Fruits. Developing solvent: anhydrous formic acid, water, methyl ethyl ketone, ethyl acetate (10:10:30:50); derivatization: NP/PEG; detection: 366 nm.**

Tracks: 1 – SST: Chlorogenic acid, hyperoside; 2 – R: Rutin, hyperoside; 3 – R1/4: Rutin, hyperoside; 4-5 – *C. laevigata*/*C. oxyacantha*; 6-8 – *C. monogyna*; 9 – *C. leiomonogyna*; 10-12 – *C. curvisepala*; 13-19 – *C. pseudokyrstostyla*; 20 – *C. fallacina*; 21 – *C. subrotunda*; 22 – *C. ambigua*; 23 – *C. pentagyna*; 24-25 – *C. pseudoheterophylla* subsp. *turkestanica*; 26-28 – *C. sanguinea*; 29 – *C. chlorosarca*; 30 – *C. pentagyna* subsp. *pseudomelanocarpa*; 31 – *C. pinnatifida*; 32-33 – *C. almaatensis*; 34 – *C. punctata*; 35 – *C. pringlei*; 36-37 – *C. festiva*; 38 – *C. douglasii*; 39 – *C. holmesiana*; 40 – *C. submollis*; 41 – *C. flabellata*; 42 – *C. canadensis*.

(Popov ex Pojark.) K.I.Chr., look slightly different and have specific marker zones. For instance, *C. pseudoheterophylla* subsp. *turkestanica* shows reddish fl zone at  $R_f \sim 0.57$  above orange fl zone corresponding to the reference substance hyperoside (red arrows); right below the position of reference substance rutin, there is another yellow fl zone (brown arrows). *C. pinnatifida* shows additional light-blue zone at  $R_f \sim 0.52$  between two orange zones (white arrow); shows additional faint yellow zones at  $R_f \sim 0.16$  and at  $R_f \sim 0.6$  (pink

arrows). *C. pentagyna* subsp. *pseudomelanocarpa* does not show orange or yellow fl zone at the position of reference substance hyperoside.

Most of the species that are widespread in North America – *C. punctata* Jacq., *C. pringlei* Sarg., *C. festiva*, *C. douglasii* Lindl., *C. holmesiana* Ashe, *C. submollis* Sarg., *C. flabellata* (Bosc ex Spach) K.Koch., *C. flabellata* (Bosc ex Spach) K.Koch. show different profiles of phenolic compounds in the upper half of the plate compared to pharmacopoeial species.

Discriminative features of these species that can be helpful for identification are shown below. Thus, *C. punctata* does not show orange or yellow fl zone at the position of reference substance hyperoside. It shows additional yellow fl zone at  $R_f \sim 0.73$  (orange arrow). *C. pringlei* shows additional yellow fl zones at  $R_f \sim 0.72$  and at  $R_f \sim 0.75$  (black arrows). In the chromatogram of the test solution zone corresponding to reference substance, the hyperoside is overlapped with light-blue fl zone, above this zone reddish fl zone at  $R_f \sim 0.57$  is seen (red arrows); in the upper third of chromatogram additional yellow fl zones at  $R_f \sim 0.65$  and at  $R_f \sim 0.92$  are present (violet arrows) (*C. festiva*). *C. douglasii* shows additional faint orange fl zone at  $R_f \sim 0.61$  above the position of reference substance hyperoside and a very faint orange fl zone above it (dark green arrows). In the chromatogram of the test solution zone corresponding to the reference substance, the hyperoside is overlapped with light-blue fl zone (*C. holmesiana*). *C. submollis* does not show orange or yellow fl zones corresponding to the reference substances rutin and hyperoside. *C. flabellata* shows reddish fl zone at  $R_f \sim 0.57$  above yellow fl zone corresponding to the reference substance hyperoside (red arrows) and additional orange fl zone at  $R_f \sim 0.75$  (dark blue arrows). *C. canadensis* does not show yellow or orange fl zone at the position of reference substance rutin.

## CONCLUSIONS

1. The evaluation and comparison of HPTLC fingerprints on phenolic constituents of 23 *Crataegus* L. species spread worldwide have been done.

2. Despite the slight variations, the similarity of phenolic constituents of nine *Crataegus* L. species native to Central and East Europe and three hawthorn species native to Central and Eastern Asia have been established. Further, phytochemical and pharmacological investigations are necessary.
3. The discriminative features in HPTLC chromatographic fingerprints for three other *Crataegus* L. species native to Central and Eastern Asia and eight hawthorn species native to North America have been established.

The data about the similarity of phenolic constituents of both pharmacopoeial and non-pharmacopoeial *Crataegus* L. species could be a ground for including new species into pharmacopoeial analysis and broadening of the herbal raw material base for the pharmaceutical market. The findings concerning discriminative features of phenolic fingerprints for some species could help to identify the possible adulteration and falsification. The results can be used for further chemotaxonomic investigation of hawthorn genus and improving "The Plant List", and should be taken into consideration for revising pharmacopoeial monograph for hawthorn fruits.

## ACKNOWLEDGEMENTS

Thanks to CAMAG and the Head of the CAMAG laboratory, Dr Eike Reich, PhD and Mr. Raphael Vizzini personally for financial and scientific support in conducting research on the base of CAMAG, Muttenz, Switzerland.

## References

- [1] Barnes J, Anderson L, Phillipson D. Herbal Medicines. London: PhP; 2007.
- [2] Derzhavnyi reiestr likarskykh zasobiv Ukrainy. (<http://www.drz.com.ua/>). Accessed March 20, 2015.
- [3] Khokhlova KO, Vyshnevskia LI, Sakharova TS. Market analysis of herbal drugs with Hawthorn raw material for cardiological treatment. Aktualni Pytannia Farmatsevtichnoi i Medychnoi Nauky ta Praktyky. 2012;9(2):107–111. [in Ukrainian].
- [4] Khokhlova KO. Quality control of hawthorn tincture by HPTLC method. Annaly Mechnykovskoho instytutu. 2016;3:56–60. [in Russian].
- [5] European Pharmacopoeia. Strasbourg: Council of Europe; 2007.
- [6] State Pharmacopoeia of Ukraine, Kharkiv: DP Ukrainyskyi naukovyi farmakopeinyi tsentr yakosti likarskykh zasobiv; 2014. [in Ukrainian].
- [7] Zerov D, ed. Flora URSS. Kyiv: Akademii nauk ukrainskoi RSR; 1954. [in Ukrainian].
- [8] Hrodzynskiy AM, ed. Medicinal plants: encyclopaedic guide. Kyiv: Holovna redaktsiia URE; 1991. [in Ukrainian].
- [9] Komarov V, Juzepchuk S, ed. Flora SSSR. Moskva: Akademii nauk SSSR; 1939. [in Russian].
- [10] The Plant List. A working list of all plant species. (<http://www.theplantlist.org/>). Accessed Jan 10, 2018.
- [11] Goncharov N, Sidora N, Kovaleva A, Komissarenko A. Phenolic compounds of North America Hawthorn species. Rossijskij Mediko-Biologicheskij Vestnik Imeni Akademika Pavlova. 2008;3:150–154. [in Russian].
- [12] Kovalova A, Sydora N, Honcharov M, Vilker A. Standardization of non-pharmacopoeial Hawthorn species. Fitoterapiia. Chasopys. 2007;2:54–56. [in Ukrainian].
- [13] Reich E, Schibli A. High-performance thin-layer chromatography for the analysis of medicinal plants. New-York, NY: Thieme; 2007.
- [14] Khokhlova K, Zdoryk O. HPTLC method in pharmacopoeial analysis of herbal raw material and herbal drug preparations. Recipe. 2017;20(4):462–469. [in Russian].
- [15] Wagner H, Bladt S, Zgainski E. Plant drug analysis. Berlin: Springer-Verlag; 1984.